IMPERIAL COLLEGE OF SCIENCE AND TECHNOLOGY

Department of Mathematics

THE STATISTICAL ANALYSIS OF SPATIAL POINT PATTERNS

by

Karen Byth

Thesis submitted for the degree of

Doctor of Philosophy in the University of London

and the

Diploma of Membership of Imperial College

MARCH, 1980

ABSTRACT

A spatial point pattern is a realisation of a stochastic process of point events in two or more dimensions. The methods of analysing such patterns fall into one of two categories: those appropriate when only sparse sampling from the pattern is performed and those possible when a complete map of the pattern exists.

Distance methods suitable in sparse sampling situations are examined. Four new tests of randomness are introduced and a semi-systematic sampling scheme is proposed. Some associated distribution theory is given. Simulation was used to compare the power of the new and other existing tests against various clustered and regular alternatives. Hopkins' statistic and its new counterpart are practicable when a semi-systematic sampling scheme is used. They performed best in the simulation study. Distance-based estimators of the intensity of the underlying process are also considered. Simulation is used to study the effect of semi-systematic sampling on the robustness of such estimators to departures from spatial randomness.

Existing methods for the analysis of complete maps assume stationarity of the underlying process under both rotations and translations. The concept of θ-stationarity is introduced. A process stationary under rotations about some preferred origin is one type of θ-stationary process. Techniques for analysing realisations of θ-stationary processes are developed and extended to include multitype processes. These methods use estimates of types of cumulative inter-point distance distribution functions. In practice the radial density of a pattern must be estimated and possible θ-stationary sectors identified. Kernel density estimates are proposed and tests of angular uniformity developed. The patterns of sporophores growing about a tree are analysed using the new methods. Some models are suggested and evidence of possible interaction between species is examined.

ACKNOWLEDGEMENTS

I am deeply indebted to my supervisor, Dr. B.D. Ripley, for introducing me to this fascinating area of research. His encouragement and patience together with the insights he provided during many hours of discussion are very much appreciated. Thanks are also due to Professor D.R. Cox for the interest he has shown in my studies, to Dr. B.W. Silverman for his helpful comments on certain aspects of density estimation and to Dr. E.D. Ford for releasing the sporophore data sets and explaining their biological background.

This work has been partly supported by a postgraduate fellowship from the Australian Federation of University Women (Queensland). I would like to record my gratitude to this organisation for its financial assistance.

Table of Contents

LIST OF TABLES

LIST OF FIGURES

CHAPTER 1: INTRODUCTION

Patterns formed by objects arranged in space are of interest in many disciplines. For example geographers may be concerned with maps of the positions of towns, ecologists with the locations of plants or animals, astronomers with the positions of stars or, on a larger scale, galaxies, and archaeologists with the positions of 'finds'. If the objects are 'small' compared with the inter-object distances they can be regarded as points. The resulting pattern of points can be considered as an outcome of a spatial point process, that is as a realisation of a stochastic process of point events in two or more dimensions. This thesis considers methods of analysing two-dimensional point patterns but obvious generalisations exist for higher dimensions.

If there is no systematic variation in a spatial point process it is said to be homogeneous (opposite heterogeneous). A spatial point pattern which has no preferred direction is said to be isotropic (opposite anisotropic). Much of the existing literature on the analysis of spatial patterns considers the case when the underlying process is both homogeneous and isotropic or, equivalently, stationary under the group of rigid motions. The Poisson process with constant intensity is perhaps the simplest process of this type and one with which other processes are usually compared. This process is a special case of the general Poisson process with non-negative bounded intensity function $\lambda(\underset{\sim}{x})$. A general Poisson process in n dimensions is a point process for which the number of points in any set $A \subset \mathbb{R}^n$ has a Poisson distribution with mean value $\int_A \lambda(\underset{\sim}{x})d\underset{\sim}{x}$. This is the usual Poisson process when $\lambda(\underset{\sim}{x}) \equiv \lambda$. If $\lambda(\underset{\sim}{x})$ depends on $\underset{\sim}{x}$ only through $|\underset{\sim}{x}|$, then the process will be said to be an isotropic Poisson process.

Methods of analysing spatial patterns may seek to describe some essential feature of the pattern by means of a convenient summary statistic such as the estimated intensity or they may attempt to fit models to the observed pattern. Usually only one realisation of the underlying process is available for study. It is necessary to assume some sort of stationarity of this underlying process before any hypothesis concerning the process can be tested on the basis of a single pattern. The stationarity assumption provides the replication necessary for subsequent inference. Some methods of analysing a spatial pattern when only a sample of measurements are available are discussed in Chapters 2 and 3. In the remaining Chapters it is assumed that a complete map of the pattern is available.

Chapter 2 is concerned with the use of 'distance' methods in the detection of nonrandomness. These methods use a sample of distances from selected positions to the neighbouring points in a pattern in order to test the null hypothesis of spatial randomness. Four new statistics are introduced and their approximate null distributions under sparse sampling are derived. Theoretical arguments are used to show that more intensive sampling is possible if a semi-systematic rather than the usual random sampling scheme is employed. This fact is verified in a simulation study. The semi-systematic sampling scheme which is proposed has the additional advantage of making Hopkins' test (Hopkins, 1954) and its new analogue practicable. In the past it has been felt that, though probably more powerful than other tests, Hopkins' test was impracticable because it required complete enumeration of the pattern. Hopkins' test and the new related test emerge as the leading contenders in a simulation study of the power of the new and other existing tests against clustered and regular alternatives.

Distance-based estimators of the average intensity of a process in some region of interest are studied in Chapter 3. Simulation is used to investigate the robustness of these estimators to changes in the underlying distribution and to study the effect of semi-systematic in place of random sampling. Both homogeneous and heterogeneous patterns are examined. Estimators based on the distances from selected positions to the r^{th} nearest point of the pattern ($r = 1,2,3$) are considered. Except in visually highly clustered patterns it appears that there is no advantage in taking $r > 1$. In highly clustered situations an estimator based on the distances corresponding to $r = 3$ is recommended in conjunction with a bias correction factor. In all other cases a 'compound' estimator based on 'T-square' distances and analogous to that recommended by Diggle (1975, 1977) appears to be the most robust of the estimators included in the simulation study. Semi-systematic sampling is recommended. For the heterogeneous patterns examined, the use of semi-systematic in place of random sampling tends to decrease the variance of the estimators without substantially increasing their absolute bias. This behaviour is to be expected on theoretical grounds.

The concept of θ-stationarity is introduced in Chapter 4 in order to analyse maps in which there is an obvious preferred origin. This concept is closely related to that of isotropy but only refers to the properties of the underlying process inside some 'sector' of interest. It is shown how the second order properties of θ-stationary simple second order processes can be described by means of a function analogous to K (Ripley, 1977), the latter being suitable only for homogeneous isotropic processes. Several clustered and regular θ-stationary processes are introduced and methods are given for simulating these

processes. It is shown how simulation can be used to test the goodness of fit of a model to a particular pattern. The ideas are extended to multitype θ-stationary point processes. A method is given for testing the independence of any two of the processes inside some 'sector' of interest.

In order to apply the techniques of Chapter 4 it is necessary either to know or to have a reliable estimate of the intensity function $\lambda(\underset{\sim}{x})$ of the underlying process inside the θ-stationary sector. The assumption of θ-stationarity means that in this region $\lambda(\underset{\sim}{x})$ depends on $\underset{\sim}{x}$ only through $|\underset{\sim}{x}|$. Thus estimating $\lambda(\underset{\sim}{x})$ in this region is equivalent to estimating the marginal radial probability density function from the appropriate 'sector' of the pattern. In Chapter 5 it is shown how kernel methods of density estimation can be used to estimate both this function and the associated marginal angular density. A test for angular uniformity which is based on the angular density estimate is introduced and its performance is assessed by means of simulation. It is possible to use the angular density estimate to partition a pattern into 'sectors' of high and low intensity if angular trend is present.

The methods developed in Chapter 5 are used to estimate the marginal radial and angular densities of the processes underlying the annual patterns of three types of sporophores found growing around a young birch tree (Ford, Pelham and Mason, 1980). Where appropriate they are also used to partition these patterns into high and low intensity 'sectors' within which the underlying process might be θ-stationary. In Chapter 6 such θ-stationarity is assumed and it is found that certain clustered models can be fitted to the sporophore patterns. The most interesting feature of the analysis for each

sporophore type is that the same fitted values for the parameters describing the mean number of sporophores per cluster and the cluster diameters appear in each year. Only the change in the total number of sporophores of that type and in the associated marginal radial density function are required to explain the differences between the annual patterns. With one possible exception the multitype analysis found no evidence of 'interactions' either within a certain sporophore type from one year to the next or between different types in any given year. The exception is one of the sporophore types which shows a tendency to grow in a similar area from year to year.

CHAPTER 2: THE USE OF DISTANCE METHODS IN THE DETECTION OF NONRANDOMNESS

2.1 Introduction

At the preliminary stage of analysis of a spatial point pattern it may be inappropriate to invest the time and money required for the detailed mapping of the region of interest. Instead only a sample of measurements are taken from this region. 'Distance' or 'nearest neighbour' methods are often used in such circumstances as an alternative to 'quadrat' methods, either to estimate the number of objects in the region or to test the 'randomness' of their pattern.

There are some statistics such as those of Clark and Evans (1954) and Brown and Rothery (1978) which use the distance from each object to its nearest neighbour in a test of 'randomness'. The following two Chapters will be concerned solely with methods requiring the sparse sampling of the region of interest. Tests of 'randomness' will be examined in this Chapter and intensity estimation in the next. Unless otherwise stated, the results of this and later Chapters will be for two dimensions only but obvious generalisations to higher dimensional spaces exist.

Even if the underlying process is Poisson, only the approximate theory of the test statistics has been derived. Very few analytical results are available for other underlying processes and those that have been found are approximations. Some of these results are given in Holgate (1965a,b), Besag and Gleaves (1974) and Diggle, Besag and Gleaves (1976) who calculate the theoretical power of several statistics against very simple clustered and regular alternatives.

The last paper and that of Hines and Hines (1979) use simulation to compare the power against more realistic alternatives.

If a complete map is available, other methods such as those recommended in Ripley (1977, 1979a) should be used.

2.2. Existing methods

For definiteness suppose that the objects of interest are plants of which N occur in the region of interest R. There are three distinct measurements used in the 'distance' methods to be discussed:

(a) u_r, the squared distance from a randomly selected point P to the r^{th} nearest plant Q_r ($r = 1,\ldots, k < N$)

(b) v, the squared distance from a randomly selected plant to its nearest neighbour

(c) t, the squared distance from Q_1 as defined in (a) to its nearest neighbour in a direction away from the initial point P. This is usually referred to as T-square sampling and was introduced in this context by Besag and Gleaves (1974).

Edge effects are made negligible by placing the study region from which random points and plants are to be selected well within R. Such a scheme will be referred to as random sampling. Figure 2.1 illustrates a random sample from a 10 metre square plot of pines (from Strand, 1972).

The squared distances are interesting quantities. With the above mentioned precaution against edge effects, πu_r, πv and $\pi t/2$ are simply the areas swept out in searching for the appropriate plant if the search is thought of in concentric circles (or in the case of t,

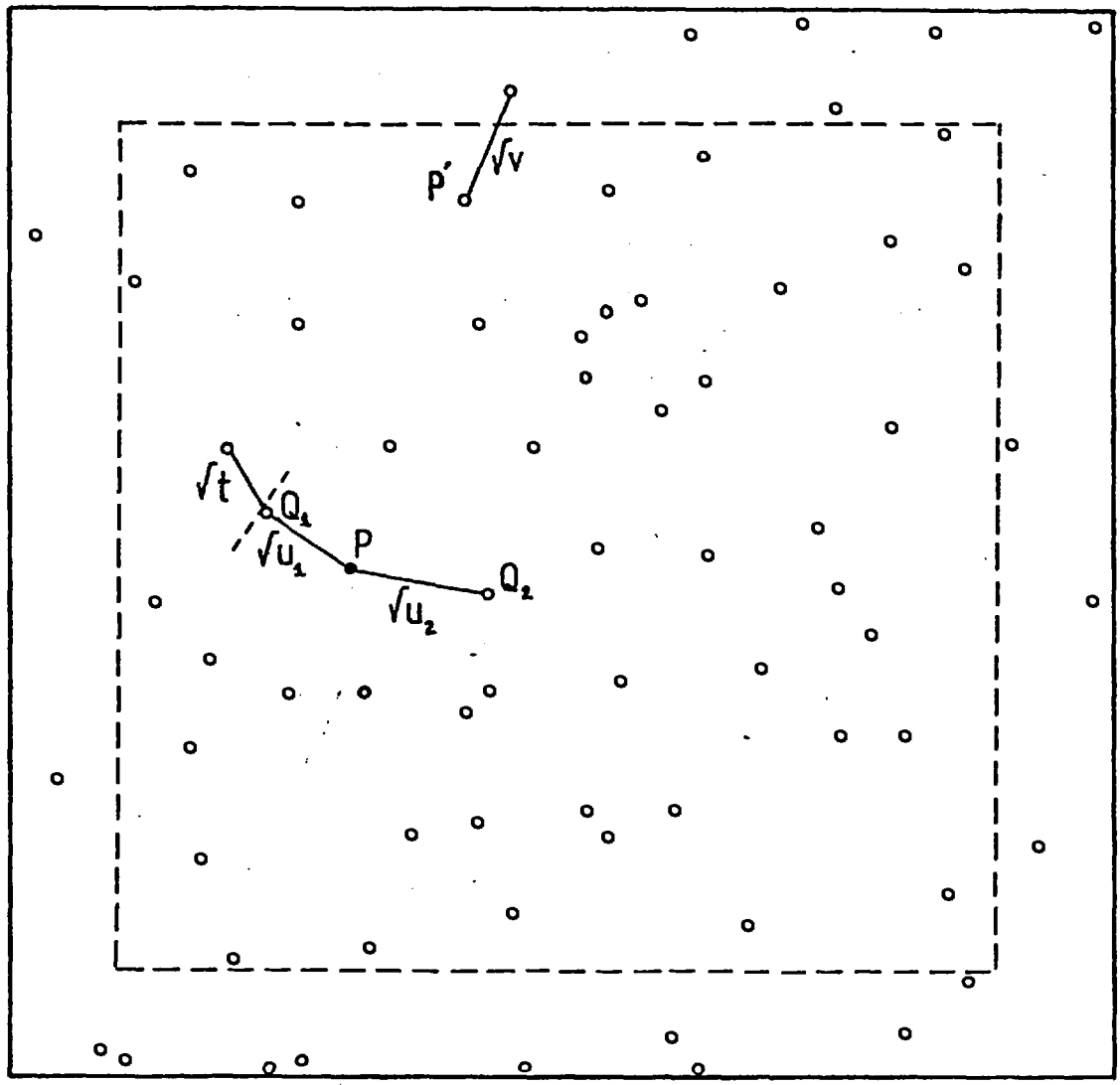

Figure 2.1

A random sample of size 1 selected from a 10 metre square stand containing 71 pines o (Strand, 1972). The boundary of this region of interest R and that of the study region S are marked ——— and - - - respectively. P is a randomly selected point from S, Q_1 and Q_2 the nearest and second nearest pines to this point. P' is a randomly selected pine from S. The distances $\sqrt{u_1}$, $\sqrt{u_2}$, $\sqrt{v}$, $\sqrt{t}$ are as indicated.

semicircles) about the chosen point or plant. A similar interpretation in terms of volumes holds in higher dimensions. The distribution theory of the 'distance' methods to be discussed assumes that for a Poisson process the πu_r's, πv's and $\pi t/2$'s are independent. For this to be true the areas searched must not overlap. This restriction clearly necessitates sparse sampling and is examined in more detail in Section 2.5.

The existing statistics considered in this Chapter are those proposed by Hopkins (1954), Holgate (1965a), Besag and Gleaves (1974) and Hines and Hines (1979). These statistics will be written as follows:

$$Hop_F = \Sigma u_{1i}/\Sigma v_i$$

(Hopkins, 1954)

$$Hol_F = \Sigma u_{1i}/\Sigma(u_{2i} - u_{1i})$$

$$Hol_N = (1/m)\,\Sigma u_{1i}/u_{2i}$$

(Holgate, 1965a)

$$T_F = \Sigma u_{1i}/\Sigma(t_i/2)$$

$$T_N = (1/m)\,\Sigma u_{1i}/(u_{1i} + t_i/2)$$

(Besag and Gleaves, 1974)

$$T_E = 2m\Sigma(2u_{1i} + t_i)/[\Sigma\{\sqrt{(2u_{1i})} + \sqrt{t_i}\}]^2$$

(Hines and Hines, 1979)

where the summation is in each case over i = 1,...,m and, with the obvious notation, u_{1i}, u_{2i}, v_i, t_i (i = 1,...,m) is a random sample of squared distances of size m hereafter written $\underset{\sim}{u}_1$, $\underset{\sim}{u}_2$, $\underset{\sim}{v}$, $\underset{\sim}{t}$. It will be convenient to consider each statistic as belonging to one of the three classes Hop, Hol or T named in a self-explanatory manner.

For a Poisson process with intensity λ it is easy to show that $\lambda\pi u_r$ (r = 1,...,k) and $\lambda\pi t/2$ have gamma (Γ) distributions with respective indices r and 1; a gamma distribution with index 1 simply being an exponential distribution with unit parameter. Equivalently twice these random variables have chi-squared (χ^2) distributions with 2r and 2 degrees of freedom respectively.

The variable $\lambda\pi v$ is, however, only approximately exponentially distributed. To see this suppose that there are $N_s \leq N$ plants in the study region S of area s. If v is to be well-defined then there must be at least one plant in S. Therefore all calculations concerning v should be conditional on $N_s \geq 1$. Consider some region of area a containing the randomly selected plant and suppose, for the moment, that this region lies wholly in S. The probability of there being no further plants in this subregion of S is therefore

$$E\{(1 - a/s)^{N_s - 1} \mid N_s \geq 1\}$$

$$= \sum_{N_s=1}^{\infty} (1 - a/s)^{N_s - 1} e^{-\lambda s} (\lambda s)^{N_s} / \{N_s!(1 - e^{-\lambda s})\}$$

$$= (e^{-\lambda a} - e^{-\lambda s}) / \{(1 - a/s)(1 - e^{-\lambda s})\}.$$

This expression is approximately $\exp(-\lambda a)$ if $a \ll s$ and $E(N_s) = \lambda s$ is sufficiently large, say ≥ 10. These conditions are

certainly satisfied in practical applications and it will in future be assumed that $\lambda\pi v$ is exponentially distributed. It should be noted that the region of area a in the above is strictly contained in S. In general the region corresponding to $\lambda\pi v$ may lie partly in $R \setminus S$, the 'border' included to make edge effects negligible. It is clear that this fact does not alter the basic conclusions.

Assuming that the variables in the random sample are jointly independent, it follows that the statistics with suffix F have F distributions with (2m,2m) degrees of freedom. Furthermore, each term summed to form the statistics with suffix N has a beta distribution with (1,1) degrees of freedom and so is uniformly distributed on [0,1]. Therefore Hol_N and T_N are the means of m independent uniform variables and, by the Central Limit Theorem, tend rapidly to the normal distribution $N(1/2, (12m)^{-1})$ as m increases. Details of these distributional results can be found for example in Holgate (1972). The statistic T_E is the Eberhardt statistic based on T-square sampling and tests for exponentiality. Hines and Hines (1979) give a table of percentage points.

Existing 'distance' methods are too numerous for each one to be considered here. The above statistics are a representative selection of the leading contenders identified in power comparisons such as those of Diggle et al (1976) and Hines and Hines (1979). In the latter study it was shown that the conditioned distance ratio method of Cox and Lewis (1976) is very similar to T_N. Perhaps the most intuitively appealing statistic and one that has generally been preferred in comparison studies is Hop_F (see Holgate, 1965b and Diggle et al, 1976). However it is usually regarded as impracticable since, to find a random plant, all plants in the study region should

be counted and a randomly numbered plant chosen. The semi-systematic sampling scheme recommended in Section 2.4 overcomes this objection.

2.3 New statistics

The first three new statistics are

$$\text{Hop}_N = (1/m) \sum_i u_{1i}/(u_{1i} + v_i)$$

$$\text{Hop}^* = (1/m^2) \sum_i \sum_j u_{1i}/(u_{1i} + v_j)$$

$$T^* = (1/m^2) \sum_i \sum_j u_{1i}/(u_{1i} + t_j/2)$$

where the summations are over $i,j = 1,\ldots,m$. Assuming that $\underset{\sim}{u}_1$, $\underset{\sim}{v}$, $\underset{\sim}{t}$ are jointly independent, the asymptotic distribution of each statistic as $m \to \infty$ can be found as follows for a Poisson process with intensity λ.

The terms summed to form each of these statistics are simply the ratios of $\lambda\pi u_{1i}$, an exponential variable, to the sum of this variable and another independent and identically distributed variable. Hence each term is uniformly distributed on [0,1]. It follows as for Hol_N and T_N that Hop_N has a $N(1/2, (12m)^{-1})$ limiting distribution as $m \to \infty$. Hop* and T* are examples of Hoeffding's U-statistics and it is easy to see that

$$E(\text{Hop}^*) = E(T^*) = 1/2$$

and that

$$\text{var}(\text{Hop}^*) = \text{var}(T^*) = \tau^2,$$

say, where

$$\tau^2 = \{1/12 + (m-1)(c_1 + c_2)\}/m^2$$

and

$$c_1 = \mathrm{cov}\{u_{1i}/(u_{1i} + v_j),\ u_{1i}/(u_{1i} + v_k)\}, \quad j \neq k,$$

$$c_2 = \mathrm{cov}\{u_{1i}/(u_{1i} + v_j),\ u_{1k}/(u_{1k} + v_j)\}, \quad i \neq k.$$

These covariance terms are

$$c_1 = \int_0^\infty \int_0^\infty \int_0^\infty \frac{u}{u+v} \frac{u}{u+w} \exp\{-(u+v+w)\}du\ dv\ dw - 1/4$$

$$c_2 = \int_0^\infty \int_0^\infty \int_0^\infty \frac{u}{u+w} \frac{v}{v+w} \exp\{-(u+v+w)\}du\ dv\ dw - 1/4$$

and may be simplified by changing the variables to

$$x = u/(u + v), \qquad y = u/(u + w), \qquad z = v$$

in c_1 and to

$$x = u/(u + w), \qquad y = v/(v + w), \qquad z = w$$

in c_2 and integrating out z to give

$$c_1 = \int_0^1 \int_0^1 2u^2v^2/(u + v - uv)^3 du\ dv - 1/4$$

$$\approx 0.0399$$

$$c_2 = \int_0^1 \int_0^1 2uv(1 - u)(1 - v)/(1 - uv)^3 - 1/4$$

$$\simeq 0.0401$$

by numerical integration. Thus the common variance of Hop* and T* is

$$\tau^2 \simeq \{1/12 + 0.080(m - 1)\}/m^2.$$

An application of Corollary 5, p.365 of Lehmann (1975) shows that, as $m \to \infty$, Hop* and T* are asymptotically normally distributed with expected value 1/2 and variance τ^2 provided that

$$\mathrm{var}[E\{u_1/(u_1 + v)\,|\,v\}] > 0$$

or that

$$\mathrm{var}[E\{u_1/(u_1 + t/2)\,|\,t\}] > 0.$$

The expressions on the left hand sides of these inequalities are equal. Putting $x = \lambda\pi u_1$ and $y = \lambda\pi v$,

$$E\{u_1/(u_1+v)\,|\,v\} = \int_0^\infty \{x/(x + y)\}\exp(-x)\,dx.$$

For $y \geq 0$,

$$x/(x + y) \quad \begin{cases} \geq 1/(1 + 2y), & x \geq 1/2 \\ \leq 1/(1 + y), & 0 \leq x \leq 1 \\ \leq 1, & x \geq 1. \end{cases}$$

It follows that

$$a \leq E\{u_1/(u_1 + v)|v\} \leq b$$

where

$$a = \{\exp(-1/2)\}/(1 + 2y)$$

and

$$b = \{1 + y \exp(-1)\}/(1 + y).$$

These bounds are plotted against y in Figure 2.2 and it is clear that $\text{var}[E\{u_1/(u_1 + v)|v\}] > 0$ as required for the asymptotic normality of Hop* and T*.

Hop_N was introduced in the hope that it might be more sensitive to changes in the relative values of u_1 and v. Hop* and T* use all possible combinations of u_{1i} and v_j and of u_{1i} and t_j $(i,j = 1,\ldots,m)$ respectively. In this sense they attempt to make maximum use of the available information on the relative values of point-plant and plant-plant distances. When tapes have been laid out to measure u_1 and u_2, the angle θ between the directions from the randomly selected point to the nearest and second nearest plants can be obtained with very little extra effort. The final new statistic which is of the Hol type incorporates this additional information on the spatial configuration.

For a Poisson process, θ is uniformly distributed on $[0,\pi]$ independently of u_1 and u_2. If u_{1i}/u_{2i} $(i = 1,\ldots,m)$ are assumed to be mutually independent, the random variable

$$s_i = \pi u_{1i}/(\theta_i\, u_{2i})$$

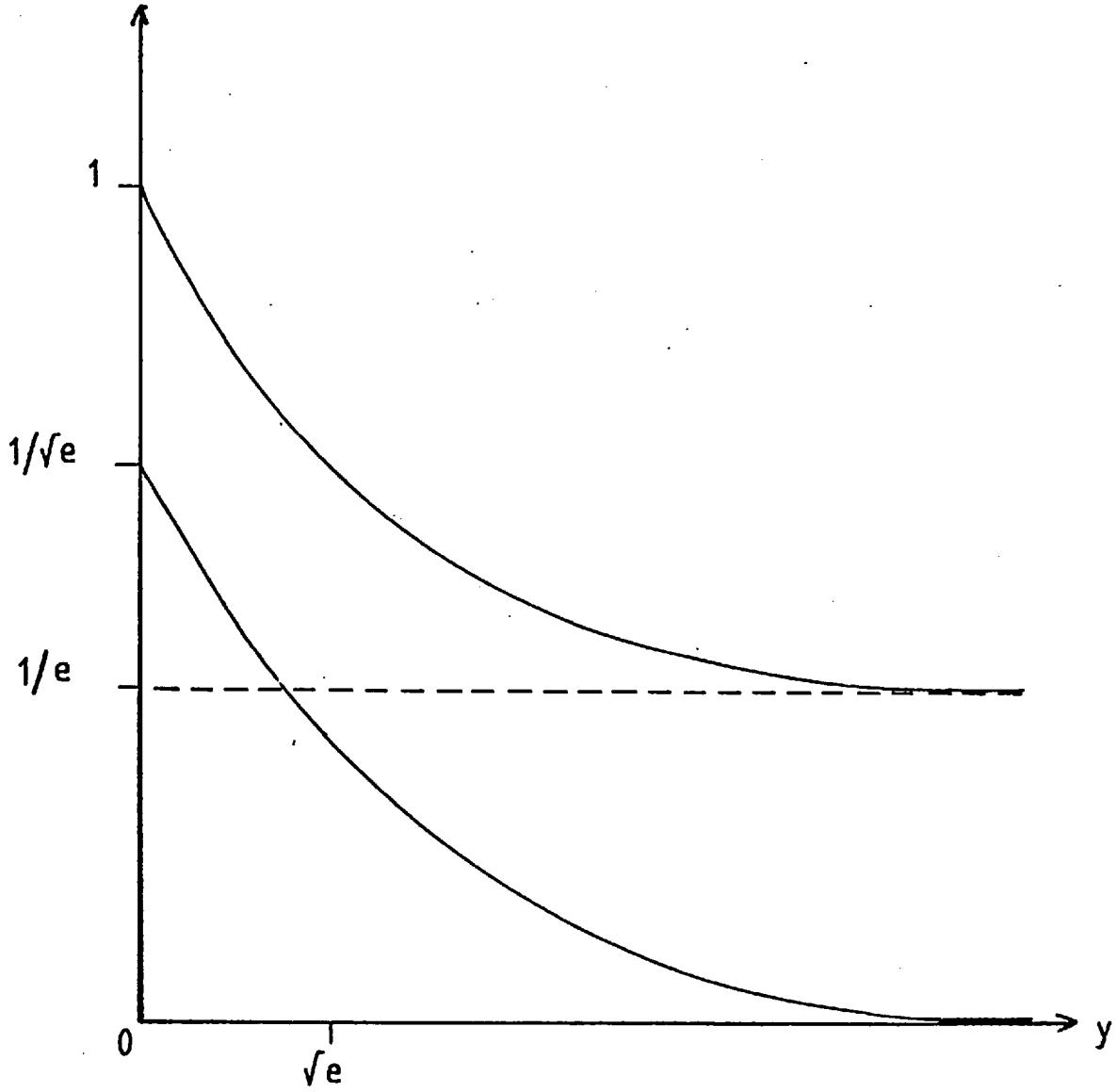

Figure 2.2

The upper and lower bounds for $E\{u_1/(u_1 + v)|v\}$ plotted against $y = \lambda\pi v$.

is simply the ratio of two independent uniform variables on [0,1] and therefore has the probability density

$$f(s) = \begin{cases} 1/2 , & 0 \leq s \leq 1 \\ (2s^2)^{-1} , & s > 1. \end{cases}$$

Both u_1/u_2 and π/θ tend to take on increasingly larger values than expected for a 'random' pattern as clustering becomes more marked and increasingly smaller ones as regularity is more marked. A test of 'randomness' can therefore be constructed from their product s by considering

$$Hol_B = Hol_B(x) = \sum_i \delta_i(x)$$

where, for some $x > 0$,

$$\delta_i(x) = \begin{cases} 0 , & \pi u_{1i}/(\theta_i u_{2i}) \leq x \\ 1 , & \pi u_{2i}/(\theta_i u_{2i}) > x. \end{cases}$$

Assuming the joint independence of u_{1i}/u_{2i} $(i = 1,\ldots,m)$, it follows that for a Poisson process Hol_B has the binomial distribution b(m,p) where $p = Pr(s > x)$. Thus to test the null hypothesis of 'randomness' H_0 against clustered alternatives at significance level α, choose a non-negative integer $r \leq m$ and compute x so that $Pr(Hol_B \geq r) = \alpha$. H_0 is then rejected at level α if the observed value $Hol_B \geq r$. A similar test in which H_0 is rejected if $Hol_B \leq r$ is available if regular alternatives are of interest. The choice of r, $0 \leq r \leq m$, (which fixes x for a given α) is arbitrary and certain values may lead to more powerful tests than others.

If a training set of observations is available, the following criterion for r may be used when m is sufficiently large for the normal approximation to the binomial to apply. Plot the standardised statistic

$$y_r = \{Hol_B(x_r) - mp_r\}/\sqrt{\{mp_r(1 - p_r)\}}$$

versus the integer r, $0 \leq r \leq m$, for the training set where p_r is a solution of

$$p_r^2(m^2 + mz_\alpha^2) + mp_r(1 - 2r - z_\alpha^2) + (r - 1/2)^2 = 0 \qquad (2.1)$$

if clustered alternatives are of interest and of

$$p_r^2(m^2 + mz_\alpha^2) - mp_r(1 + 2r + z_\alpha^2) + (r + 1/2)^2 = 0 \qquad (2.2)$$

if regular alternatives are of interest where z_α is the upper α-percentile of the standard normal distribution and

$$x_r = \begin{cases} (2p_r)^{-1} & , \quad 0 \leq p_r \leq 1/2, \\ (2 - 2p_r)^{-1} & , \quad 1/2 < p_r \leq 1. \end{cases} \qquad (2.3)$$

The value of r which maximises y_r is the value to be used in testing H_0 and can easily be computed.

Equation (2.1) is simply the quadratic in p_r obtained when the approximate expression

$$(r - 1/2 - mp_r)/\sqrt{\{mp_r(1 - p_r)\}} \approx z_\alpha$$

is considered to be exact. This approximate expression follows from

$$\alpha = \Pr(\mathrm{Hol}_B(x_r) \geq r) \approx \Pr(Z \geq (r - 1/2 - mp_r)/\sqrt{\{mp_r(1 - p_r)\}})$$

where Z is a standard normal variate. Similar considerations lead to (2.2). Equation (2.3) is found by inverting

$$p_r = \int_{x_r}^{\infty} f(s)ds = \begin{cases} 1 - 1/(2x_r) , & 0 \leq x_r \leq 1, \\ 1/(2x_r) , & x_r > 1 . \end{cases}$$

If no training set is available, simulation results suggest that it is reasonable to set $r = [9m/10] = r^*$, say, for clustered alternatives and $r = m - r^*$ for regular alternatives where $[\cdot]$ denotes 'the integer part of'.

The test statistics given in this and the preceding Section have been arranged to take on large values for clustered patterns and small ones for regular patterns. The associated tests of 'randomness' may be one or two-sided for all but Hol_B which can either test against clustering or regularity but not both simultaneously. A definite advantage shared by the above tests is that, unlike such methods as that of Pielou (1959) (corrected by Mountford, 1961), no knowledge of the usually unknown underlying intensity is required.

2.4 Semi-systematic sampling

Finney (1947, 1948, 1950, 1953) and Quenouille (1949) were among the first to investigate the possible advantages of sampling systematically rather than at random from a spatial pattern which does not display fairly marked periodicity. If the points or plants from which the squared distance measurements are made are selected in a semi-systematic manner, it will be shown that a higher sampling intensity is possible than for random sampling and that Hop methods can be used without the complete enumeration of the study region.

Suppose the plants in the region of interest were generated by a Poisson process of intensity λ. The area swept out in searching for the nearest plant from any position which is uniformly distributed over the study region has an exponential distribution, mean $1/\lambda$. Randomly selected points are such positions as are points chosen according to the semi-systematic scheme described below. It has been shown that, approximately, randomly selected plants also have this property. It will be seen that, under certain circumstances, this is equally true of plants selected according to the following semi-systematic sampling scheme illustrated in Figure 2.3 for the plot of pines from Strand (1972):

(a) set up a fairly regular grid of 2 m points within the study region

(b) from half these points measure the squared distance to the nearest and second nearest plants and obtain the angular measurements θ and the T-square plant-plant squared distances in the obvious way

(c) around each remaining point lay out a small plot of constant area (usually a circle or square) and count the plants in each plot

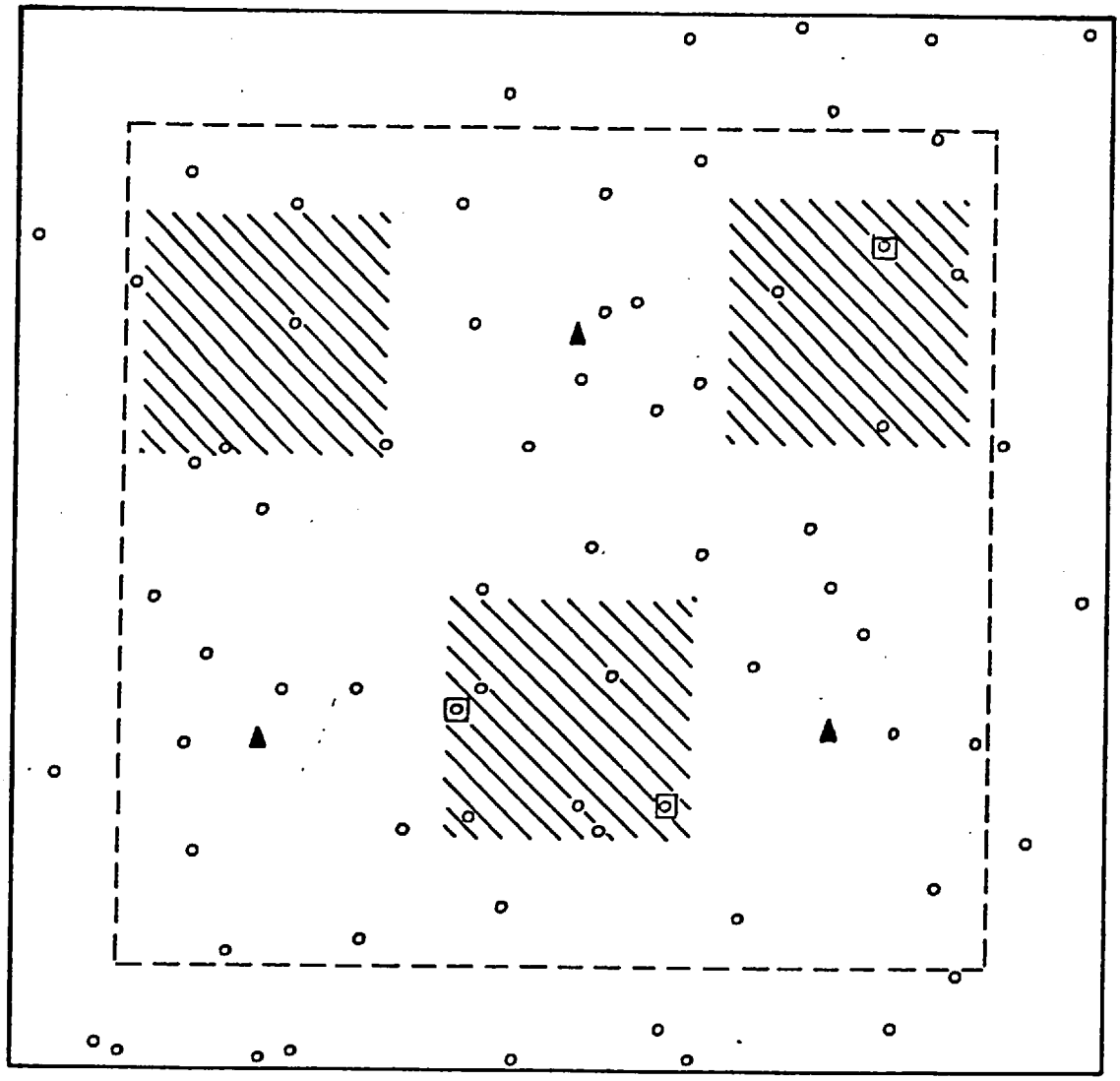

Figure 2.3

The points ▲ and pines ⊡ from which distances to neighbouring pines o are measured in a semi-systematic sample of size m = 3 from a 10 metre square stand containing 71 pines (Strand, 1972). The boundary of this region of interest R and that of the study region S are marked ——— and - - - respectively. The enumerated region is shown ▨

(d) select m plants at random from those enumerated and measure the squared distance from each to its nearest neighbour.

Values for $\underset{\sim}{u}_1$, $\underset{\sim}{u}_2$, $\underset{\sim}{v}$, $\underset{\sim}{t}$, $\underset{\sim}{\theta}$ obtained in this way will be referred to as a semi-systematic sample.

The necessary conditions for $\lambda\pi v$ to have approximately an exponential distribution can be found in the following way. Suppose that the total area of the enumerated plots is e, that each of these plots lies wholly within the study region S of area s and that there are N_e plants enumerated. Clearly $N_e \geq 1$ if v is to be well-defined under semi-systematic sampling. Consider some subregion of S about a plant selected at random from those enumerated. Let b and c be the areas of those parts of this subregion which fall respectively inside and outside the enumerated region. Then the probability that the subregion contains no further points is

$$e^{-\lambda c}\, E\{(1 - b/e)^{N_e - 1} \mid N_e \geq 1\}$$

$$= e^{-\lambda c}\, (e^{-\lambda b} - e^{-\lambda e})/\{(1 - b/e)(1 - e^{-\lambda e})\}.$$

This expression is approximately $\exp(-\lambda a)$ where $a = (b + c)$ is the area of the subregion if $b \ll e$ and $\lambda b \ll \lambda e$.

Each enumerated plot is obviously of area e/m. If $\lambda e/m = 5$ there are on average 5 plants per plot and in this case it is clear that $b \ll e$ and that $\lambda b \ll \lambda e$ since $(\lambda e - \lambda b) \approx \lambda e = 5m$. In practice, parts of some of the plots or of the circular subregion corresponding to $\lambda\pi v$ may lie in the 'border' region $R \setminus S$ but this does not affect the conclusions. Simulation results reported in Section 2.6 confirmed the validity of the null distribution theory of Hop statistics given

earlier when now semi-systematic sampling is used and plots of area sufficient to contain on average 5 plants are enumerated.

An even more attractive sampling scheme would be simply to choose one plant at random from each of the small plots laid out in step (c) and to measure $\underset{\sim}{v}$ from these plants. This would necessitate only one visit to each plot. However plants chosen in this way are not equally likely to be selected, a plant lying in a plot containing few plants being more likely to be chosen than one in a plot with many plants. Hence $\underset{\sim}{v}$ then contains inflated values for the plant-plant measurements and the null distribution theory given for Hop statistics is no longer valid.

A possibility is to estimate the intensity using each plot separately, giving estimates $\hat{\lambda}_i \propto n_i$ $(i = 1,\ldots,m)$, as well as using all the plots simultaneously to find $\hat{\lambda} \propto \bar{n} = \sum_i n_i/m$ where n_i is the number of plants in the i^{th} plot. A modified version of each Hop statistic can then be constructed by considering $\hat{\lambda}\pi u_{1i}$ and $\hat{\lambda}_i \pi v_i$ $(i = 1,\ldots,m)$ rather than $\lambda\pi u_{1i}$ and $\lambda\pi v_i$. (For example, Hop_F becomes $\bar{n}\,\Sigma u_{1i}/\Sigma(n_i v_i)$.) The distributions of these modified statistics are clearly not the same as those derived for the Hop statistics assuming the independence of $\underset{\sim}{u}_1$ and $\underset{\sim}{v}$. Simulation studies revealed that the sampling distributions of the modified Hop statistics agree with the quoted null distributions only for dense patterns and very sparse sampling (need at least 360 plants in the study region if selecting a sample of size 9 from plots covering a quarter of the region). It will be seen in the next Section that the first semi-systematic scheme proposed allows more intensive sampling and correspondingly less dense patterns. Attention will therefore be restricted to this semi-systematic and to the random sampling schemes.

2.5 Some null hypothesis distribution theory

If the spatial pattern is an outcome of a Poisson process of intensity λ, it has already been stressed that the null distributions quoted are valid only when the areas searched do not overlap. Consider the areas $\lambda\pi u_{1i}$, $\lambda\pi v_i$ $(i = 1,\ldots,m)$ which are approximately exponentially distributed with unit mean. The following heuristic argument shows that there is about a 5% probability that two areas overlap if the minimum distance between the sampled positions (points or plants) is at least $3/\sqrt{(\pi\lambda)}$. Let d_1 and d_2 be the distances from two positions to their respective nearest plants. The closest admissible configuration for the two positions is if the same plant Q_1 is nearest to both and if the two positions and this plant are colinear as illustrated in Figure 2.4. The inter-position distance is then $(d_1 + d_2)$, a quantity which can never exceed $\sqrt{\{2(d_1^2 + d_2^2)\}}$. Now $\lambda\pi(d_1^2 + d_2^2)$ has a Γ distribution with index 2 if the areas do not overlap. Thus the areas searched overlap no more than 5% of the time if the inter-position distance is at least $\sqrt{\{2 \times 4.744/(\pi\lambda)\}} \approx 3/\sqrt{(\pi\lambda)}$ where 4.744 is the upper 5% point of a Γ distribution with index 2. This bound on the inter-position distance can be checked in the field because the usual estimate of $1/\sqrt{(\pi\lambda)}$ is the root mean square distance from a point to the nearest plant (see, for example, Holgate, 1972).

For m positions selected by random sampling, the average distance between positions is clearly about $\sqrt{\{s/(\pi m)\}}$ for a study region of area s. Thus, for random sampling, the number of sample positions should not exceed $1/3^2 \approx 10\%$ of the number of plants in the study region. This conclusion is confirmed in the simulation study reported in the next Section. If semi-systematic sampling is used, the average

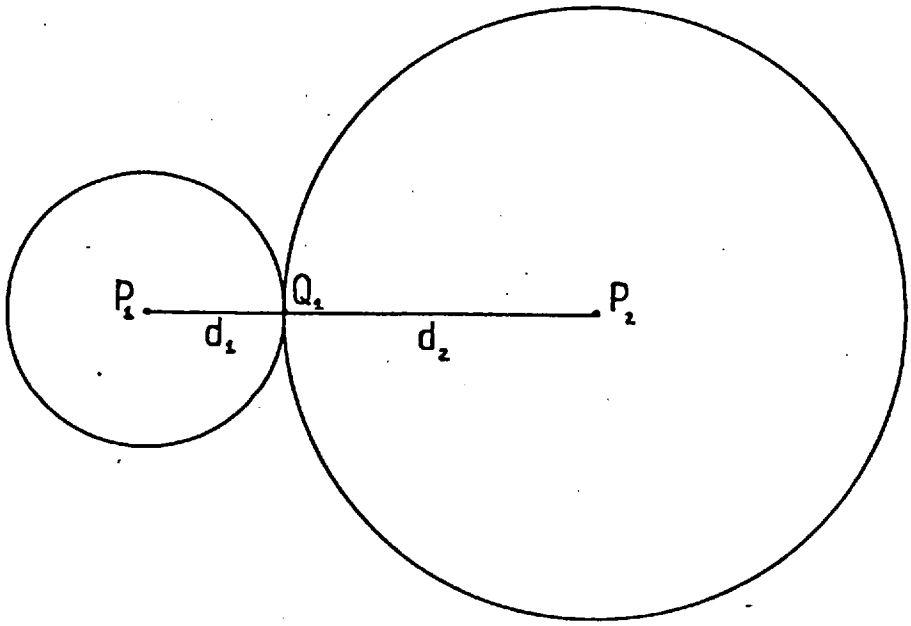

Figure 2.4

The closest admissible configuration for two positions P_1 and P_2 if the same plant Q_1 is nearest to both and if the circular areas searched in finding Q_1 from P_1 and from P_2 do not overlap.

distance between sites becomes $\sqrt{(s/m)}$ for the usual square grid of m sample positions in a square study region. The sampling intensity can therefore be increased by a factor of about 3, a fact also verified by simulation.

2.6 Simulation results

All the new and existing statistics discussed above were tested for 'random' processes and clustered and regular alternatives with both the random and the semi-systematic sampling schemes. The region of interest R was the unit square and the study region S the subregion $[0.2, 0.8]^2$ lying well inside R. In every case the total number of plants N in R was fixed, so the sampling intensity $\rho \approx m/(0.36N)$ for a sample of size m. For convenience m was taken to be a perfect square and semi-systematic sampling involved laying out two square grids of m vertices, one for point-'plant' and the other for 'plant'-'plant' measurements. The minimum distance between the vertices in each grid was $0.6/\sqrt{m}$. One grid was placed randomly inside the study region and the other was then aligned as shown in Figure 2.5 in such a way that it too lay in S. All the 'plants' in the small square plots about the vertices of the grid used for 'plant'-'plant' readings were counted.

Since N was fixed, a 'random' pattern was the outcome of a binomial process with N trials on the unit square. The x and y coordinates of 'plants' in such a pattern were simulated by generating 2N independent uniformly distributed variables on [0,1]. Diggle et al (1976) reported consistency with the null distributions of all the statistics except T_E for $\rho \leq 10\%$ on the basis of 57

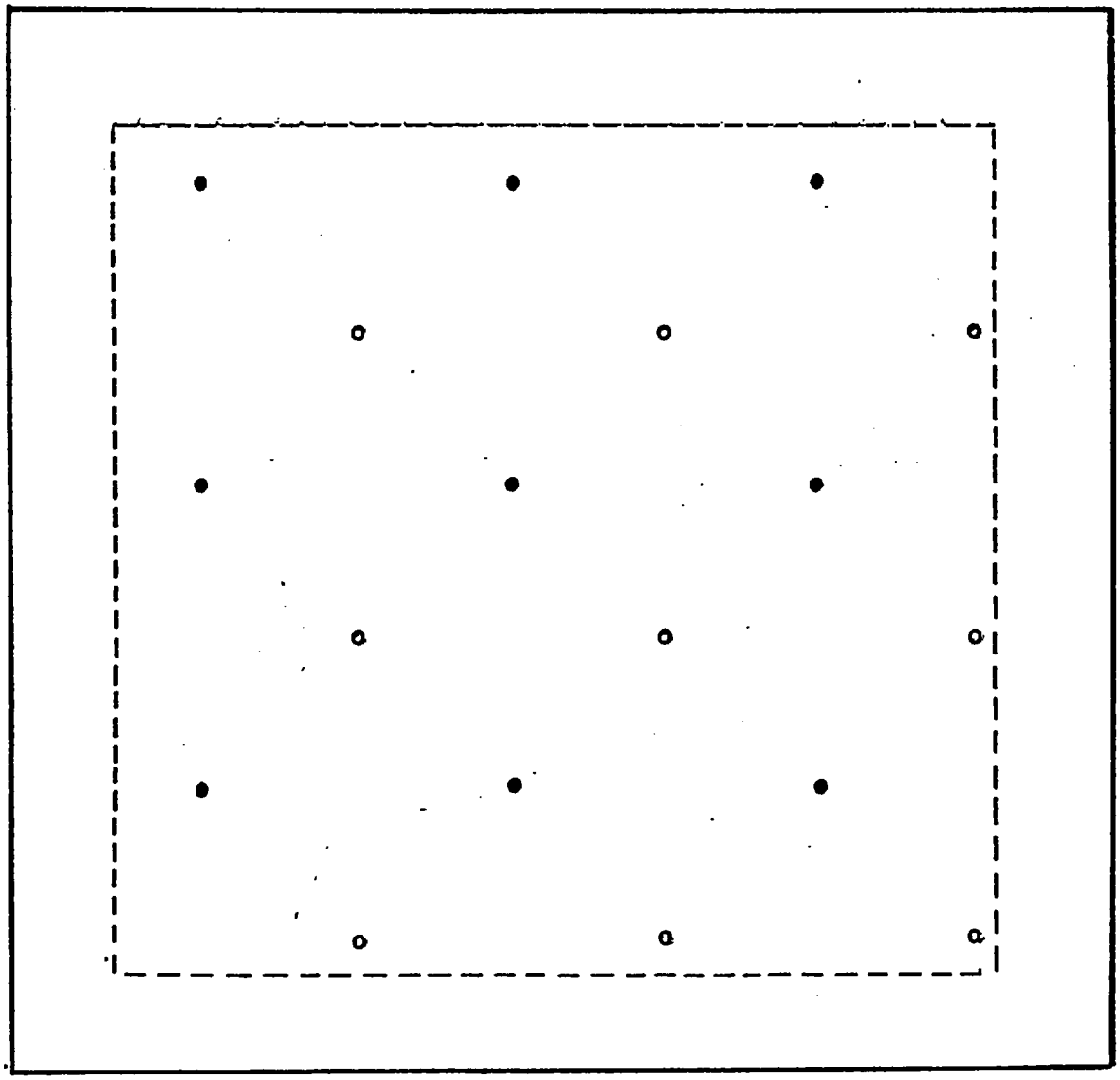

Figure 2.5

A possible configuration for the 9 vertices of each of the square grids used in a semi-systematic sample of size m = 9. The vertices used for point-plant measurements are shown • and those used in finding plant-plant measurements o . The boundary of the region of interest R and that of the study region S are marked ——— and - - - respectively.

realisations with m = 25. My results for the statistics were based on 1000 realisations for each of a variety of combinations of ρ and N ($\equiv \lambda$). They suggest that 10% is an acceptable bound for Hol and T statistics but is too high for Hop statistics: with m = 9, 71, 68 and 69 values out of 1000 for Hop_F, Hop_N and Hop* respectively lay beyond the 5% point of the appropriate theoretical distribution. The bound $\rho \leq 5\%$ seems adequate. The theory of Section 2.5 indicates that such a smaller bound is to be expected for Hop statistics which need <u>two</u> separate sets of m sample positions. When semi-systematic sampling was used, ρ could be at least as high as 25% for Hol and T statistics. For Hop statistics $\rho \leq 10\%$ sufficed if half the area was enumerated, $\rho \leq 5\%$ if one quarter. These bounds corresponded to enumerating an average five 'plants' per small plot.

Matérn cluster processes (Matérn, 1971) modified to contain a fixed number of plants N were used as clustered alternatives. Realisations were simulated by generating a Poisson number of cluster centres N_c, mean μ, and distributing these independently and uniformly within the unit square. The remaining $(N - N_c)$ 'plants' were then each distributed uniformly within a disc of diameter D centred on a cluster centre chosen at random, independently for each 'plant'. If the 'plant' so added fell outside the unit square, the procedure was repeated for this 'plant'. Figure 2.6 illustrates a realisation of such a process with D = 0.1, N = 600, μ = 100 giving a mean cluster size C = 6.

Strauss processes (Strauss, 1975, Kelly and Ripley, 1976, Ripley 1977, 1979b) were used as regular alternatives, D measuring the range of inhibition and c the strength. A process with c = 0 consists of non-overlapping discs of diameter D about each 'plant'.

Figure 2.7 illustrates a realisation of a Strauss process with $N = 240$, $D = 0.04$, $c = 0.1$.

The power comparisons are based on 100 realisations with $m = 9$, $\rho \leq 5\%$ and 5% equal-tailed tests for all except Hol_B which used the appropriate 2½% one-sided test. The results are reported in Tables 2.1 and 2.2. The choice of sampling scheme did not appreciably affect the estimated power of Hol and T statistics. Therefore only the average of the 200 results for semi-systematic (one quarter of the total area enumerated) and random sampling is presented for these statistics. The results shown for Hol_B are for $r = 8$ and 1 respectively in Tables 2.1 and 2.2. These values of r gave reasonable power against the appropriate alternatives. For any of the other statistics at most 3% of the estimated power against clustered or regular alternatives arose from values falling in the 2½% lower or upper tails respectively. Tables 2.1 and 2.2 may therefore be used to compare the power of all statistics against one-sided alternatives at the 2½% significance level, or of all except Hol_B against two-sided alternatives at the 5% level.

It was disappointing to find that the new U-statistics Hop* and T* are not obviously more powerful than their counterparts Hop_N and T_N. There is no apparent advantage in using the information provided by <u>all</u> combinations of point-plant and plant-plant measurements in this way : the double summation merely smooths the contribution from each u_{1i}, v_i, t_i $(i = 1,\ldots,m)$.

The statistic Hol_B is certainly more powerful than Hol_F or Hol_N against regular alternatives. However in situations where the clusters are not well separated, the angular measurement θ may often be taken from a point lying within or very close to a cluster and

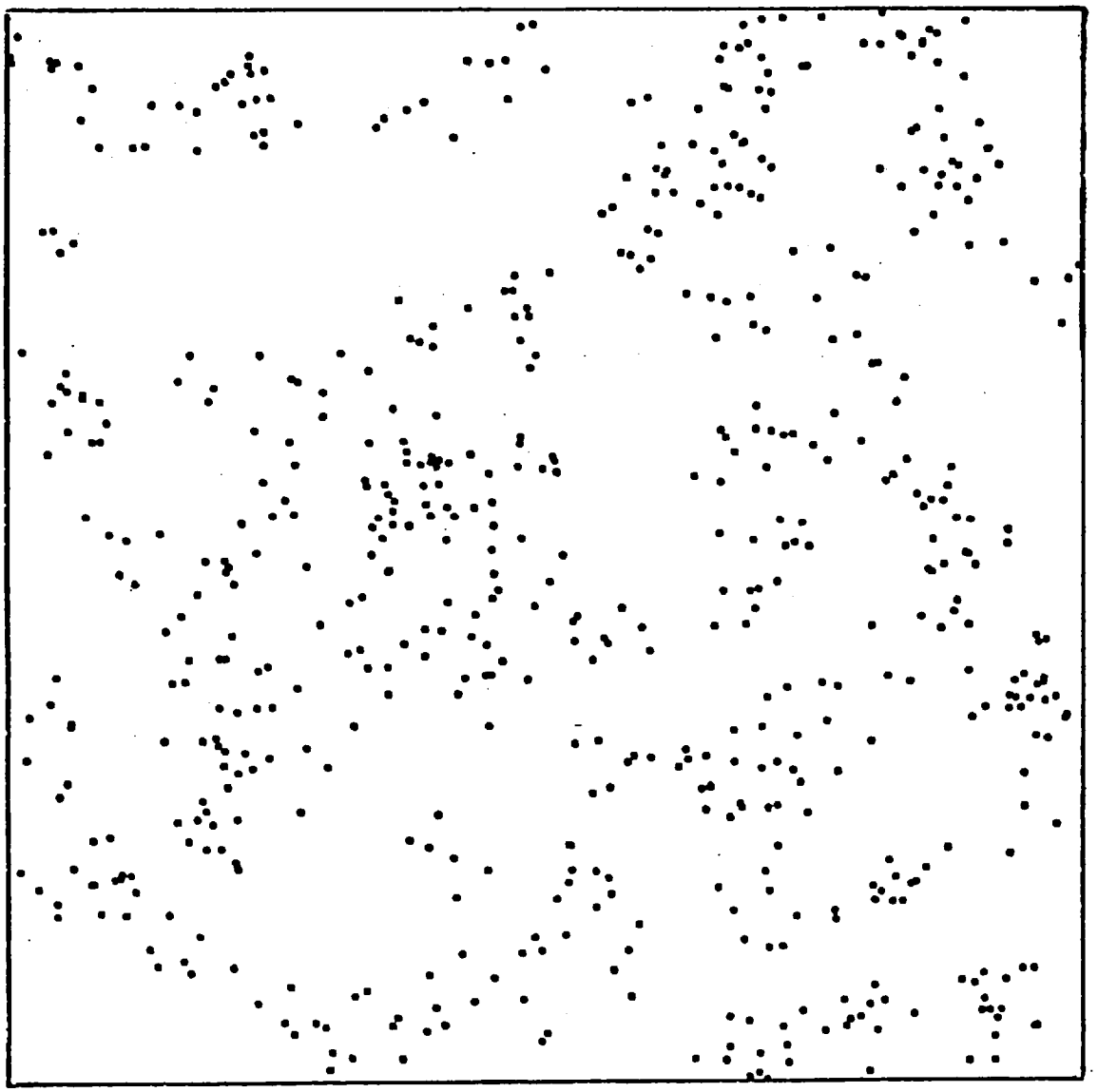

Figure 2.6

A realisation on the unit square of a modified Matérn cluster process having N = 600 points, mean cluster size C = 6 and cluster diameter D = 0.1.

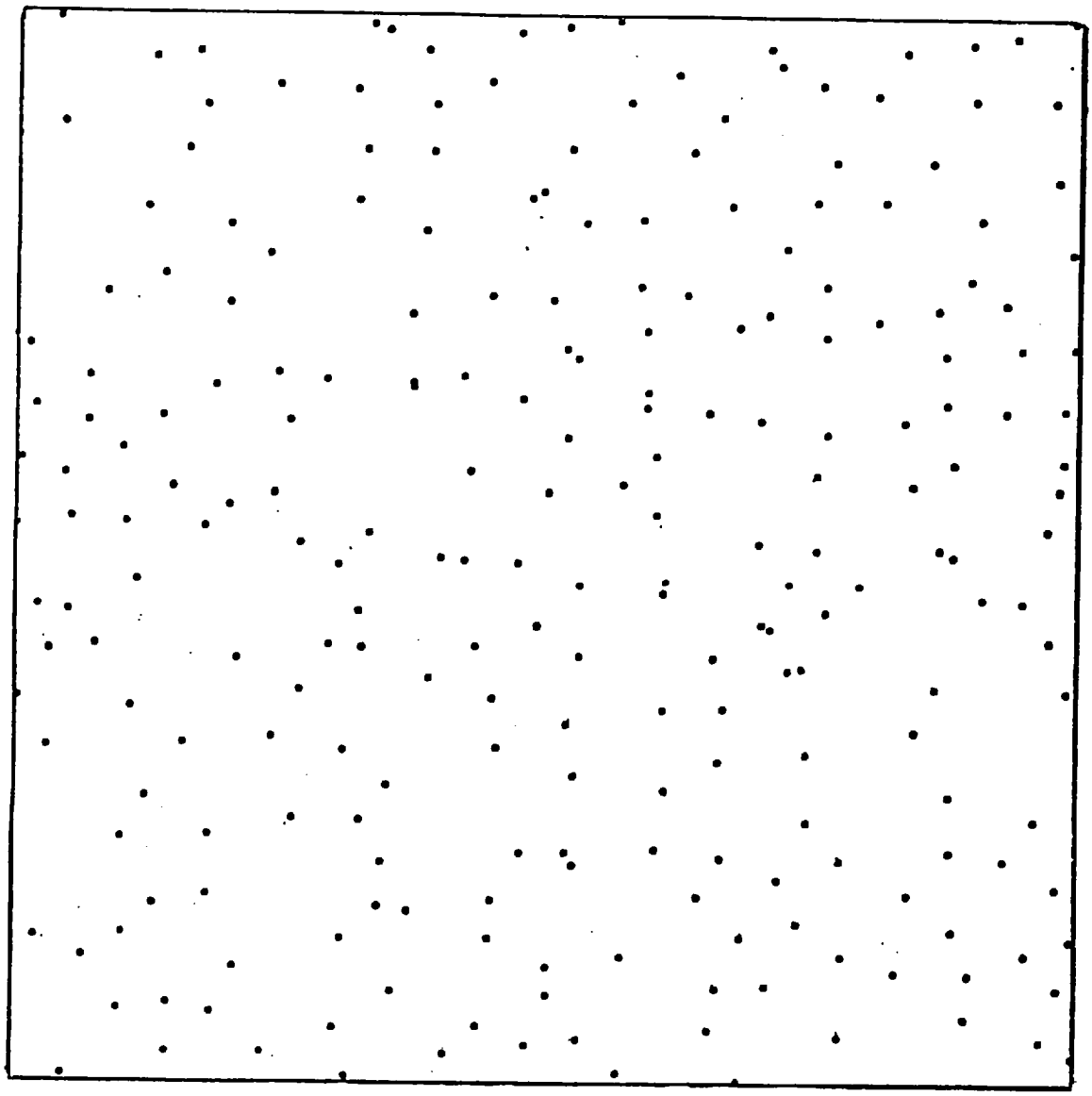

Figure 2.7

A realisation on the unit square of a Strauss process having N = 240 points, range of inhibition D = 0.04 and coefficient of inhibition c = 0.1.

C	D	Hop_F		Hop_N		Hop*		T_F	T_N	T*	T_E	Hol_F	Hol_N	Hol_B
		R	S	R	S	R	S							
2	.05	58	35	42	27	44	26	43	36	38	36	22	19	25
	.02	80	55	92	67	92	71	50	79	79	85	38	43	51
3	.1	34	28	13	16	13	16	22	9	9	21	9	5	5
	.05	85	71	67	65	69	61	70	65	66	68	36	23	43
	.03	97	87	95	92	97	93	86	92	92	96	65	56	70
6	.15	40	37	19	16	21	18	23	11	8	29	11	8	7
	.1	69	75	45	48	46	45	65	36	32	59	27	10	20
	.07	96	98	69	74	70	78	91	76	77	88	61	26	46

TABLE 2.1

Estimated power in percent against clustered alternatives with mean cluster size C and cluster diameter D. R and S respectively denote the columns containing the results for the appropriate Hop statistic under random and semi-systematic sampling. The entries for T and Hol statistics are the average of the results under both sampling schemes.

D	c	Hop_F		Hop_N		Hop*		T_F	T_N	T*	T_E	Hol_F	Hol_N	Hol_B
		R	S	R	S	R	S							
.03	0	19	20	50	47	50	48	11	20	20	22	7	9	16
.0325	0	27	36	64	60	67	73	12	25	25	29	7	10	24
.035	.25	20	19	31	25	30	25	7	10	10	15	7	6	10
	0	30	43	68	68	67	66	13	30	32	33	5	6	21
.04	.25	16	23	21	31	21	31	10	17	21	15	4	5	10
	.1	33	38	48	46	48	44	10	24	24	30	9	11	22
	0	49	48	84	80	86	82	18	33	36	45	17	15	30

TABLE 2.2

Estimated power in percent against regular alternatives with coefficient of inhibition c and range of inhibition D. R and S respectively denote the columns containing the results for the appropriate Hop statistic under random and semi-systematic sampling. The entries for T and Hol statistics are the average of the results under both sampling schemes.

need not be small. In such cases $\pi u_1/(\theta u_2)$ is not large. For this reason Hol_B is not always more powerful than Hol_F against clustered alternatives. Taken as a whole, Hol statistics are definitely inferior to Hop and T statistics. This confirms the results reported by Diggle et al (1976) and Hines and Hines (1979).

Hopkins' original test (that is Hop_F using random sampling) is best against clustered alternatives with both Hop_F and T_E doing well under semi-systematic sampling. For regular alternatives Hop_N is clearly best and does not appear to lose power when semi-systematic sampling is used. It is interesting to note the substantial decrease in power against regular alternatives for all statistics when the strength of inhibition is slightly weakened from the case of non-overlapping discs, $c = 0$. For example, compare $c = 0$ with $c = 0.1$ for $D = 0.04$. Both Diggle et al (1976) and Hines and Hines (1979) considered as regular alternatives only simple sequential inhibition processes which are very similar to the case $c = 0$.

2.7 Recommendations

The study shows Hop statistics are worthy of consideration. The semi-systematic sampling scheme allows Hop tests to be used without the necessity of complete enumeration and permits more intensive sampling if complete enumeration or T statistics are used. A recommended strategy to test for significant pattern in a region is to

(a) lay out a fairly regular grid of 2m points lying inside the study region and to proceed as explained for semi-systematic sampling in Section 2.4, making sure that each plot is of area sufficient to contain on average five plants

(b) calculate Hop_F and Hop_N and use these as tests of 'randomness'; Hop_F when clustering is suspected and Hop_N for regular alternatives.

If T statistics must be used, T_E and a semi-systematic scheme are recommended, the latter as a precaution against over-sampling.

CHAPTER 3: THE USE OF DISTANCE METHODS IN ROBUST INTENSITY ESTIMATION

3.1 Introduction

It is often of considerable interest to estimate the average intensity of the point process underlying an observed pattern in some region. For example it may be of economic or ecological importance to have a reliable estimate of the number of trees in a forest. Counts in randomly located quadrats can be used to give unbiased estimates of the average intensity irrespective of the form of the underlying process. This is not true of 'distance' methods. Nevertheless 'distance' methods are often preferred since they can be easier to use in the field. It is therefore important to establish which distance-based estimators of the average intensity in a region are robust to changes in the distribution of the underlying process. This is the aim of this Chapter.

The distance-based estimators then available were reviewed by Persson (1971). Their bias was calculated for regular lattice processes and for randomly distributed point cluster processes. Diggle (1975, 1977) considered estimators of the inverse of the intensity for some homogeneous processes. He introduced several 'compound' estimators which are combinations of the usual estimators based on the means of the squared distances $\underset{\sim}{u}_1$, $\underset{\sim}{v}$ or $\underset{\sim}{t}$ of Chapter 2. In the first paper he showed analytically that for specific regular and clustered processes the 'compound' estimators have smaller bias than the usual estimators. In the second paper he used simulation to verify that the 'compound' estimators also give more reliable estimates for certain more realistic clustered processes.

In this Chapter some analogues of Diggle's 'compound' estimators are considered. These new functions estimate the average intensity and not its inverse. Estimators based on the distances not only to the nearest object but also to the second and third nearest objects are examined. In addition to estimators based on the mean squared distances others based on the squares of the mean distances and of the median distances are compared in a simulation study. The empirically based estimator of Batcheler and Hodder (1975) is included in this study. So too is the estimator introduced by Morisita (1957) and formed from the mean of the inverses of the squared distances to the third nearest object. Morisita claimed that this estimator should be robust if the pattern consists of areas of different intensity within each of which the process is Poisson.

Simulation is used to study the bias and variance of both the new and the existing estimators under the random and semi-systematic sampling schemes of Chapter 2. The results for homogeneous and for heterogeneous patterns are summarised in the final Section.

3.2 The estimators

For definiteness again suppose that the objects of interest are plants of which there are N in the region of interest $R \subset \mathbb{R}^2$. Furthermore suppose that the intensity of the underlying process at the point $\underset{\sim}{x} \in \mathbb{R}^2$ is given by $\lambda(\underset{\sim}{x})$. So as to minimise edge effects it is necessary to measure distances from points or plants selected from a study region S lying well within R. The average intensity in S is given by

$$\bar{\lambda} = \int_S \lambda(\underset{\sim}{x})\, d\nu(\underset{\sim}{x}) \Big/ \int_S d\nu(\underset{\sim}{x})$$

where $\nu(\cdot)$ is Lebesgue measure on $\mathbb{R}^2$. It is this quantity $\bar{\lambda}$ for which robust estimators are required.

Under either random or semi-systematic sampling as defined in Chapter 2 let

(a) x_r be the distance from the selected point P to the r^{th} nearest plant Q_r

(b) y_r be the distance from the selected plant to the r^{th} nearest plant

(c) z_r be the distance from Q_1 to the r^{th} nearest plant in a direction away from P, that is the T-square distance to the r^{th} nearest plant from Q_1

(d) w be the distance from Q_1 to the nearest plant.

With the notation of Chapter 2 this means that

$$u_r = x_r^2, \qquad v = y_1^2, \qquad t = z_1^2 .$$

Samples of size m are denoted in the obvious way by

$$\underset{\sim}{x}_1, \ldots, \underset{\sim}{x}_r, \qquad \underset{\sim}{y}_1, \ldots, \underset{\sim}{y}_r, \qquad \underset{\sim}{z}_1, \ldots, \underset{\sim}{z}_r, \underset{\sim}{w}.$$

In this Chapter the distances corresponding to $r \leq 3$ are of interest and sampling is again assumed to be sufficiently sparse to ensure the independence of the samples.

Estimators of $\bar{\lambda}$ based on the measurements $\underset{\sim}{y}_r$ are only practicable under semi-systematic sampling. Random sampling necessitates complete enumeration of the N_S plants in the study region S and $N_S/\int_S d\nu(\underset{\sim}{x})$

would then be an excellent estimator of $\overline{\lambda}$. A modest amount of enumeration is required when finding $\underset{\sim}{y}_r$ under semi-systematic sampling. Before estimators which use $\underset{\sim}{y}_r$ are recommended, they must therefore be more robust than others which do not. Although impracticable, estimators which use $\underset{\sim}{y}_r$ are considered under random sampling in the simulation study. The inclusion of these estimators allows the effect of semi-systematic sampling to be assessed for a wider variety of estimators.

The most analytically tractable case to consider is the homogeneous Poisson process with constant intensity $\lambda(\underset{\sim}{x}) \equiv \lambda \equiv \overline{\lambda}$. As explained in Chapter 2, $\lambda\pi x_{ri}^2$, $\lambda\pi y_{ri}^2$ and $\lambda\pi z_{ri}^2/2$ $(r = 1,2,3;\ i = 1,\ldots,m)$ are approximately jointly independent and distributed as Γ variates with index r for such a process under the assumption of sparse sampling. Following Persson (1964) it is therefore easy to show that if

$$d_{ri} = x_{ri} \text{ or } y_{ri} \text{ or } z_{ri}/\sqrt{2} \qquad (r = 1,2,3;\ i = 1,\ldots,m)$$

and if

$$\overline{d_r^2} = \sum_{i=1}^{m} d_{ri}^2/m$$

$$\overline{d}_r^2 = \left(\sum_{i=1}^{m} d_{ri}/m\right)^2$$

$$d_r^* = \text{median of } d_{r1},\ldots,d_{rm}$$

$$\overline{1/d_r^2} = \left(\sum_{i=1}^{m} 1/d_{ri}^2\right)/m$$

then, at least asymptotically as $m \to \infty$, the method of moments estimators of λ given in Table 3.1 are unbiased and have the given asymptotic variances. Estimators based on the function $\overline{1/d_r^2}$ for $r = 1,2$ are not included in Table 3.1 because the expectation of $1/d_{1i}^2$ and the variance of $1/d_{ri}^2$ $(r = 1,2)$ are infinite for a homogeneous Poisson process. For such a process the asymptotic variance of the estimator based on $\overline{d_r^2}$ is as small as that based on any other function of $\underset{\sim}{d}_r$ since it is the maximum likelihood estimator. Of course for other processes this need not be so.

The 'compound' estimators of $\overline{\lambda}$ to be studied in this Chapter are analogues of the 'compound' estimators $\tilde{\gamma}$, $\tilde{\gamma}_T$, γ^* and γ_T^* of the inverse of the intensity introduced by Diggle (1975). These new estimators are arithmetic and geometric means of usual estimators based on point-plant and on plant-plant distances. The usual intensity estimators tend to be biased in opposite directions for clustered processes; those based on point-plant distances tend to underestimate the average intensity whilst those which use plant-plant distances tend to overestimate this quantity. The converse is true for regular processes (see Diggle, 1975). It is hoped that the 'compound' estimators are more robust than the usual estimators used in their formation: the opposing effects on the bias of the usual estimators should at least partially cancel each other out in the 'compound' estimators.

The plant-plant distances may tend to zero in a highly clustered pattern although the point-plant distances must remain finite for any reasonably shaped study region S. Thus the intensity estimated in any of the usual ways from the plant-plant distances may tend to infinity whilst that estimated from the point-plant distances must be bounded away from zero. This illustrates the asymmetric behaviour of the biases of the usual estimators. Because of this asymmetry the

$f(d_r)$	$\hat{\lambda}$	var $(\hat{\lambda})$
$\overline{d_1^2}$	$1/(\pi\overline{d_1^2})$	λ^2/m
$\bar{d}_1^2$	$1/(4\bar{d}_1^2)$	$1.09296\ \lambda^2/m$
d_1^{*2}	$0.069315/(\pi d_1^{*2})$	$2.08138\ \lambda^2/m$
$\overline{d_2^2}$	$2/(\pi\overline{d_2^2})$	$0.5\ \lambda^2/m$
$\bar{d}_2^2$	$9/(16\bar{d}_2^2)$	$0.52707\ \lambda^2/m$
d_2^{*2}	$1.67835/(\pi d_2^{*2})$	$0.90408\ \lambda^2/m$
$\overline{d_3^2}$	$3/(\pi\overline{d_3^2})$	$0.\dot{3}\ \lambda^2/m$
$\bar{d}_3^2$	$225/(256\bar{d}_3^2)$	$0.34599\ \lambda^2/m$
d_3^{*2}	$2.67406/(\pi d_3^{*2})$	$0.57495\ \lambda^2/m$
$\overline{1/d_3^2}$	$2(\overline{1/d_3^2})/\pi$	λ^2/m

Table 3.1

The function $f(\cdot)$ of the distance measurements $\underset{\sim}{d}_r$ $(r = 1,2,3)$ used in forming the method of moments estimator $\hat{\lambda}$ of the intensity λ of a homogeneous Poisson process. The estimators based on $\overline{d_r^2}$ are also the maximum likelihood estimators. At least asymptotically as the sample size $m \to \infty$, each estimator is unbiased and the asymptotic variance, var $(\hat{\lambda})$, is shown. The distances d_{ri} may be either x_{ri} or y_{ri} or $z_{ri}/\sqrt{2}$ $(i = 1,\ldots,m)$.

'compound' estimators which are geometrical means of the usual estimators might be more robust than their arithmetic mean analogues. Certainly such is the case for the 'compound' estimators of the inverse of the intensity investigated by Diggle (1975, 1977).

For each function $\overline{d_r^2}$, $\bar{d}_r^2$, d^{*2} and $\overline{1/d_r^2}$ of the distance measurements to the r^{th} nearest plant there are four corresponding new 'compound' estimators. For example the estimators based on $\overline{d_1^2}$ are

$$(m/2)\{1/(\pi\Sigma x_{1i}^2) + 1/(\pi\Sigma y_{1i}^2)\} \tag{3.1}$$

$$(m/2)\{1/(\pi\Sigma x_{1i}^2) + 2/(\pi\Sigma z_{1i}^2)\} \tag{3.2}$$

$$m\sqrt{[\{1/(\pi\Sigma x_{1i}^2)\}\{1/(\pi\Sigma y_{1i}^2)\}]} \tag{3.3}$$

$$m\sqrt{[\{1/(\pi\Sigma x_{1i}^2)\}\{2/(\pi\Sigma z_{1i}^2)\}]} \tag{3.4}$$

where the summation is in each case over $i = 1,\ldots,m$. The other new estimators are defined in the obvious way using the remaining nine estimators given in Table 3.1. Thus there are in all forty 'compound' estimators to be compared in addition to the usual estimators formed by using either the point-plant or the plant-plant distance measurements in the estimators of Table 3.1.

The estimator suggested on empirical grounds by Batcheler and Hodder (1975) is also considered. This estimator is

$$m/(\pi\Sigma x_{1i}^2 \times 3.473 \times 3.717^{-1.9131X})$$

where

$$X = \sqrt{[\{m\Sigma x_{1i}^2 - (\Sigma x_{1i})^2\}/(\Sigma x_{1i}\Sigma w_i)]}.$$

It is possible to construct 'compound' estimators based on distance measurements from selected points to the r^{th} nearest plant and from selected plants to the s^{th} nearest plant where $r \neq s$. There is no reason to expect these 'compound' estimators to be more robust than those described already. They are not included in the present study.

The standardised bias B and the standardised variance V of an estimator $\hat{\lambda}$ of the average intensity $\overline{\lambda}$ in the study area S are defined by

$$B = E(\hat{\lambda}/\overline{\lambda} - 1)$$

and

$$V = \text{var}(\hat{\lambda}/\overline{\lambda}) .$$

With the exception of the Batcheler and Hodder estimator it is clear that for a homogeneous Poisson process, at least asymptotically as $m \to \infty$, $B \to 0$ for each estimator under investigation. In the next two Sections simulation is used to study the robustness of the estimators to changes in the form of the underlying process. An estimator is said to be robust if B is close to zero and if V is not excessively large for a wide variety of processes. This restriction on the size of V ensures the efficiency of the estimator.

3.3 The homogeneous case

The simulation study splits into two parts. The first part which is presented in this Section looks at the robustness of the estimators of the intensity for homogeneous processes. The second part presented in the next Section examines the robustness of the estimators of the average intensity in the study area S for heterogeneous processes. Since so many estimators are being compared the full set of tables of

results are not given. Instead the main features of these tables are described and the actual results are given in each case for the most robust estimator.

In all cases 25 realisations of each process were used to estimate B and V for the various estimators under consideration. For the 'compound' estimators m = 9 whilst for the usual estimators m = 18. Thus the results concerning either type of estimator are based on the same total number of distance measurements. This ensures that the effort required to collect the data used in a particular estimate is comparable with that needed to form any other estimate. The simulated patterns were all restricted to have a total number of N = 500 points in the unit square R. The points or plants from which distance measurements were made were selected according to the random and semi-systematic sampling schemes of Chapter 2. They were chosen from within the square study area $S = [0.1, 0.9]^2$ so as to minimise edge effects. The results of Chapter 2 suggest that the resulting sampling intensity is sufficiently small to ensure the approximate validity of the assumptions made under sparse sampling.

The standardised bias of the usual estimator based on the function $f(\cdot)$ of $\underset{\sim}{x}_r$ given in Table 3.1 is denoted $B(\underset{\sim}{x}_r, f(d_r))$. For example, the standardised bias of $m/(\pi\Sigma x_{1i}^2)$ is $B(\underset{\sim}{x}_1, \overline{d_1^2})$. The standardised biases of the 'compound' estimators in equations (3.1)-(3.4) are denoted respectively $B(\underset{\sim}{x}_1, \underset{\sim}{y}_1, +, \overline{d_1^2})$, $B(\underset{\sim}{x}_1, \underset{\sim}{z}_1, +, \overline{d_1^2})$, $B(\underset{\sim}{x}_1, \underset{\sim}{y}_1, \surd, \overline{d_1^2})$ and $B(\underset{\sim}{x}_1, \underset{\sim}{z}_1, \surd, \overline{d_1^2})$. The standardised biases of the other 'compound' estimators are written in the obvious way.

The clustered and regular homogeneous processes considered in this Section are respectively the modified Matérn cluster process and the Strauss process introduced in Chapter 2. As Bartlett (1963) points

out, it is possible to consider such a cluster process as a heterogeneous process but such an interpretation is not used here.

For regular patterns Diggle (1977) recommends using γ_T^* to estimate the inverse of the intensity. The intensity estimator given in equation (3.4) is $1/\gamma_T^*$. The simulation results for a variety of Strauss processes show that estimators based on the distances to the 2^{nd} and 3^{rd} nearest plants are very slightly more robust than the corresponding estimator which uses the distance to the nearest plant. However, the improvement is so slight as to be scarcely worth the additional effort involved in finding these larger distances. For example $B(\underset{\sim}{x}_1, \underset{\sim}{z}_1, \surd, \bar{d}_1^{\,2}) \approx 0.02$ whilst $B(\underset{\sim}{x}_3, \underset{\sim}{z}_3, \surd, \bar{d}_3^{\,2}) \approx 0.01$ under semi-systematic sampling for a Strauss process with coefficient of inhibition $c = 0.4$ and range of inhibition $D = 0.015$. The use of semi-systematic rather than random sampling appears to have no obvious effect on the estimated bias and variance. The results of Chapter 2 would therefore suggest the use of the former so as to avoid over-sampling. The estimated values of $|B|$ and V for the estimator

$$E^* = m^2/\{(2\Sigma x_{1i})(\sqrt{2}\ \Sigma z_{1i})\} \qquad (3.5)$$

analogous to (3.4) but based on $\bar{d}_1^{\,2}$ are among the smallest for all the estimators in each situation considered. In particular there appears to be no advantage in using estimators based on the plant-plant distances $\underset{\sim}{y}_r$. The use of semi-systematic sampling and the estimator E^* are therefore recommended for regular homogeneous patterns.

Realisations of modified Matérn cluster processes having a mean number $\mu = 2$, 4 or 5 points per cluster and a cluster diameter $D = 0.05$, 0.1 and 0.2 were simulated. Increasing μ or decreasing D

produces more obvious visual clustering in the simulated patterns. When D = 0.05 the simulated patterns are highly clustered whilst the patterns for $\mu = 2$ and D = 0.2 are visually similar to homogeneous Poisson patterns; see Figures 3.1(a)-(d).

The 'compound' estimators are more robust than the usual estimators in all except the highly clustered situations (D = 0.05). For moderately clustered patterns there seems to be no advantage in using the distances from the selected point or plant to the 2^{nd} or 3^{rd} nearest plant. Nor is there any apparent advantage in choosing estimators which make use of $\underset{\sim}{y}_r$ and so require partial enumeration. In the situations considered the performance of such estimators is comparable with or worse than that of the analogous estimators which use $\underset{\sim}{z}_r$. Except for the highly clustered patterns, the estimator E* is again at least as robust as any other estimator considered. The use of semi-systematic instead of random sampling appears to generally improve the performance of E*. Certainly it is a safeguard against oversampling. The standardised bias and variance of E* for the moderately clustered patterns are shown in Table 3.2. The corresponding values of the estimator

$$E^{+} = (m^2/2)[1/\{4(\Sigma x_{1i})^2\} + 2/\{4(\Sigma z_{1i})^2\}]$$

and those of $m^2/\{4(\Sigma x_{1i})^2\}$ are included in this Table for comparison.

In highly clustered situations all the estimators have considerable bias. The estimator $3m/(\pi\Sigma x_{3i}^2)$ based on the distances x_3 under semi-systematic sampling generally appears to have bias comparable with and variance less than the best of the other estimators in such cases. Under semi-systematic sampling $B(\underset{\sim}{x}_3, \overline{d_3^2}) \approx -0.15, -0.26, -0.41$ and the

(a)

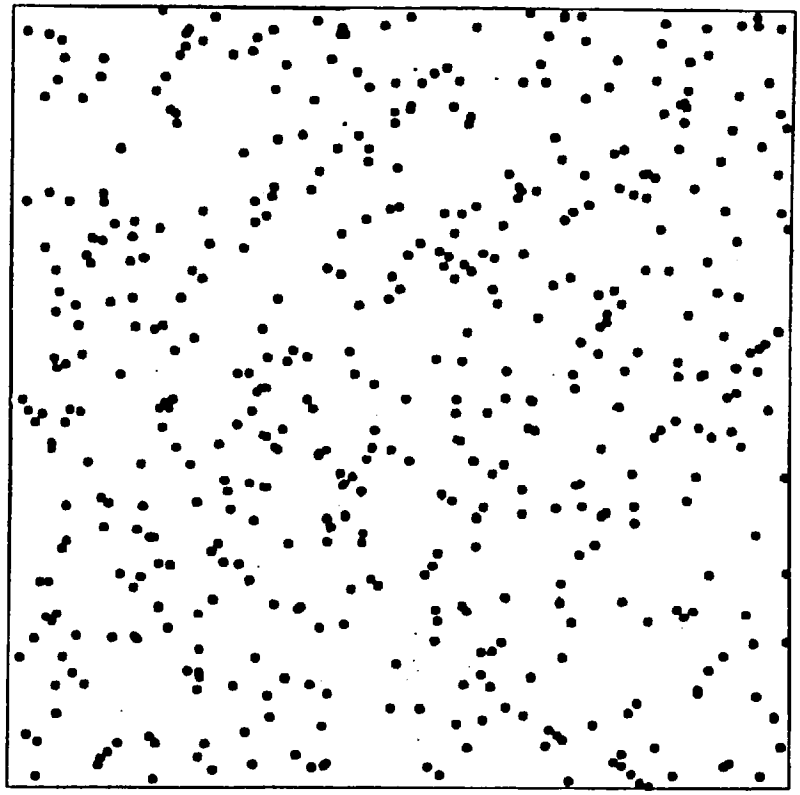

(b)

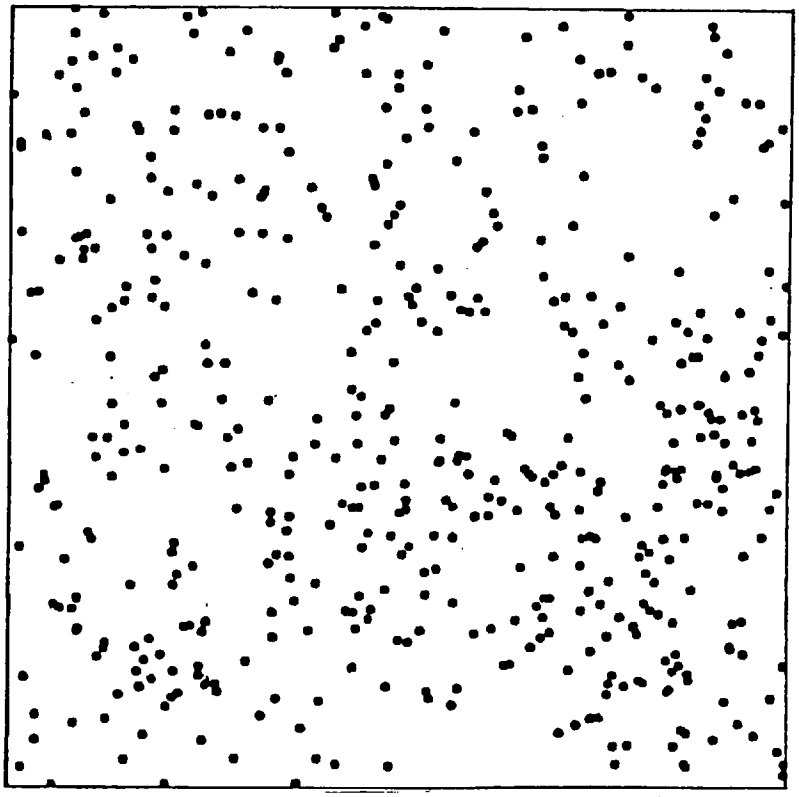

Figure 3.1(a), (b). Realisations on the unit square of (a) a homogeneous Poisson process (b) a modified Matérn cluster process with on average $\mu = 2$ points per cluster of diameter $D = 0.2$. Each realisation consists of 500 points.

(c)

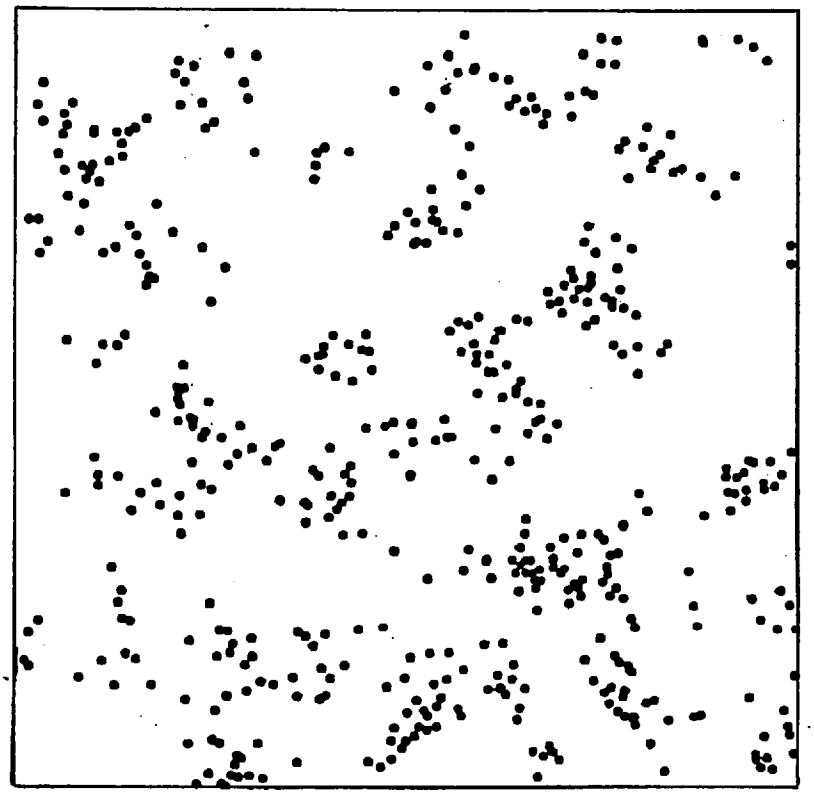

(d)

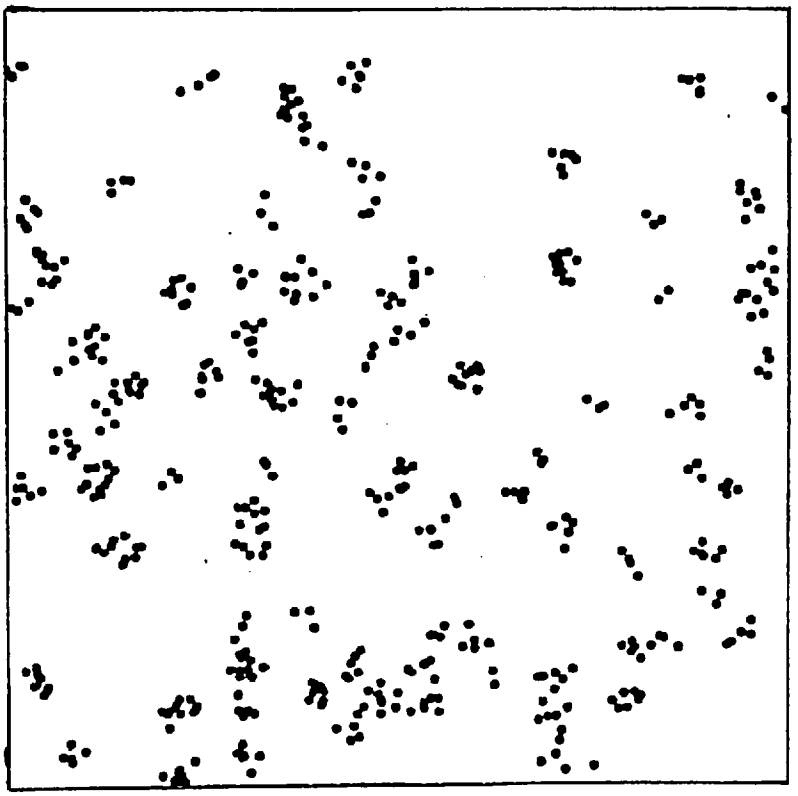

Figure 3.1 (c),(d). Realisations on the unit square of modified Matérn cluster processes with (c) $\mu = 4$, $D = 0.1$ (d) $\mu = 4$, $D = 0.05$. Each realisation consists of 500 points.

μ	D	$m^2/\{4(\sum x_{2i})^2\}$ R	$m^2/\{4(\sum x_{2i})^2\}$ S	E^+ R	E^+ S	E* R	E* S
2	0.2	-4	4	11	13	6	7
		(3)	(7)	(10)	(8)	(8)	(7)
	0.1	-13	-22	2	9	-2	-1
		(5)	(2)	(8)	(13)	(7)	(9)
4	0.2	-4	-2	6	8	4	2
		(3)	(3)	(6)	(5)	(6)	(4)
	0.1	-25	-39	10	21	-1	3
		(9)	(3)	(16)	(16)	(11)	(9)
5	0.2	-2	-14	12	17	7	1
		(15)	(3)	(19)	(10)	(17)	(7)
	0.1	-42	-48	23	20	3	-2
		(4)	(3)	(29)	(22)	(18)	(11)

Table 3.2

Some results of the simulation study for homogeneous modified Matérn cluster processes consisting of clusters of diameter D each containing an average of μ points. The percentage results are shown for random R and semi-systematic S sampling. Each result is based on 25 patterns each of 500 points. The estimated standardised bias is listed and the estimated standardised variance is given beneath in parentheses.

corresponding estimated standardised variances are 0.01, 0.01, 0.02 according as $\mu = 2, 4, 5$ when $D = 0.05$. There is a further advantage in using this estimator. If the field worker has some idea of the average number μ of points in each cluster, not an unreasonable assumption in a highly clustered situation, then $B(\underset{\sim}{x}_r, \overline{d_r^2})$ is about $(r/\mu - 1)$ for $r \leq \mu$. In such situations it is therefore possible to approximately correct for bias.

To see how the correction term arises suppose that the clusters are randomly distributed point clusters each containing exactly μ points. Then for $r \leq \mu$, $\underset{\sim}{x}_r$ are the distances from selected points to the nearest cluster and the cluster intensity is λ/μ. Thus the expected squared distance from a selected point to the nearest cluster is $\mu/(\pi\lambda)$. Hence the estimate $rm/(\pi\Sigma x_{ri}^2)$ should be about $r/(\pi\mu/\pi\lambda) = r\lambda/\mu$. In other words, for $r \leq \mu$, $B(\underset{\sim}{x}_r, \overline{d_r^2}) \approx (r/\mu - 1)$. For the recommended estimator $r = 3$ and $(r/\mu - 1) = -0.25$ and -0.4 for $\mu = 4$ and 5. These values are in close agreement with the estimated standardised bias of -0.26 and -0.41 in the highly clustered case $D = 0.05$.

3.4 The heterogeneous case

The analytical result of Matérn (1960, p.81) concerning the variance of an estimator based on systematic sampling suggests that semi-systematic sampling should yield more efficient intensity estimators than random sampling when there is strong local positive correlation in the pattern. Many authors have been concerned about the possible bias introduced under systematic sampling in the presence of periodic variation (for example see Finney, 1947, 1948, 1950). Milne (1959) points out that five conditions must be satisfied before 'centric'

systematic sampling gives rise to a severely biased estimate. The probability of the simultaneous occurrence of these five conditions is so small that he contends that "the risk of periodic variation defeating the 'centric' systematic sample ..... can justifiably be ignored."

In this Section simulation is used to examine the performance of the intensity estimators under random and semi-systematic sampling in the presence of trend. The simplest situation to consider is a general Poisson process in which $\lambda(\underset{\sim}{x})$ is <u>not</u> constant over the region R. In the simulation study R is the unit square, $S = [0.1, 0.9]^2$ and for $\underset{\sim}{x} = (x_1, x_2) \in R$

$$\lambda(\underset{\sim}{x}) \propto \alpha(x_1 - 1/2)^2 + 1/2$$

where $\alpha \in \mathbb{R}_+$ is a parameter which may be varied. The cases $\alpha = 2, 4, 6$ were considered, $\alpha = 0$ corresponding to a homogeneous Poisson process. Realisations of some nonhomogeneous Poisson processes are illustrated in Figure 3.2. The x coordinates of the points in each pattern were generated by acceptance sampling from the distribution with density proportional to $\alpha(x - 1/2)^2 + 1/2$, $x \in [0,1]$, whilst the y coordinates were random numbers generated from a uniform distribution on $[0,1]$.

The estimators based on the distances from selected points or plants to the nearest plant performed best. This is probably due to the fact that the larger distances to other plants are more affected by the underlying trend. On the whole the 'compound' estimators seem to be more reliable than the usual estimators. In nearly all cases considered the use of semi-systematic in place of random sampling led to a decrease in both the estimated absolute bias and the variance of each estimator. The estimator E* is again the most robust. The results of the study for E* are presented in Table 3.3.

(a)

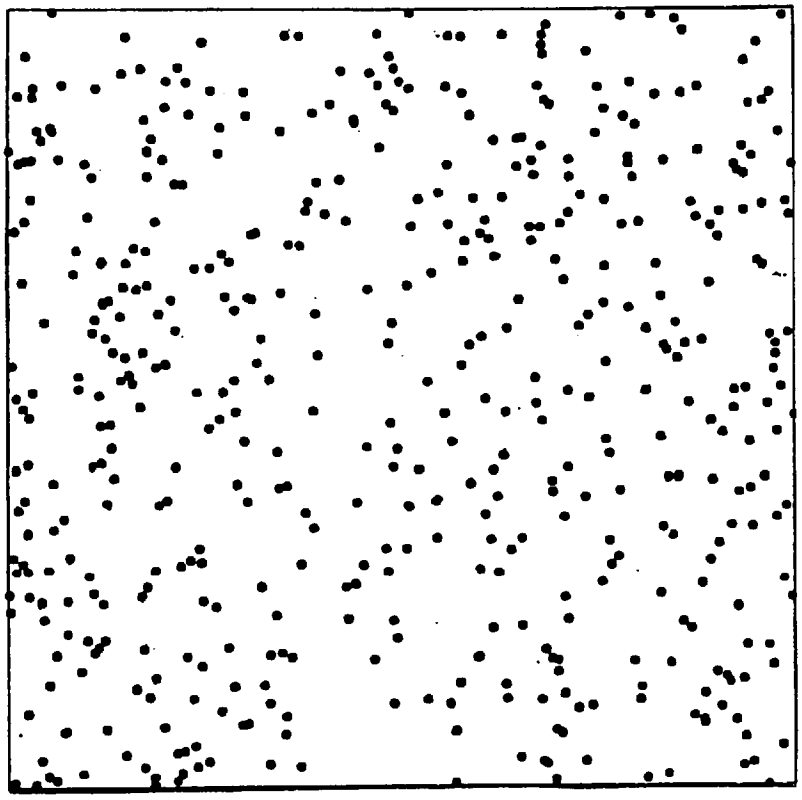

(b)

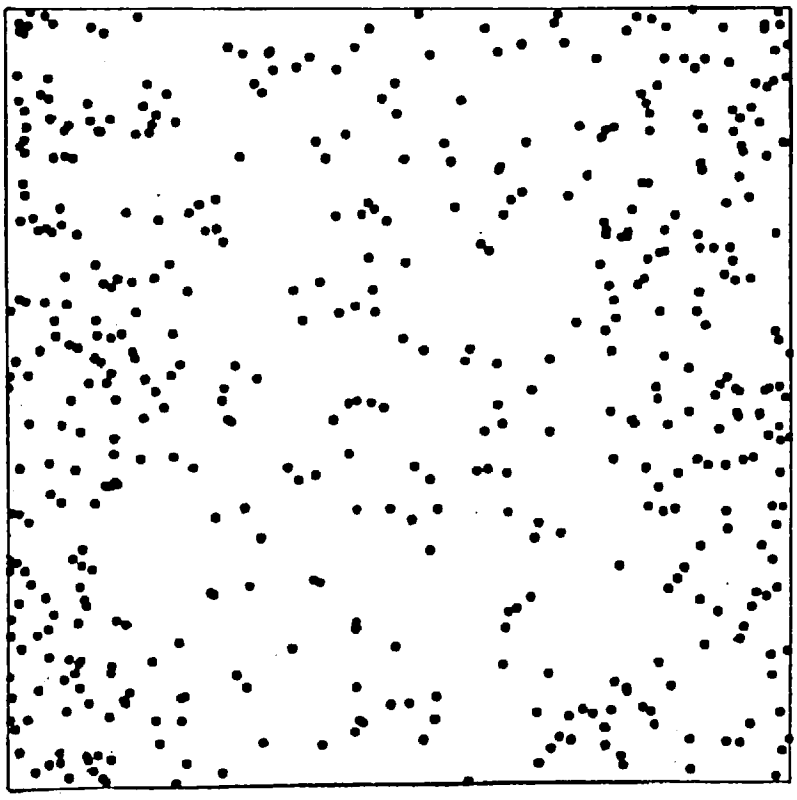

Figure 3.2. Realisations on the unit square R of a general Poisson process with intensity $\lambda(\underset{\sim}{x}) \propto \alpha(x_1 - 1/2)^2 + 1/2$, $\underset{\sim}{x} = (x_1, x_2) \in R$ where (a) $\alpha = 2$ (b) $\alpha = 4$. Each realisation consists of 500 points.

Percentage standardised	$\alpha = 2$		$\alpha = 4$		$\alpha = 6$	
	R	S	R	S	R	S
(i) bias	5	3	3	2	10	4
(ii) variance	5	3	6	5	7	5

Table 3.3

Results for E* of the simulation study for general Poisson processes with intensity $\lambda(\underset{\sim}{x})$, $\propto \alpha(x_1 - 1/2)^2 + 1/2$ for $\underset{\sim}{x} = (x_1, x_2) \in [0,1]^2$. Each result is based on 25 patterns each of 500 points. Both random R and semi-systematic S sampling are considered.

The other heterogeneous processes which were considered are extensions of modified Matérn cluster processes. They are simulated in the same way as these processes except that the cluster centres are now a realisation of a general Poisson process with intensity

$$\lambda(\underset{\sim}{x}) \propto \alpha(x_1 - 1/2)^2 + 1/2 \quad \text{for} \quad \underset{\sim}{x} = (x_1, x_2) \in [0,1]^2.$$

Thus there are three parameters needed to describe such processes: the trend parameter α, the mean number of points per cluster μ and the cluster diameter D. The cases $\alpha = 2$ and 4 were considered. These represent slight and moderate trend respectively. The same combinations of μ and D were examined as in the homogeneous case. Realisations of some heterogeneous cluster processes are illustrated in Figure 3.3. The results of the simulation study for these heterogeneous cluster processes closely parallel those summarised earlier for the homogeneous cluster processes. The only obvious difference is that, as expected in the heterogeneous case, the use of semi-systematic sampling tends to decrease the variance of all the estimators without causing large increases in their absolute biases. Indeed the absolute bias is often reduced as can be seen from Table 3.4 for the estimator E* which is again recommended for all except highly clustered patterns. For these patterns the estimator $3m/(\pi\Sigma x_{3i}^2)$ is again recommended in conjunction with the correction factor given earlier. When D = 0.05 and μ = 4, 5, the estimated standardised biases of this estimator are -0.25, -0.38 for $\alpha = 2$ and -0.30, -0.44 for $\alpha = 4$ compared with the values $(3/\mu - 1) = -0.25, -0.40$.

(a)

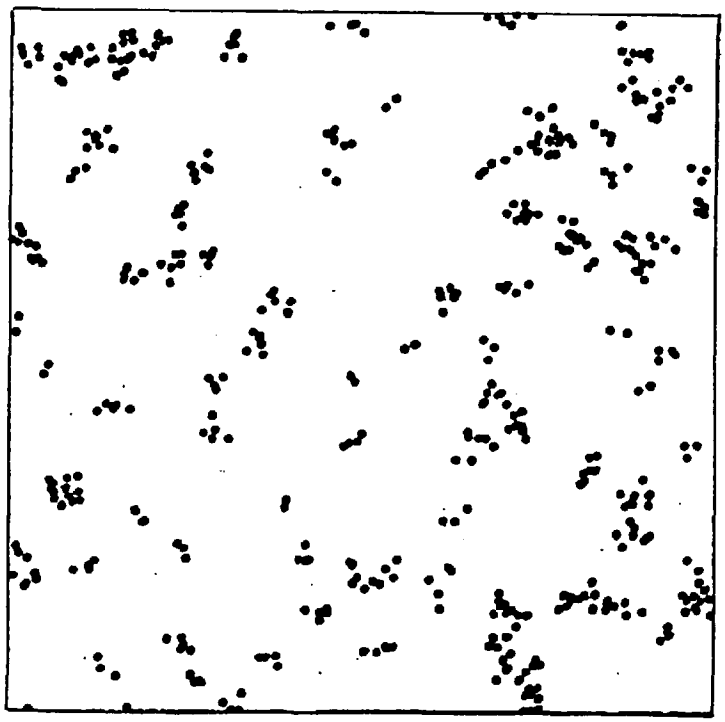

(b)

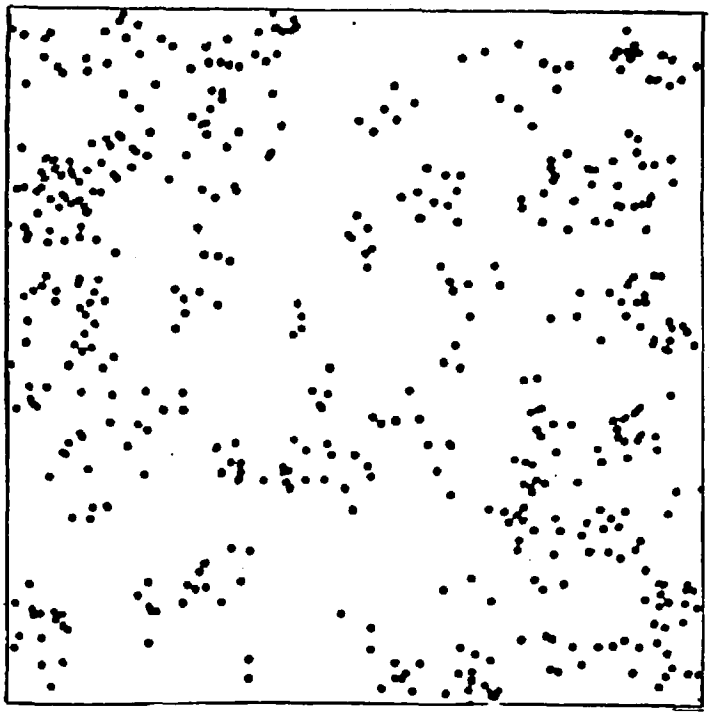

Figure 3.3. Realisations on the unit square R of heterogeneous cluster processes. Each cluster contains 4 points on average and is of diameter D. The cluster centres are a realisation of a Poisson process with intensity $\lambda(x) \propto 4(x_1 - 1/2)^2 + 1/2$, $x = (x_1, x_2) \in R$. (a) $D = 0.05$ (b) $D = 0.1$.

		$\alpha = 2$		$\alpha = 4$	
μ	D	R	S	R	S
2	0.2	7	8	3	3
		(11)	(3)	(13)	(6)
	0.1	-1	1	6	-3
		(9)	(8)	(4)	(3)
4	0.2	-4	-1	-3	0
		(6)	(4)	(14)	(10)
	0.1	7	9	-2	-4
		(17)	(11)	(8)	(6)
5	0.2	-3	1	12	-7
		(12)	(7)	(13)	(5)
	0.1	-13	3	-9	-3
		(11)	(12)	(10)	(11)

Table 3.4

The percentage results for E* of the simulation study for heterogeneous cluster processes in which the cluster centres are a realisation of a general Poisson process with intensity $\lambda(\underset{\sim}{x}) \propto \alpha(x_1 - 1/2)^2 + 1/2$ for $\underset{\sim}{x} = (x_1, x_2) \in [0,1]^2$. The estimated standardised bias is listed and the estimated standardised variance is given beneath in parentheses. Both random R and semi-systematic S sampling are considered. Each result is based on 25 patterns each of 500 points.

3.5 Conclusions

In all except highly clustered situations the 'compound' estimators are certainly more robust than their usual analogues based on either point-plant or plant-plant distance measurements alone. Semi-systematic sampling is recommended in preference to random sampling. In the homogeneous case it is a precaution against over-sampling. As expected in the heterogeneous cases considered, it has the added advantage of usually decreasing the estimated variance of the intensity estimators without seriously increasing their estimated absolute bias. The 'compound' estimators based on the 'T-square' distances $\underset{\sim}{x}_r$, $\underset{\sim}{z}_r$ do not require partial enumeration of the pattern. For the situations considered their performance is either comparable with or better than that of the analogous estimators formed from $\underset{\sim}{x}_r$ and $\underset{\sim}{y}_r$. In general there is no advantage in using any 'compound' estimators other than those based on the distances from selected points and plants to the nearest plant ($r = 1$).

It is recommended that the 'compound' estimator E* be used to estimate the average intensities of the processes underlying all except highly clustered patterns. The performance of this estimator is in all cases comparable with or better than that of $1/\gamma_T^*$ where γ_T^* is the estimator of the inverse of the intensity recommended by Diggle (1975, 1977). The improvement is possibly due to the fact that γ_T^* is a function of $\Sigma x_{1i}^2/m$ and $\Sigma z_{1i}^2/m$ whilst E* is based on $(\Sigma x_{1i}/m)^2$ and $(\Sigma z_{1i}/m)^2$, the latter being less affected by an unusually large observation. Use of the estimator $3m/(\pi\Sigma x_{3i}^2)$ in conjunction with a bias correction factor is recommended for visually highly clustered patterns.

The results of this simulation study support and extend the work of Diggle (1975, 1977). It should be noted that neither the estimator suggested by Batcheler and Hodder (1975) nor that introduced by Morisita (1957) are particularly robust to the types of changes in the underlying distributions considered here.

CHAPTER 4: A GENERALISATION OF $\hat{K}$ TO θ-STATIONARY SIMPLE SECOND ORDER POINT PROCESSES.

4.1 Introduction

The positions of three types of sporophores which grew about a single birch tree in the years 1975, 1976 and 1977 (Ford, Pelham and Mason, 1980) are illustrated in Figures 4.1(a), (b) and (c). If the sporophores are considered as points then these Figures can be interpreted as maps of part of the realisations of spatial point processes in some region of interest. A quick glance reveals that the intensity of each underlying process changed with the radial distance from the tree. Therefore these processes cannot be considered to be homogeneous.

The tree is an obvious reference point for the sporophore patterns and will hereafter be taken to be the mathematical origin. Other examples of patterns with an obvious origin might include the locations of diseased trees in a forest in successive years after the introduction of the disease at some known (or unknown) site and the positions of fortifications in the countryside near the site of an historically important city. In the former the origin would be the initial point of infection and, in the latter, the position of the old city.

Virtually all existing methods of analysing maps of spatial patterns test for departures from null hypotheses involving processes which are both homogeneous and isotropic or, equivalently, stationary under the group of rigid motions. Diggle (1979) and Ripley (1979a) compare some of these methods. In most cases the null hypothesis is that the observed pattern is part of an outcome of a Poisson or

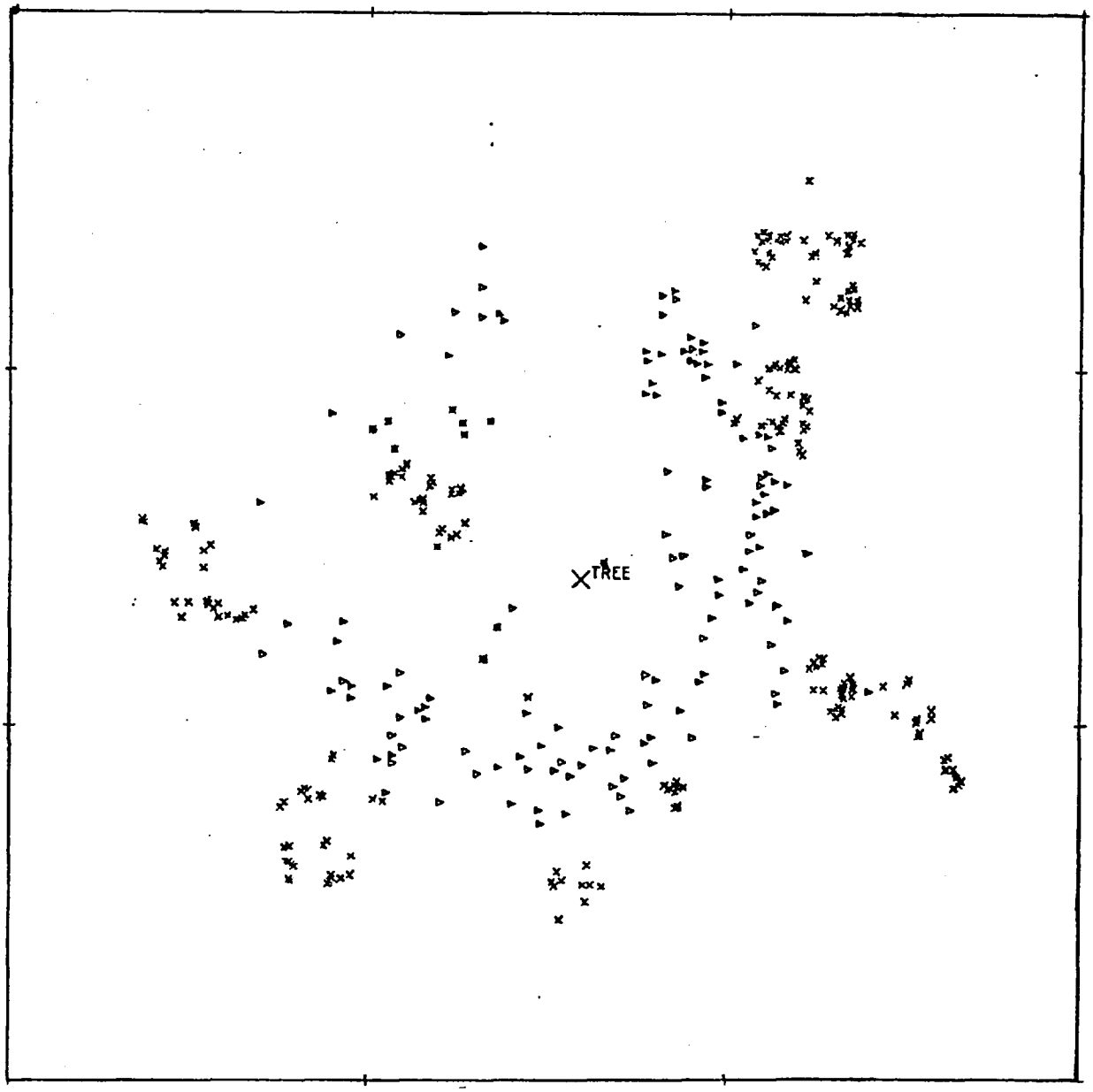

Figure 4.1(a)

The pattern of sporophores growing about the birch tree in 1975.

▷ Hebeloma spp., × Laccaria laccata, * Lactarius pubescens.

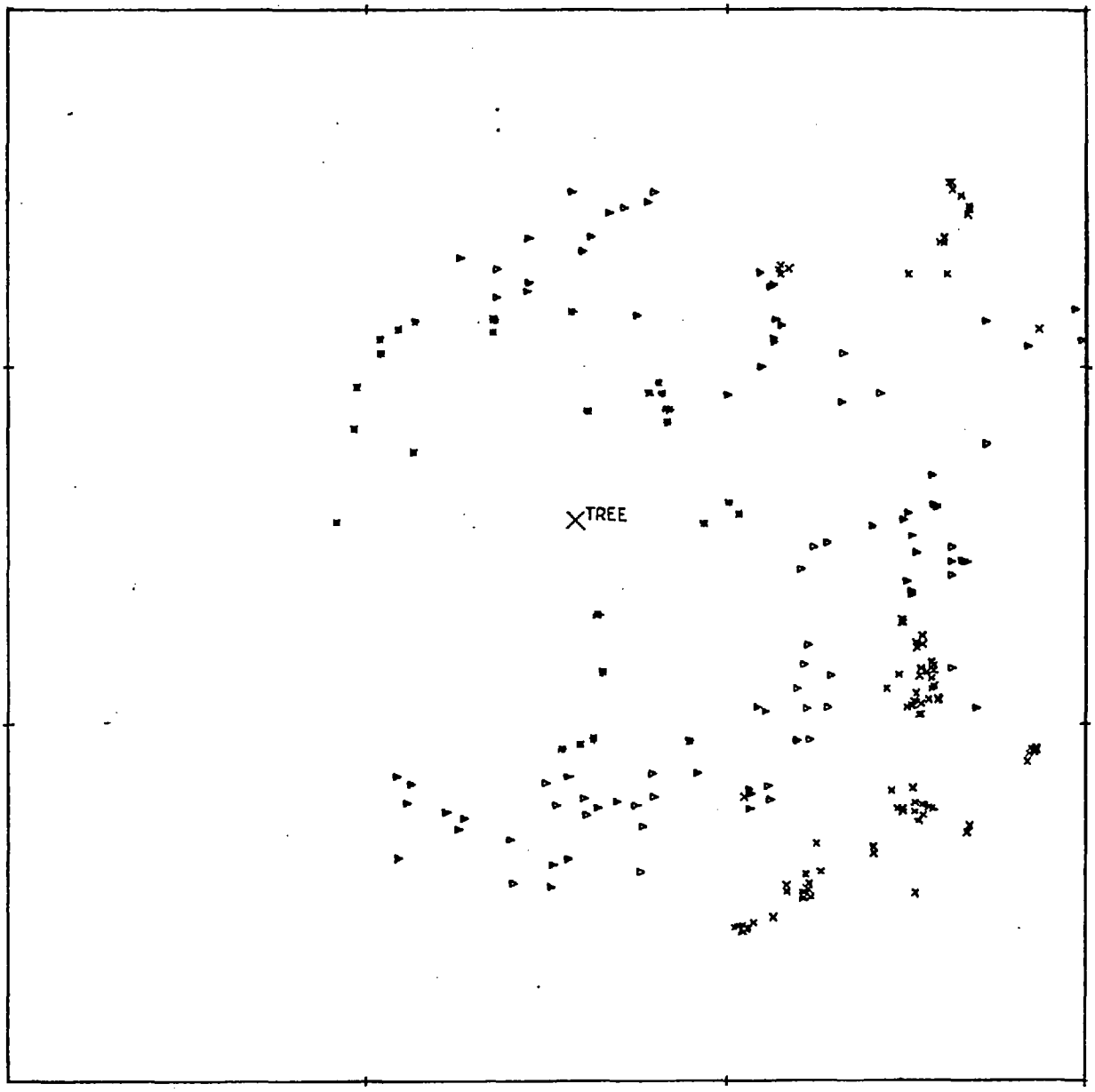

Figure 4.1(b)

The pattern of sporophores growing about the birch tree in 1976.

▷ Hebeloma spp., × Laccaria laccata, * Lactarius pubescens

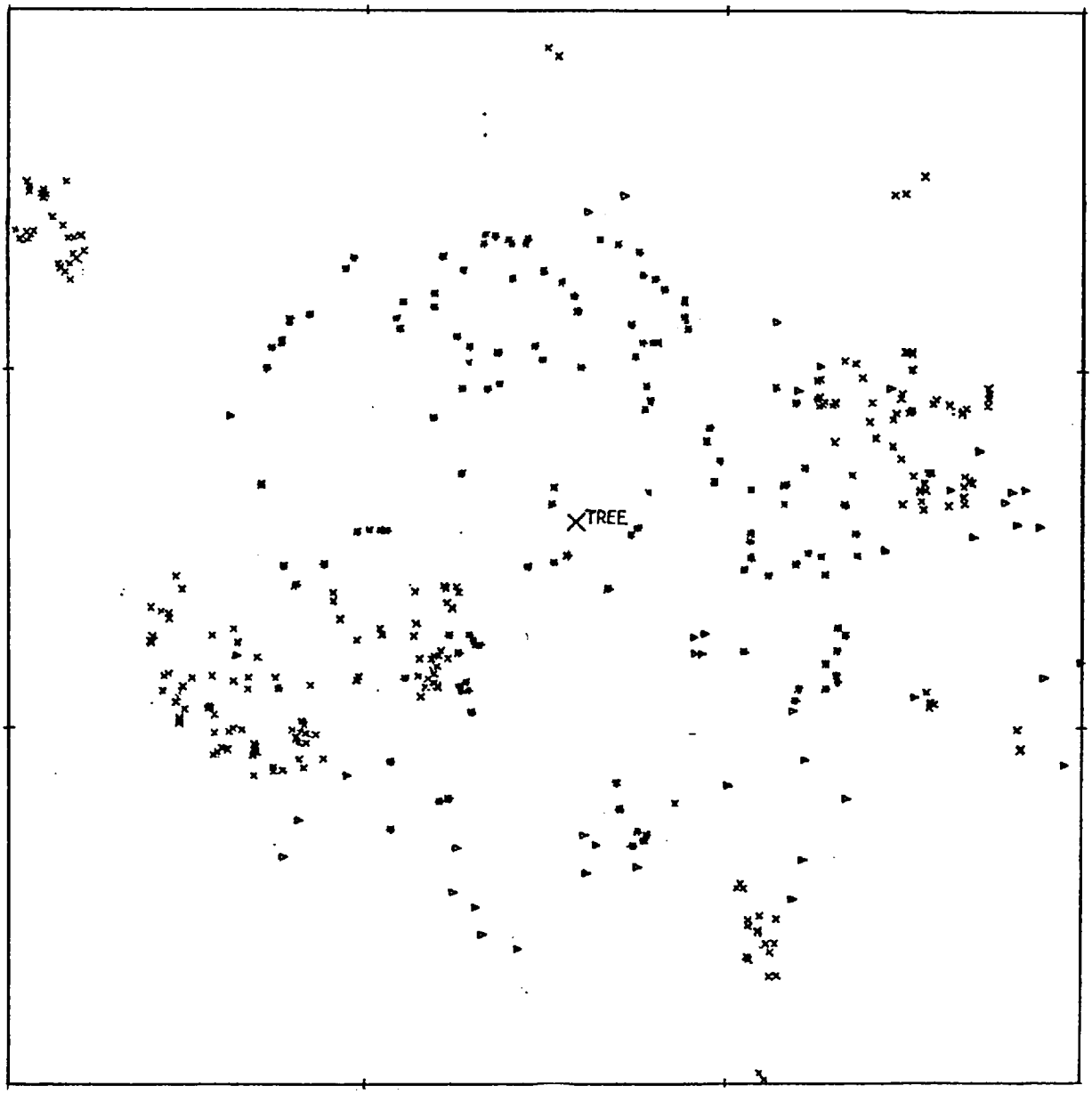

Figure 4.1(c)

The pattern of sporophores growing about the birch tree in 1977.

▷ Hebeloma spp., × Laccaria laccata, * Lactarius pubescens.

binomial process. There is very little published work on what may be done when the observed pattern is obviously not part of a realisation of a process that is stationary under the group of rigid motions.

One possibility is to partition the region of interest into subregions within which it is reasonable to assume isotropy and homogeneity of the underlying process. Each subregion is then analysed in turn and the results compared in some way. It is visually obvious, however, that no partition of the sporophore patterns into subregions each containing a reasonable number of sporophores of each type, say more than twenty, is likely to produce subregions in which this property may be assumed. Even if such a partition were possible, an analysis within each subregion would not make use of all the information concerning the spatial relationships between the subregions. Some alternative approach is required.

As a first approximation it seems reasonable to assume that the underlying process associated with each sporophore type in each year is stationary under rotations about the origin. A less restrictive approximation made later involves the concept of θ-stationarity which describes a similar assumption about the underlying process only in some sector of interest. This Chapter contains a theoretical development of generalisations of Ripley's $\hat{K}$ method which are applicable in such situations where there is an obvious point of reference or origin. One of these new methods is used to analyse the sporophore patterns in Chapter 6 after their marginal radial and angular distributions have been estimated in Chapter 5.

4.2 θ-stationary simple second order point processes

Ripley (1976a) has defined point processes, in particular simple second order point processes, on a topological space X. Briefly, each realisation of a simple second order point process consists of a countable set of distinct points from X. If the random variable Z(A) denotes the number of points in each Borel subset A of X, then for a second order point process $E\{Z(A)\}$ and $E[\{Z(A)\}^2]$ are finite whenever A is bounded.

The first and second moment structures of a point process Z on X are described by the first and second moment measures, respectively

$$\mu^1(A_1) = E\{Z(A_1)\}$$

and

$$\mu^2(A_1 \times A_2) = E\{Z(A_1)Z(A_2)\}$$

where $A_1, A_2 \in C$, the class of bounded measurable sets in X. If G is the group of rotations about the origin then Z will be said to be isotropic if its distribution is invariant under G. For a simple point process it is only necessary to check invariance for the finite dimensional hitting probabilities for sets from, say, the class of open discs (Ripley, 1976b). Unless otherwise stated it will be assumed that Z is an isotropic simple second order point process on X.

Ripley (1976c) has shown that, under certain conditions, if T is the quotient space of the equivalence relation defined by G on $Y = X^2$ and if $p : Y \to T$ is the quotient map, then for all Borel sets $A \subset Y$

$$\mu^2(A) = \int_T \nu_t(A)dK(t) \qquad (4.1)$$

where ν_t is a unique invariant Radon measure on Y, concentrated on $Y_t = p^{-1}(\{t\})$, and K is a unique σ-finite measure on T. It follows that the first two moment measures may be summarised by $\lambda(\underset{\sim}{x})$, the intensity of the process Z at the point $\underset{\sim}{x}$, and K, the reduced second moment measure.

In particular, for an isotropic process on $X = \mathbb{R}^2$ any $(\underset{\sim}{x},\underset{\sim}{y}) \in Y$ belongs to some equivalence class which may be characterised by $t = (|\underset{\sim}{x}|, |\underset{\sim}{y}|, \xi)$ where $\xi = \cos^{-1}\{\underset{\sim}{x}.\underset{\sim}{y}/(|\underset{\sim}{x}||\underset{\sim}{y}|)\}$. For example, Figure 4.2(a) illustrates two pairs $(\underset{\sim}{x}_1,\underset{\sim}{y}_1)$ and $(\underset{\sim}{x}_2,\underset{\sim}{y}_2)$ in the same equivalence class. In this case $\lambda(\underset{\sim}{x})$ depends on $\underset{\sim}{x}$ only through $|\underset{\sim}{x}|$. For notational convenience $\lambda(\underset{\sim}{x})$ will be written $\lambda(|\underset{\sim}{x}|)$ with the obvious interpretation.

With the above characterisation of T for an isotropic process on $X = \mathbb{R}^2$,

$$K : \mathbb{R}^+ \times \mathbb{R}^+ \times [0,\pi] \to \mathbb{R}^+ .$$

The moment decomposition equation (4.1) may then be written

$$\begin{aligned} \mu^2(A_1 \times A_2) &= E\{Z(A_1)Z(A_2)\} \\ &= \int_{A_1 \cap A_2} \lambda(|\underset{\sim}{x}|)\, d\nu(\underset{\sim}{x}) \\ &+ \int_{\mathbb{R}^+ \times \mathbb{R}^+ \times [0,\pi]} \nu_{(r,s,\theta)}(A_1 \times A_2)\, dK(r,s,\theta) \end{aligned} \qquad (4.2)$$

where ν is Lebesgue measure on $\mathbb{R}^2$ and $\nu_{(r,s,\theta)}$ can be shown to be proportional to the invariant Radon measure on $Y_{(r,s,\theta)}$.

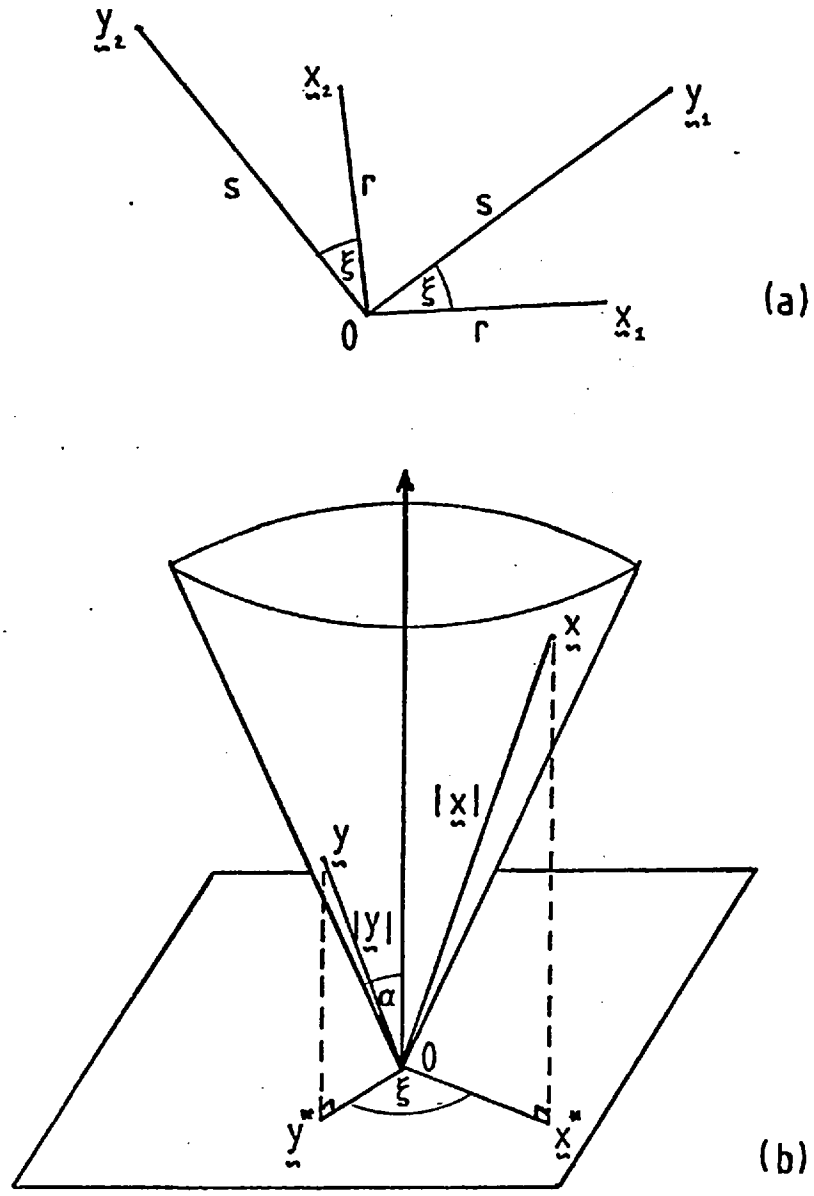

Figure 4.2

(a) Points $(\underset{\sim}{x}_1,\underset{\sim}{y}_1)$, $(\underset{\sim}{x}_2,\underset{\sim}{y}_2) \in Y = \mathbb{R}^2 \times \mathbb{R}^2$ in the same equivalence class characterised by $t = (r,s,\xi)$.

(b) A point $(\underset{\sim}{x},\underset{\sim}{y}) \in Y = X^2$ where X is the surface of the cone with half-angle α. This point is in the equivalence class characterised by $t = (|\underset{\sim}{x}|, |\underset{\sim}{y}|, \xi)$.

The expressions in equation (4.2) have the following intuitive interpretations:

$\mu^2(A_1 \times A_2)$ = expected number of ordered pairs $(\underset{\sim}{x},\underset{\sim}{y})$ of points, one point from A_1 and the other from A_2

= (a) + (b)

where

(a) = expected number of ordered 'pairs' $(\underset{\sim}{x},\underset{\sim}{x})$ of points, the same point from A_1 and A_2

$$= \int_{A_1 \cap A_2} \lambda(|\underset{\sim}{x}|)d\nu(\underset{\sim}{x})$$

and

(b) = expected number of ordered pairs $(\underset{\sim}{x},\underset{\sim}{y})$ of distinct points, one point from A_1 and the other from A_2

$$= \int_{\mathbb{R}^+ \times \mathbb{R}^+ \times [0,\pi]} \nu_{(r,s,\theta)}(A_1 \times A_2)dK(r,s,\theta)$$

where

$\nu_{(r,s,\theta)}(A_1 \times A_2)$ = probability that a pair of points in the equivalence class characterised by (r,s,θ) lies in $(A_1 \times A_2)$

and

$K(r,s,\theta)$ = expected number of ordered pairs $(\underset{\sim}{x},\underset{\sim}{y})$ of distinct points such that $|\underset{\sim}{x}| \leq r$, $|\underset{\sim}{y}| \leq s$ and $\cos^{-1}\{\underset{\sim}{x}.\underset{\sim}{y}/(|\underset{\sim}{x}||\underset{\sim}{y}|)\} \leq \theta$.

Precisely the same moment decomposition equation (4.2) will arise if the process Z is defined for some fixed $\alpha \in (0,\pi/2]$ on the two-dimensional manifold

$$X = \{\underset{\sim}{x} : \underset{\sim}{x} = (x_1,x_2,x_3) \in \mathbb{R}^3,\ x_1^2 + x_2^2 = (x_3 \tan \alpha)^2\}.$$

Clearly X is the surface of a cone with half-angle α. If $(\underset{\sim}{x},\underset{\sim}{y}) \in Y$ lies in the equivalence class corresponding to $t \in T$, then the required characterisation is $t = (|\underset{\sim}{x}|, |\underset{\sim}{y}|, \xi)$ where this time

$$\xi = \cos^{-1}\{\underset{\sim}{x}^*.\underset{\sim}{y}^*/(|\underset{\sim}{x}^*||\underset{\sim}{y}^*|)\} \quad \text{and} \quad \underset{\sim}{x}^* = (x_1,x_2,0), \quad \underset{\sim}{y}^* = (y_1,y_2,0)$$

are the orthogonal projections of $\underset{\sim}{x}$, $\underset{\sim}{y}$ onto the plane perpendicular to the axis of the cone and passing through the origin. Figure 4.2(b) illustrates these relationships. It follows that the earlier case $X = \mathbb{R}^2$ arises here as the particular case $\alpha = \pi/2$.

If Z is a simple second order point process on $\mathbb{R}^2$ and $\underset{\sim}{x} \in \mathbb{R}^2$ is written (r,θ) in polar coordinates, let Z_θ denote the restriction of the Z process to the 'sector'

$$S = \{\underset{\sim}{x} : r \in \mathbb{R}^+, \ \theta \in H\}$$

where either

$$H = [\theta_1, \theta_2] \quad , \quad 0 \leq \theta_1 < \theta_2 < 2\pi,$$

or

$$H = [\theta_1, 2\pi) \cup [0,\theta_2], \quad 0 \leq \theta_2 < \theta_1 < 2\pi.$$

If the process Z_θ is stationary under rotations on the cone formed by identifying the edges of the 'sector' S, then the process Z will be said to be <u>θ-stationary</u> on S. The sector S will be called a <u>θ-stationary sector</u> of Z. Toroidal edge corrections are used as boundary conditions for homogeneous, isotropic processes defined on a bounded set (for example see Ripley, 1977, 1979a). The concept of θ-stationarity performs the same function for isotropic processes defined on a 'sector'.

Any isotropic process on $\mathbb{R}^2$ is clearly θ-stationary on any 'sector' S but θ-stationarity on some 'sector' S does not imply isotropy on $\mathbb{R}^2$ unless $S = \mathbb{R}^2$. For example, if Z is a Poisson process on $\mathbb{R}^2$ with varying intensity

$$\lambda(\underset{\sim}{x}) = \begin{cases} \lambda_1 > 0 , & \underset{\sim}{x} \in S \\ \lambda_2 > 0 , & \underset{\sim}{x} \in S^c \end{cases}$$

where $\lambda_1 \neq \lambda_2$, then Z is not isotropic but is θ-stationary on both S and S^c. Figure 4.3 illustrates a realisation of such a process.

Hereafter 'small' objects such as sporophores will be represented by points. A <u>model</u> will be a family of processes which are restrictions of simple second order θ-stationary point processes to some θ-stationary 'sector'. It will be assumed that for a realisation of a spatial pattern it is possible to observe all points in some known set E, the <u>sampling window</u>. Although it is not necessary for much of the theory of this Chapter, it will also be assumed that $E = \{\underset{\sim}{x} : r \leq r_0, \theta \in H_0\}$ for some $r_0 < \infty$, $H_0 \subset H$; that is E is a sector lying inside some θ-stationary 'sector' and so contains the origin.

The cumulative distribution function K of the σ-finite measure on T is used in preference to the corresponding density for the reasons cited by Ripley (1977). In particular any estimate of this density would have to be smoothed. This would require a subjective choice of the amount of smoothing for a function of several variables.

It is possible to consider the analogue of Ripley's function p(t). For an isotropic process this is given by

$$p(r,t) = \Pr\{Z(b(\underset{\sim}{x},t)) > 0 \;\big|\; |\underset{\sim}{x}| = r\}$$

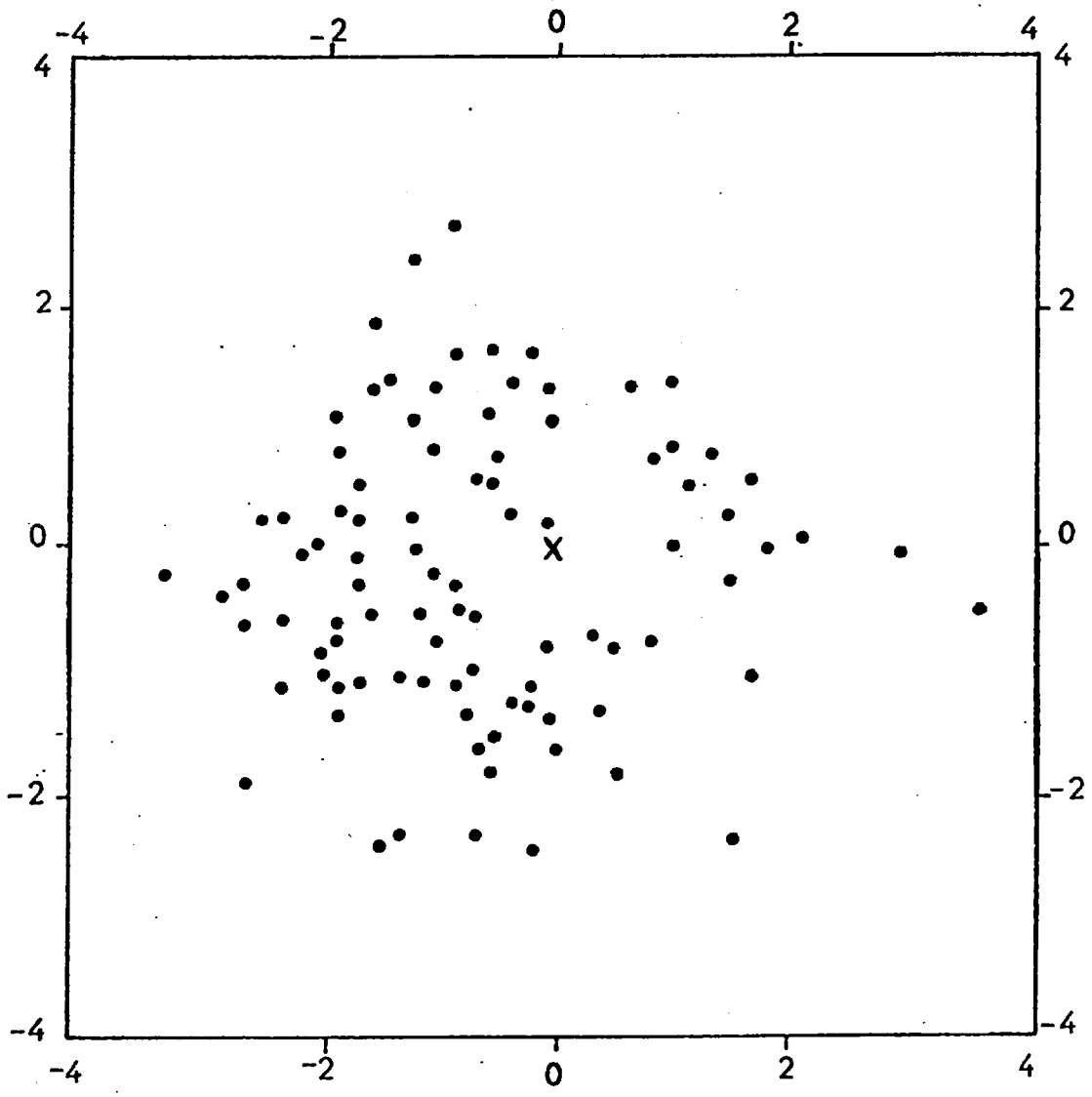

Figure 4.3

A realisation consisting of 100 points from a general Poisson process. The process is θ-stationary on the left and right half-planes but is not isotropic. The intensity at a specified radial distance is three times larger on the left half-plane than on the right. The origin is marked X.

where

$$b(\underset{\sim}{x},t) = \{\underset{\sim}{y} : |\underset{\sim}{x} - \underset{\sim}{y}| < t\}$$

for any $\underset{\sim}{x} \in \mathbb{R}^2$ and $t > 0$. This function is the 'first order' part of the description of an isotropic process in terms of the hitting distribution for all finite collections of open discs. Unlike $p(t)$ which was introduced to detect heterogeneity, $p(r,t)$ can have no such obvious use due to the admissible variation in the intensity. The functions $p(t)$ and $p(r,t)$ provide information on only the distribution of the distance from a randomly chosen position to the nearest point. In many applications the estimate of $p(t)$ merely provides further evidence supporting the conclusions reached on the basis of the estimate of $K(t)$. It is reasonable to expect that this would also be the case with $p(r,t)$ and $K(r,s,\theta)$. For these reasons it was decided to concentrate attention on $K(r,s,\theta)$.

4.3 Some models

For convenience the models described in this Section will be families of isotropic processes on $\mathbb{R}^2$. Isotropy ensures that the intensity at the point $\underset{\sim}{x} = (r,\theta)$ is given by $\lambda(\underset{\sim}{x}) = \lambda(r)$. In all cases analogous models consisting of θ-stationary processes can be formed simply by considering the restrictions of isotropic processes to θ-stationary sectors and using appropriate boundary conditions to eliminate edge effects.

The Poisson model is the simplest to be considered. It is comprised of the family of isotropic Poisson processes with variable radial intensity $\lambda(r)$. Figure 4.4(a) illustrates a realisation of such a process. It is clear that for such processes

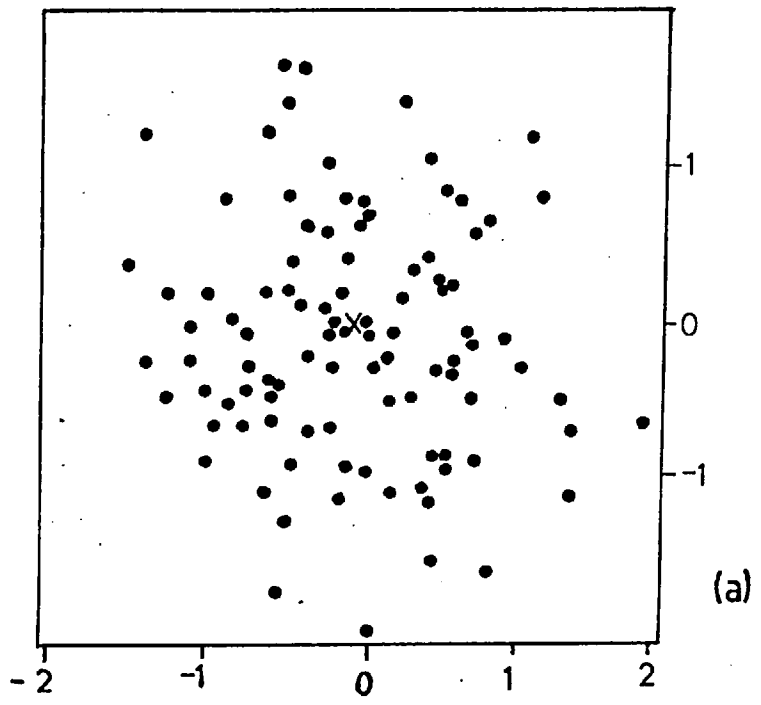

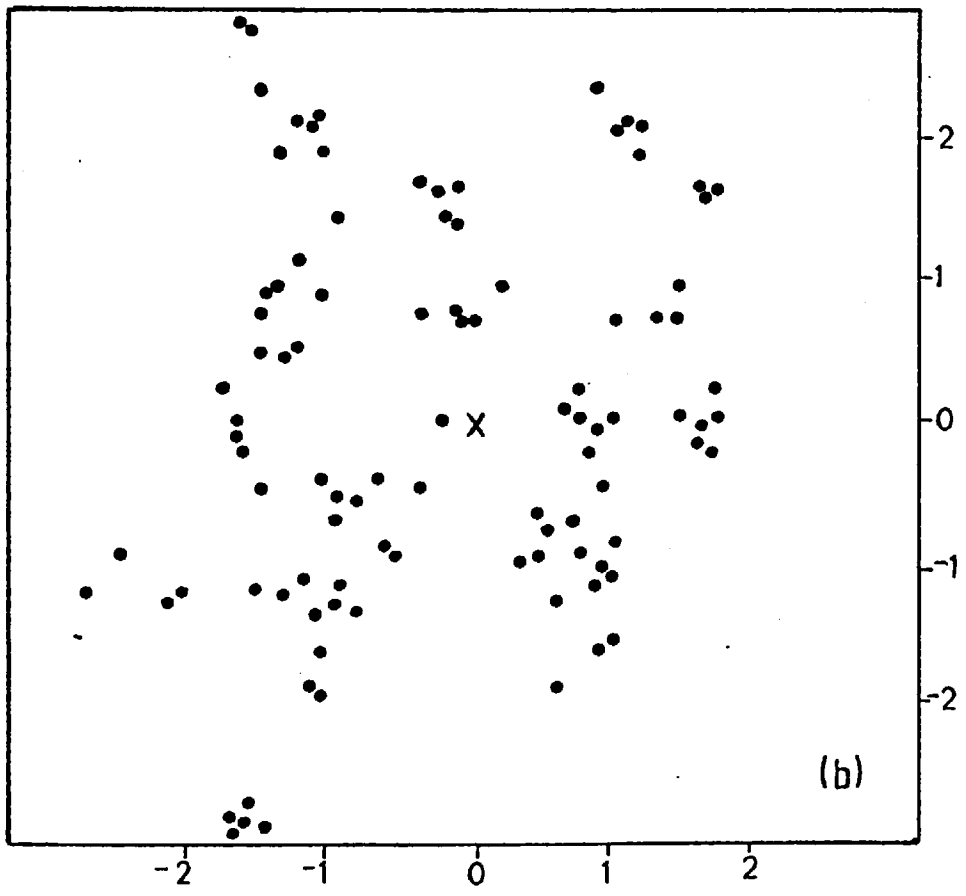

Figure 4.4

(a) A realisation consisting of 100 points from an isotropic Poisson process with radial intensity $\lambda(r) \propto \exp(-r^2)$.

(b) A realisation consisting of 100 points from a simple cluster process. The mean number of points per cluster $\mu = 4$ and the cluster diameter $D = 0.8$. The origin is marked X.

$$K(r,s,\theta) = \int_0^r \lambda(x)2\pi x \int_{-\theta}^{\theta} \int_0^s \lambda(y)y \, dy \, d\theta \, dx$$

$$= 4\pi\theta \int_0^r \lambda(x)x \, dx \int_0^s \lambda(y)y \, dy.$$

This function depends on the intensity which is usually unknown. It might therefore be more convenient to consider

$$K^*(r,s,\theta) = K(r,s,\theta)/\{\text{av } \lambda(r). \text{ av } \lambda(s)\}$$

where

$$\text{av } \lambda(r) = \int_0^r \lambda(x)2\pi x \, dx/(\pi r^2)$$

is the mean intensity inside the circle of radius r. For a Poisson process

$$K^*(r,s,\theta) = \pi\theta r^2 s^2$$

which is independent of $\lambda(r)$.

In Section 4.5 it is shown that the function

$K_1(r,t)$ = expected number of ordered pairs $(\underset{\sim}{x},\underset{\sim}{y})$ of distinct points such that $|\underset{\sim}{x}| \leq r$, $|\underset{\sim}{x} - \underset{\sim}{y}| \leq t$

is even more useful than K^* for reasons of parsimony and ease of graphical representation. For an isotropic Poisson process

$$K_1(r,t) = \int_0^r \lambda(x_1)2\pi x_1 \int_{b((x_1,0),t)} \lambda(|\underset{\sim}{y}|)d\nu(\underset{\sim}{y})dx_1$$

where ν is Lebesgue measure on $\mathbb{R}^2$ and $b(\underset{\sim}{x},t) = \{\underset{\sim}{y} : |\underset{\sim}{y}-\underset{\sim}{x}| \leq t\}$. Provided that $\lambda(\underset{\sim}{y}) \approx \lambda(\underset{\sim}{x})$ for $|\underset{\sim}{x} - \underset{\sim}{y}| \leq t$, a condition which should be satisfied for small values of t by the smoothly varying intensity functions usually met in practice, it follows that for an isotropic Poisson process

$$K_1(r,t) \approx \int_0^r \lambda(x)2\pi x\pi t^2\lambda(x)dx$$

$$= 2\pi^2t^2 \int_0^r x\lambda^2(x)dx.$$

Unlike K or K^*, K_1 does not completely specify the second moment measure. However, if $\lambda(\underset{\sim}{y}) \approx \lambda(\underset{\sim}{x})$ for $|\underset{\sim}{x}-\underset{\sim}{y}| \leq t$, it seems reasonable to expect that K_1 will contain much of the information about the second moment structure of a process in which there are no substantial long range interactions between points. This is confirmed by the results reported in the following Sections.

For any isotropic process

$$K(r,s,\theta) = \int_0^r \lambda(x_1)2\pi x_1 \int_{c(x_1,s,\theta)} \lambda(\underset{\sim}{y}|x_1)d\nu(\underset{\sim}{y})dx_1$$

where

$$c(x_1,s,\theta) = \{\underset{\sim}{y} : \underset{\sim}{y} = (y_1,y_2) \in \mathbb{R}^2,\ |\underset{\sim}{y}| \leq s,\ \cos^{-1}(y_1/|\underset{\sim}{y}|) \leq \theta\}$$

and

$\lambda(\underset{\sim}{y}|x_1)$ = the conditional intensity at $\underset{\sim}{y}$ given there is a point at $(x_1,0)$.

In the same way

$$K_1(r,t) = \int_0^r \lambda(x_1) 2\pi x_1 \int_{b((x_1,0),t)} \lambda(\underset{\sim}{y}|x_1) d\nu(\underset{\sim}{y}) dx_1 .$$

For an isotropic Poisson process

$$\lambda(\underset{\sim}{y}|x_1) = \lambda(\underset{\sim}{y}) = \lambda(|\underset{\sim}{y}|).$$

A process will be said to be <u>clustered</u> at the radial distance x_1 if

$$\lambda(\underset{\sim}{y}|x_1) > \lambda(|\underset{\sim}{y}|) \quad , \quad d((x_1,0),\underset{\sim}{y}) < \delta,$$

and to be <u>regular</u> at the radial distance x_1 if

$$\lambda(\underset{\sim}{y}|x_1) < \lambda(|\underset{\sim}{y}|) \quad , \quad d((x_1,0),\underset{\sim}{y}) < \delta,$$

where $d(\ ,\ )$ is the distance function between two points and δ is some positive constant. If a process is clustered for some interval of radial distances, it follows that for some values of (r,s,θ) and (r,t)

$$K^*(r,s,\theta) > \pi\theta r^2 s^2$$

and that

$$K_1(r,t) > 2\pi^2 t^2 \int_0^r x\lambda^2(x)dx.$$

The expressions on the right hand sides of these inequalities are just the exact and approximate values of K^* and K_1 respectively under a Poisson hypothesis. Processes which are regular over some interval of radial distances obviously satisfy the above with the inequality reversed.

These inequalities suggest that estimates of K^* or K_1 might be used to test the fit of a model in a similar manner to that proposed by Ripley (1977) for homogeneous isotropic processes. This idea is pursued further in Section 4.5. Many of the clustered and regular processes described in Ripley (1977) have obvious isotropic analogues with variable radial intensity. Some of these are described below. All of the processes mentioned are either clustered or regular over the whole range of radial distances. It would of course be possible to construct a process which was, say, clustered for certain intervals of radial distances and regular for distances outside these intervals.

Two clustered processes are considered. The first is an isotropic generalisation of one of Matérn's cluster processes (Matérn, 1971) and will be called a simple cluster process. This process consists of an isotropic Poisson parent process on $\mathbb{R}^2$ with intensity $\lambda_0(\underset{\sim}{x}) = \lambda_0(|\underset{\sim}{x}|)$ and a daughter process ϕ. The process ϕ is the restriction of another independent Poisson process with constant intensity λ_1 to a disc of diameter D. The parent process is sampled and each point is taken as the centre of a disc associated with an independent copy of ϕ. The simple cluster process is made up of both the parent process and the superimposed daughter processes. It is obviously an isotropic process and the mean number of points per cluster is $\mu = (\lambda_1 \pi D^2/4 + 1)$. Figure 4.4(b) illustrates an outcome of such a process.

It is possible to find an expression for $\lambda(r)$, the variable radial intensity of a simple cluster process. This function is composed of two terms: the first is a contribution from the parents, $\lambda_0(r)$, and the second is a contribution from the offspring. In nearly all cases one is interested in radial distances $r \geq D/2 = R$. Here the offspring

contribution is

$$2\lambda_1 \int_{r-R}^{r+R} \theta(x) x \lambda_0(x) dx \qquad (4.3)$$

where

$$\theta(x) = \sin^{-1}[\{R^2 - (r^2 + R^2 - x^2)/(4r^2)\}^{\frac{1}{2}}/x].$$

To see how this term arises, consider Figure 4.5. A daughter at P can be the offspring of a parent located anywhere inside the circle of radius R centred on P. The contribution from offspring of parents at radial distance x is, with the notation on the Figure,

$$\lambda_1 \, 2\theta(x) x \lambda_0(x)$$

and this must be integrated over the possible values of x, $r-R \leq x \leq r+R$, to give (4.3). Thus, for $r \geq D/2$,

$$\lambda(r) = \lambda_0(r) + 2\lambda_1 \int_{r-R}^{r+R} \theta(x) x \lambda_0(x) dx.$$

The expression for $\theta(x)$ follows from the two equations

$$x^2 = r^2 + R^2 - 2r\,R\cos\phi(x)$$

and

$$\sin\phi(x) = x \sin\{\theta(x)\}/R.$$

The functions K* and K_1 are essentially determined by the conditional intensity $\lambda(\underset{\sim}{y}|x_1)$, a complicated expression even for a simple cluster process. However, it is clear that this function must

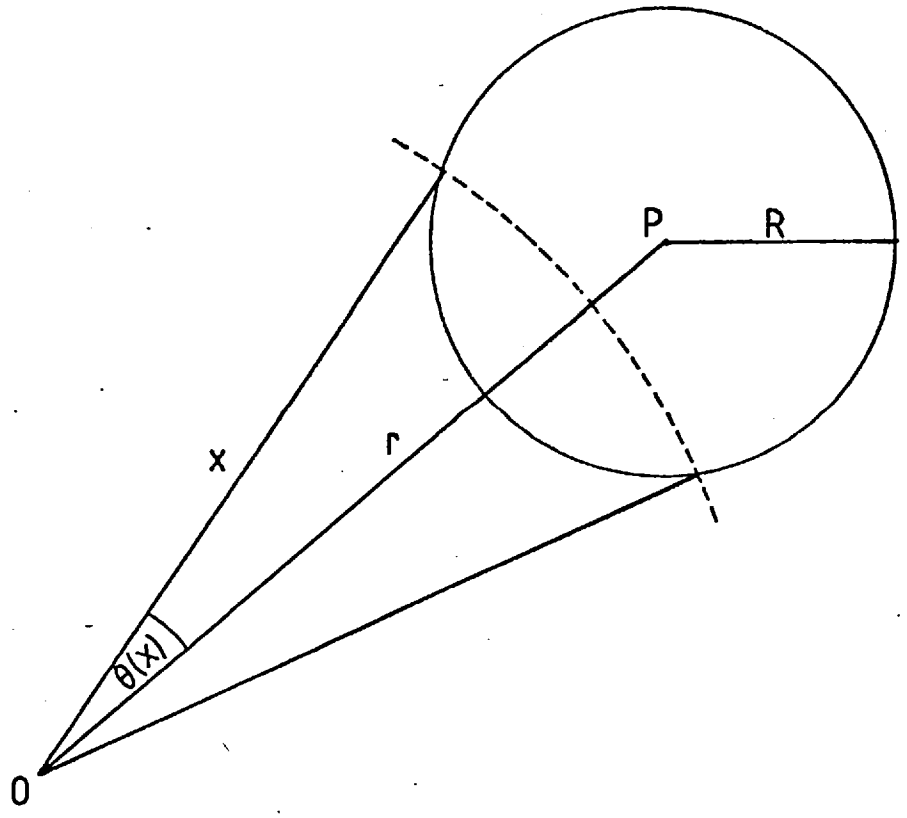

Figure 4.5

The relationships between x, r, R and $\theta(x)$ required to find the offspring contribution to the radial intensity of a simple cluster process.

be the sum of two terms, one arising when the two points are from different clusters and the other when they are in the same cluster. The first term is simply $\lambda(|\underset{\sim}{y}|)$. The second must be positive if $|\underset{\sim}{x}-\underset{\sim}{y}| \leq D$ and zero when $|\underset{\sim}{x}-\underset{\sim}{y}| > D$ where $\underset{\sim}{x} = (x_1, 0)$. Thus a simple cluster process is indeed clustered according to the definition given earlier.

The other clustered process to be considered will be called a double cluster process. It consists of an isotropic Poisson parent process on $\mathbb{R}^2$ with intensity $\lambda_0(\underset{\sim}{x}) = \lambda_0(|\underset{\sim}{x}|)$, a process ϕ_L and a process ϕ_S. The Poisson process, ϕ_L and ϕ_S are jointly independent. The processes ϕ_S and ϕ_L are the restrictions of Poisson processes with constant intensities λ_S and λ_L to discs of diameter D_L and D_S respectively. The parent process is sampled and each point is taken as the centre of a disc of diameter D_L associated with an independent copy of ϕ_L. The ϕ_L processes are then sampled and each resulting point is taken as the centre of a disc of diameter D_S associated with an independent copy of ϕ_S. The double cluster process consists of only those points arising from the ϕ_S processes. Figure 4.6(a) illustrates a realisation of such a process. It is clearly made up of a number of large clusters each of which is comprised of smaller clusters of points. The average number of small clusters within each large cluster is $\mu_S = \lambda_L \pi D_L^2/4$ and the small clusters each contain a mean number $\lambda_S \pi D_S^2/4$ of points. The conditional and unconditional intensity functions for a double cluster process are complicated expressions which have not been evaluated analytically. Similar considerations to those used in the case of a simple cluster process reveal that the double cluster process must also be clustered in the sense defined earlier.

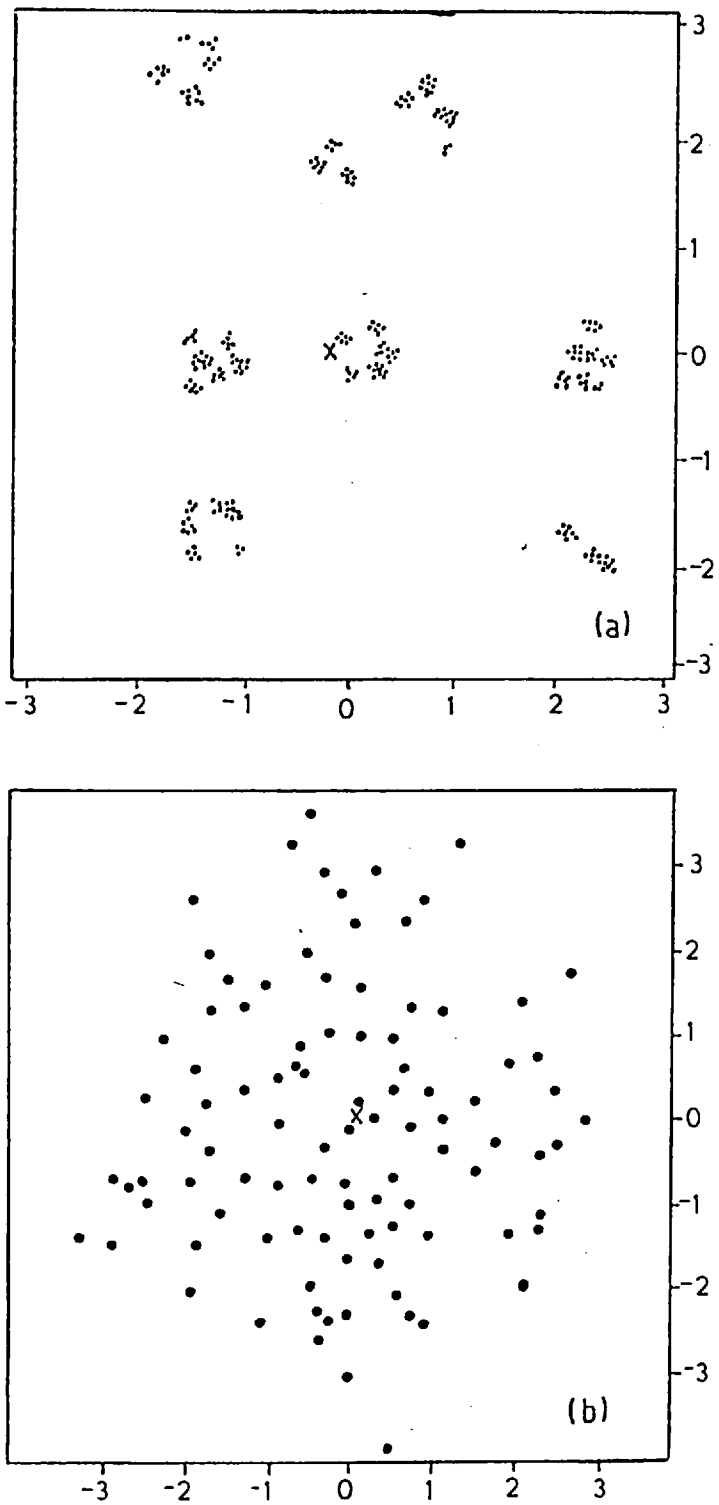

Figure 4.6. (a) A realisation consisting of 240 points from a double cluster process. There are on average $\mu = 6$ points per small cluster of diameter $D_S = 0.3$ and each large cluster contains an average of $\mu_S = 5$ small clusters. The diameter of the large clusters $D_L = 1.0$.
(b) A realisation consisting of 100 points from a fixed range interaction process with coefficient of inhibition $c = 0.1$ and range of interaction $D = 0.3$. The origin is marked X.

All of the hard core models mentioned in Ripley (1977) have obvious isotropic analogues. Instead of sampling a Poisson process of constant intensity α, sample an isotropic Poisson process with radial intensity $\lambda_0(r)$ and then apply the same criteria to the resulting point pattern. For example, the first of Matérn's hard core models is obtained by deleting any point within a distance D of any other whether or not this has already been deleted. The process so defined is clearly isotropic and its unconditional and conditional intensities are given by

$$\lambda(r) = \lambda_0(r)\exp\{-\int_{b((r,0),D)} \lambda_0(|\underset{\sim}{x}|)d\nu(\underset{\sim}{x})\}$$

and

$$\lambda(\underset{\sim}{y}|x_1) = \begin{cases} \lambda(|\underset{\sim}{y}|) & , \quad |\underset{\sim}{x}-\underset{\sim}{y}| > D, \\ 0 & , \quad |\underset{\sim}{x}-\underset{\sim}{y}| \leq D, \end{cases}$$

respectively, where $\underset{\sim}{x} = (x_1,0)$. This process is therefore regular according to the earlier definition. The restriction of such a process to some bounded set C can be simulated by simulating the underlying Poisson process on $\{\underset{\sim}{y} : \exists\ \underset{\sim}{x} \in C,\ d(\underset{\sim}{x},\underset{\sim}{y}) \leq D\}$ and deleting points as explained.

Isotropic analogues of fixed range and pairwise interaction processes are defined on a bounded set $C \subset \mathbb{R}^2$ by f, the Radon-Nikodym derivatives of their distributions with respect to that of an isotropic Poisson process with radial intensity $\lambda_0(r)$. Suppose that x is a realisation, that is a collection of points in C, and let the interaction between any two points $\underset{\sim}{\xi}$, $\underset{\sim}{\eta} \in C$ depend only on the distance $d(\underset{\sim}{\xi},\underset{\sim}{\eta})$ between them. Following Ripley (1977) set

$$f(x) = ab^{n(x)} \prod_{\substack{\underset{\sim}{\xi},\underset{\sim}{\eta}\in x \\ \underset{\sim}{\xi}\neq\underset{\sim}{\eta}}} h\{d(\underset{\sim}{\xi},\underset{\sim}{\eta})\}$$

when $a,b > 0$, $n(x)$ is the number of points in x and the interaction function $h : (0,\infty) \to [0,\infty)$ is bounded and vanishes on $(0,D)$.

Fixed range interaction processes correspond to taking

$$h(d) = \begin{cases} c, & d < D \\ 1, & d \geq D . \end{cases}$$

Let ν_0 be the measure induced by the isotropic Poisson process with radial intensity $\lambda_0(r)$. Then for a pairwise interaction process the conditional density with respect to ν_0 of a point $\underset{\sim}{\xi}$ given the realisation in $C \setminus \{\underset{\sim}{\xi}\}$ depends only on the number of points in the realisation less than a distance D from $\underset{\sim}{\xi}$, that is on the number of neighbours of $\underset{\sim}{\xi}$. This characterisation is proved by Kelly and Ripley (1976). The case $c = 0$ corresponds to one type of hard core model whilst $c = 1$ is simply the Poisson process. Figure 4.6(b) illustrates a realisation.

More complicated isotropic pairwise interaction processes could be obtained by making the interaction between $\underset{\sim}{\xi}$ and $\underset{\sim}{\eta}$ depend not only on $d(\underset{\sim}{\xi},\underset{\sim}{\eta})$ but also on $|\underset{\sim}{\xi}|$ and $|\underset{\sim}{\eta}|$.

4.4 Simulation

Simulations of the proposed process will be required when testing the goodness of fit of a model. In general a simulated pattern is the restriction of a realisation of the process to some bounded set $C \subset \mathbb{R}^2$ and consists of a number N of points. In what follows N is fixed and the bounded set is the window sector $E = \{\underset{\sim}{x} : r \leq r_0, \theta \in H_0\}$ where $\underset{\sim}{x} = (r,\theta)$ in polar coordinates as defined in Section 4.2.

For a general Poisson process the numbers of points in any two disjoint sets are independent. This fact makes it particularly simple to simulate an isotropic Poisson process with radial intensity $\lambda(x)$. The probability density function $f_r(x)$ of the marginal distribution of the radial distance to a point in the process is proportional to $x\lambda(x)$ for <u>any</u> isotropic process. Provided $x\lambda(x)$ is bounded on $[0, r_0]$, acceptance sampling can be used to generate a sample of N values of the radial distance on $[0, r_0]$. These values are taken as the radial coordinates of the N points in the simulated Poisson process, the angular coordinates being N independent values generated from a uniform distribution on H_0.

Boundary conditions must be imposed when clustered on regular patterns are simulated. One method is to impose a type of periodic boundary condition by identifying the two straight edges of the sector E and simulating the pattern on that part of the surface of the resultant cone within a distance $(r_0 + R)$ of the origin where R is some specified constant. Denote this part of the surface by S and let $S_0 = \{\underset{\sim}{x} : \underset{\sim}{x} \in \mathbb{R}^2, r \leq r_0 + R, \theta \in H_0\}$ be obtained by opening out S along, say, the line $x_1 = (x_2 \tan \alpha)$ where α is the half-angle of the cone; see Figure 4.7. The required simulated pattern is that in $E \subseteq S_0$.

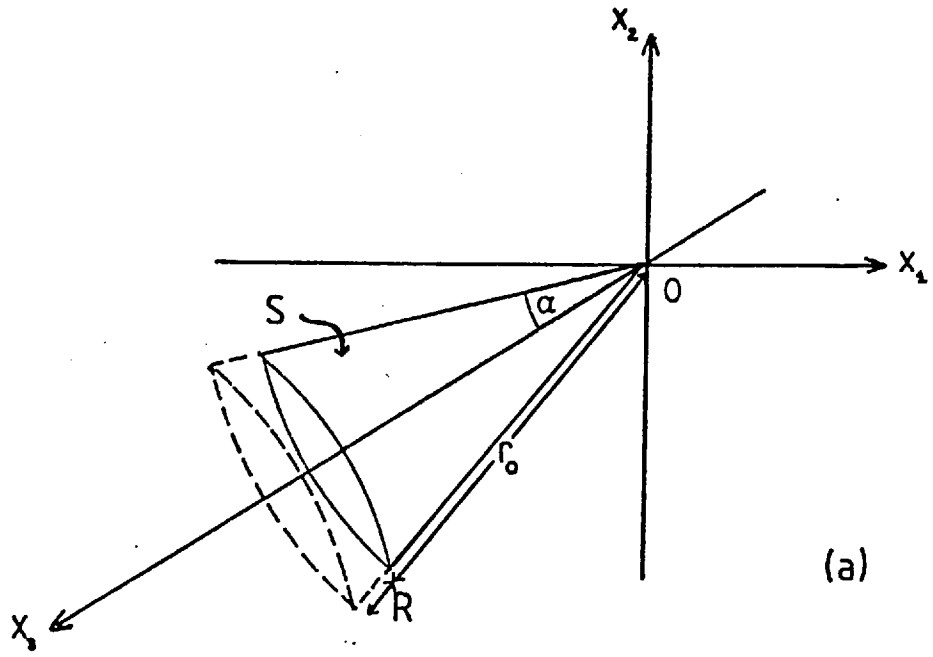

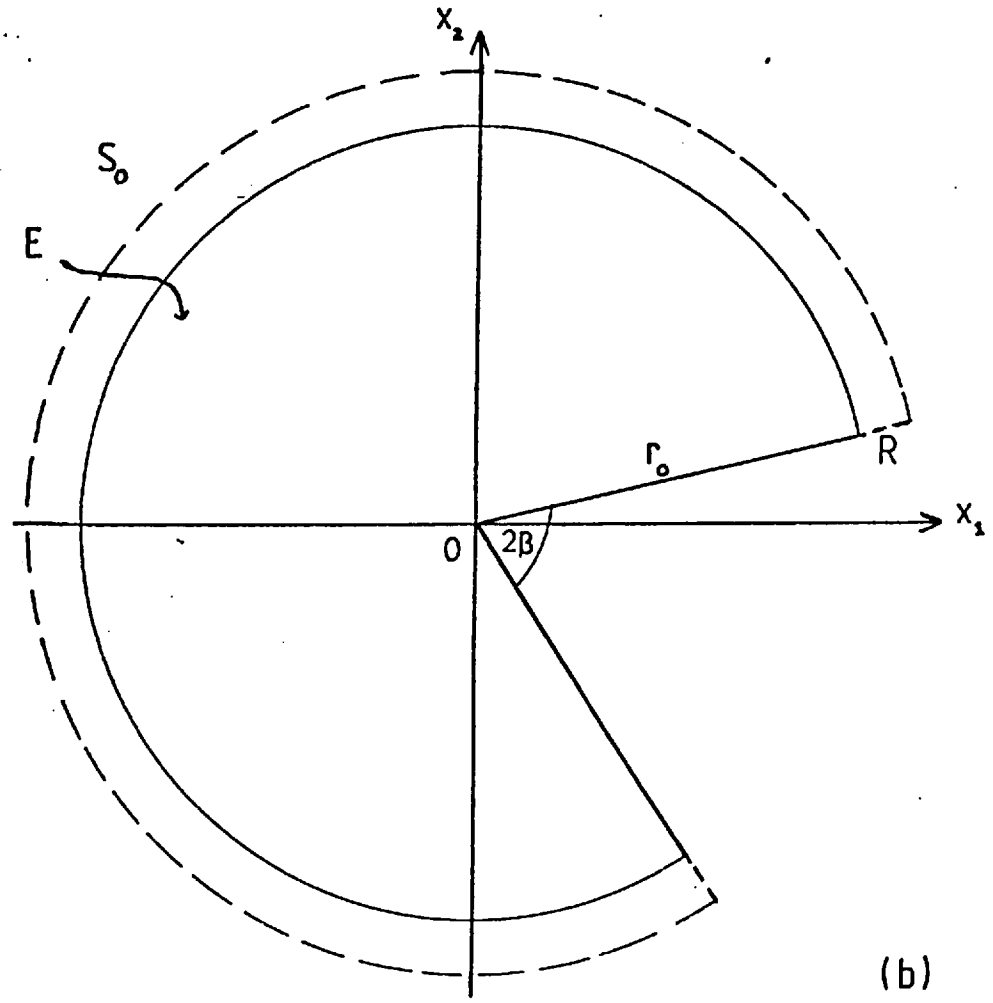

Figure 4.7

(a) The surface S of the cone with half-angle α on which the processes are simulated.
(b) The set $S_0 \subset \mathbb{R}^2$ obtained by 'opening out' S. The window sector $E \subset S_0$ and $\beta = \pi(1 - \sin \alpha)$.

To be specific, first consider simple cluster processes and use the notation for these processes given in Section 4.3. Let $R = D/2$ and generate a single Poisson number N_c, mean $\mu = \int_E \lambda_0(|\underset{\sim}{x}|)d\nu(\underset{\sim}{x})$. Simulate an isotropic Poisson pattern with radial intensity $\lambda_0(\cdot)$ on S in the obvious way, adding each point in turn until N_c points no more distant than r_0 from the origin have been added. The $(N_c + n)$ points, $n \geq 0$, of this pattern on S are taken to be the cluster centres. A centre is picked at random and a point is placed independently and at random inside a 'disc' of diameter D centred on the chosen cluster centre, the 'disc' of course lying on the surface of the cone. If the point so added is further than $(r_0 + R)$ from the origin, it is discarded and the procedure is repeated. Points are added independently in this fashion until $(N-N_c)$ such additional points lie within a distance r_0 of the origin. The pattern of the N points in $E \subseteq S_0$ formed by opening out the cone is the required simulation. A similar method can be used to simulate double cluster processes on E, this time taking $R = (D_L + D_S)/2$ with the notation of Section 4.3.

Fixed range interaction processes may be simulated by appropriate generalisations of the method given in Ripley (1977, 1979b). Let $R = 0$ and simulate an isotropic Poisson process with radial intensity $\lambda_0(\cdot)$ on S conditional on there being N points in S. Denote the pattern so obtained by x. Delete a point chosen at random from this pattern. Generate another point $\underset{\sim}{\xi}$, $|\underset{\sim}{\xi}| \leq r_0$, from the isotropic Poisson process. Accept this point with probability proportional to $f(x \cup \underset{\sim}{\xi})/f(x)$ where x denotes the reduced pattern of (N-1) points. Here f refers to the Radon-Nikodym derivative of the distribution of the fixed range interaction process with respect to that of the

isotropic Poisson process when both processes are defined in the obvious way on the surface of the cone. Thus the probability of accepting the point $\underset{\sim}{\xi}$ is proportional to $c^{\#(\underset{\sim}{\xi})}$ where $\#(\underset{\sim}{\xi})$ is the number of neighbours of $\underset{\sim}{\xi}$ in x and 0^0 is defined to be 1. Points $\underset{\sim}{\xi}$ are generated in this way until one is accepted. The whole procedure of deletion and acceptance is repeated a total of 2N times. The required simulation is the resulting pattern of N points on E formed by opening out S.

The edge effects introduced by setting R = 0 should be negligible provided that the range of interaction D is small and that N is not close to the maximum possible number of points in E for the hard core model, c = 0, with this range. If these conditions are not satisfied, one can simulate patterns on S corresponding to R = 2D, say, and accept only those patterns for which there are N points not more than a distance r_0 from the origin. If, as in the examples to be discussed, $\lambda(r) = 0$ for $r > r_0$, there are clearly no difficulties with edge effects. Pairwise interaction processes may be simulated in a similar way.

4.5 Fitting models

Ripley (1977) described how a single sample can be used in testing the goodness of fit of a model under conditions of homogeneity and isotropy. There are obvious generalisations of this method which can be used to fit models under only isotropic hypotheses, the assumption of isotropy providing the necessary replication. These methods use estimates of K^* or K_1 in the following manner.

Suppose that $\hat{K}^*(r,s,\theta)$ and $\hat{K}_1(r,t)$ are estimators of $K^*(r,s,\theta)$ and $K_1(r,t)$ respectively. Possible forms for the estimators will be given later. Except when specific values of (r,s,θ) and (r,t) are involved, $\hat{K}^*(r,s,\theta)$ and $\hat{K}_1(r,t)$ will be written $\hat{K}^*$ and $\hat{K}_1$ respectively. The estimates $\hat{K}^*$ and $\hat{K}_1$ are useful summary statistics even when modelling the stochastic process which generated the observed pattern is of no interest.

The goodness of fit criteria involve a comparison of $\hat{K}^*$ or $\hat{K}_1$ for the data pattern of N points with estimates of K^* or K_1 from a number (n-1) of simulated patterns which are realisations of the hypothesised process P_0. Each simulated process consists of N points. Let $\hat{K}^*_{max}(r,s,\theta)$ and $\hat{K}^*_{min}(r,s,\theta)$ denote the maximum and minimum values respectively of the (n-1) estimates of $K^*(r,s,\theta)$ obtained from the simulated patterns. Define $\hat{K}_{1max}(r,t)$ and $\hat{K}_{1min}(r,t)$ in a similar manner.

If the particular point (r,s,θ) is of interest, a Monte Carlo test of size 2/n of the null hypothesis that the data pattern is a realisation of the process P_0 is to accept the null hypothesis if $\hat{K}^*(r,s,\theta) \in [\hat{K}^*_{min}(r,s,\theta), \hat{K}^*_{max}(r,s,\theta)]$ and to reject it otherwise. Usually one is interested in a set of points, say

$$\{(r,s,\theta) : 0 \leq r \leq r_1, \quad 0 \leq s \leq s_1, \quad 0 \leq \theta \leq \theta_1\},$$

and the null hypothesis is accepted if $\hat{K}^* \in [\hat{K}^*_{min}, \hat{K}^*_{max}]$ for <u>all</u> these points and rejected otherwise. The size of this test is certainly no more than 2/n and can be estimated by the rejected proportion of a further group of patterns each of N points simulated from the process P_0. The analogous tests involving $\hat{K}_1$ are obvious. One-sided tests are possible if clustered or regular alternatives are of interest.

Often the data must be used to fit certain parameters of the model. Provided the number of estimated parameters is small compared with N, this should not noticeably affect the significance levels given above.

If the observed pattern consists of the set of points $\{\underset{\sim}{x}_i\}$, $i = 1,\ldots,N$, falling inside the window sector E defined earlier, then the estimators $\hat{K}^*$ and $\hat{K}_1$ are given by

$$\hat{K}^*(r,s,\theta) = (2\pi)^2 \Sigma^* k(\underset{\sim}{x}_i,\underset{\sim}{x}_j)/\{h_0^2 \text{ ave } \lambda(r).\ \text{ave } \lambda(s)\}$$

and

$$\hat{K}_1(r,t) = (2\pi)^2 \Sigma_1 k(\underset{\sim}{x}_i,\underset{\sim}{x}_j)/h_0^2.$$

The summations are over all ordered pairs of distinct points $(\underset{\sim}{x}_i,\underset{\sim}{x}_j)$ such that, in the case of Σ^*, $|\underset{\sim}{x}_i| \leq r$, $|\underset{\sim}{x}_j| \leq s$, $\cos^{-1}\{\underset{\sim}{x}_i \cdot \underset{\sim}{x}_j/(|\underset{\sim}{x}_i||\underset{\sim}{x}_j|)\} \leq \theta$ and, in the case of Σ_1, $|\underset{\sim}{x}_i| \leq r$, $|\underset{\sim}{x}_i - \underset{\sim}{x}_j| \leq t$. The function $k(\underset{\sim}{x}_i, \underset{\sim}{x}_j)$ is the reciprocal of the proportion of the perimeter of the circle centred on $\underset{\sim}{x}_i$ and passing through $\underset{\sim}{x}_j$ which is within E. The 'length' in radians of the angular interval H_0 associated with E is h_0.

The estimator $\hat{K}^*(r,s,\theta)$ is well-defined if $r,s \leq r_0$ and $\theta \leq h_0$. Consider the case $r,s \leq r_0/3$ when $h_0 = 2\pi$, that is when the window is a disc of radius r_0 centred at the origin. Then $\hat{K}^*$ is unbiased and $k(\underset{\sim}{x}_i, \underset{\sim}{x}_j) = 1$ for each term in the summation Σ^*. Usually the radial intensity function $\lambda(\cdot)$ is unknown and ave $\lambda(r)$ must be estimated by $2n(r)/(h_0 r^2)$ where $n(r)$ is the number of points no more than a distance r from the origin. It was found by simulation that only a very small possible bias of $\hat{K}^*$ was introduced in the above case when such an approximation was made for a variety of intensity functions.

If $\lambda(\cdot)$ is a constant function in which case the underlying process is both homogeneous and isotropic, $k(\underset{\sim}{x}_i, \underset{\sim}{x}_j)$ is inversely proportional to the probability that a point the distance of $\underset{\sim}{x}_j$ from $\underset{\sim}{x}_i$ had of being recorded. Then $\hat{K}^*(r,s,\theta)$ is unbiased even when $\max(r,s) > r_0/3$ or $h_0 < 2\pi$. However this is no longer true when variable radial intensity functions are considered. Indeed the bias can be substantial even when it is not necessary to estimate ave $\lambda(r)$.

There are other practical objections to the estimator $\hat{K}^*$ when testing the goodness of fit of a model. Suppose one is interested in a set of values $\{(r,s,\theta) : 0 \leq r \leq r_1, 0 \leq s \leq s_1, 0 \leq \theta \leq \theta_1\}$. It is reasonable to compare $\hat{K}^*$ with $\hat{K}^*_{min}$ and $\hat{K}^*_{max}$ at m equally-spaced values of each of r, s and θ. This requires $O(m^3)$ operations and is thus computationally time-consuming even for moderate values of m. Furthermore, there is no obvious graphical method of clearly displaying the relative values of these functions of three variables without using m plots, each plot showing the relationships for, say, different values of r and s with θ held constant. These objections do not apply to the function of two variables $\hat{K}_1$.

The estimator $\hat{K}_1(r,t)$ is well-defined if $r \leq r_0$ and $t \leq t_0 = \sup\{|\underset{\sim}{x}-\underset{\sim}{y}| : \underset{\sim}{x},\underset{\sim}{y} \in E\}$. It has been shown that $\hat{K}_1(r,t)$ should provide useful information about the second moment structure of the underlying process when $\lambda(\underset{\sim}{x}) \approx \lambda(\underset{\sim}{y})$ for $|\underset{\sim}{x}-\underset{\sim}{y}| \leq t$. In all that follows it will be assumed that t is taken sufficiently small for this assumption to hold. This is not a severe restriction in practice as one is usually interested in small interpoint distances $t << r_0$ and $\lambda(\cdot)$ usually varies smoothly. When $|\underset{\sim}{x}_i-\underset{\sim}{x}_j| \leq t$ the function $k(\underset{\sim}{x}_i, \underset{\sim}{x}_j)$ is approximately inversely proportional to the probability that a point the distance of $\underset{\sim}{x}_j$ from $\underset{\sim}{x}_i$ had of being recorded. Thus $\hat{K}_1(r,t)$ is approximately unbiased. It was found by simulation for a variety of radial intensity

functions that this bias appears to be small.

The sampling fluctuations of $\hat{K}_1$ have not been investigated analytically. The goodness of fit test described earlier uses simulation to find confidence regions for $\hat{K}_1$. If one is interested in the set of values $\{(r,t) : 0 \leq r \leq r_1, 0 \leq t \leq t_1\}$, then comparing $\hat{K}_1$ with $\hat{K}_{1min}$ and $\hat{K}_{1max}$ at m equally-spaced values of each of r and t involves only $O(m^2)$ operations. Moreover it is easy to represent the results on a single plot: simply print +, 0, - at the point (r,t) according as $\hat{K}_1(r,t)$ lies above, inside or below the simulation envelope at the point (r,t).

Such a plot is illustrated in Figure 4.8(a). The outcome of the isotropic Poisson process with radial intensity

$$\lambda(r) \propto \exp(-r^2)$$

illustrated in Figure 4.4(a) was used as the data set. The envelope values $\hat{K}_{1min}$ and $\hat{K}_{1max}$ were computed from 50 simulations of the same process and, as expected, $\hat{K}_1$ lay within this envelope at each evaluation point (r,t). Each pattern consisted of a total of N = 100 points.

Unfortunately the radial intensity function is not usually known in practice and must be estimated. Some methods of estimation are discussed in Chapter 5. If the estimator $\hat{\lambda}(r)$ deviates markedly from $\lambda(r)$, spurious effects of clustering or regularity may be detected. For example, suppose the radial intensity $\lambda(r)$ of the pattern in Figure 4.4(a) is estimated by

$$\hat{\lambda}(r) \propto \exp(-r^2/2).$$

When $\hat{K}_1$ was compared with the envelope values computed from 50 simulations of an isotropic Poisson process with radial intensity $\hat{\lambda}(r)$, each consisting of N = 100 points, the plot illustrated in Figure 4.8(b)

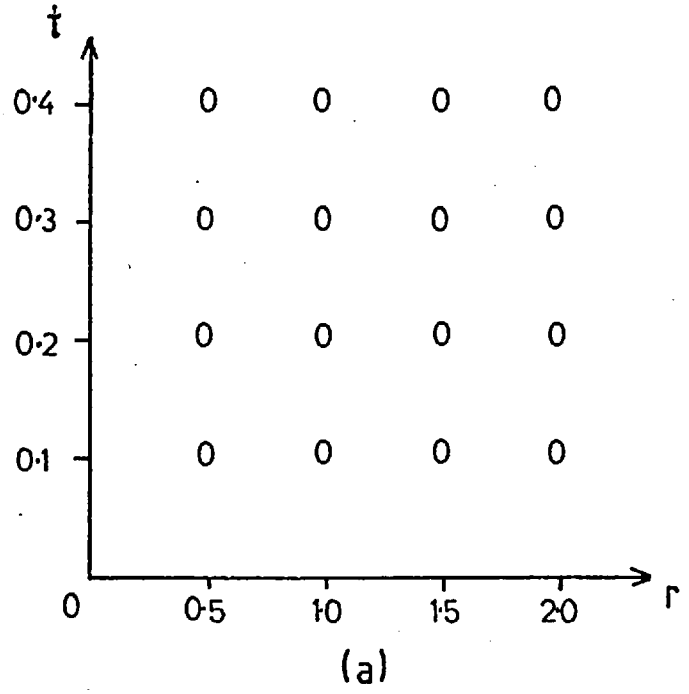

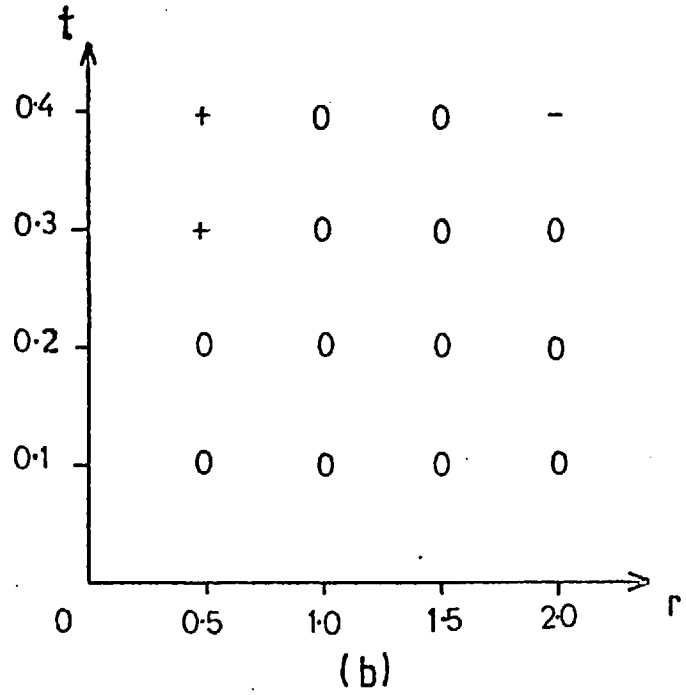

Figure 4.8

Results of $\hat{K}_1$ analyses of the pattern illustrated in Figure 4.4(a). The simulation envelope is based in each case on 50 simulations of a pattern of 100 points from an isotropic Poisson process with (a) $\lambda(r) \propto \exp(-r^2)$ and (b) $\lambda(r) \propto \exp(-r^2/2)$. The entry +, o or - at the point (r,t) indicates that $\hat{K}_1$ lay above, inside or below the envelope for the radial distance r and the interpoint distance t.

was obtained. This plot would indicate that the observed pattern was clustered at small radial distances and regular at large ones. However it is known that the pattern is a realisation of an isotropic Poisson process. The spurious effects arise since $\lambda(r)$ has not been well-estimated; the patterns simulated to form the envelope having on average fewer points close to the origin and more further from the origin than the data pattern of Figure 4.4(a).

A series of isotropic Poisson, clustered and regular patterns with several different radial intensities were generated to compare the performance of K_1 and K^* in correctly fitting such models. There was no substantial difference and, in view of this and the difficulties associated with K^*, it was decided to use only K_1 in future analyses.

There is of course a limit to the amount of information contained in the first and second moments of a spatial process. This fact was stressed by several contributors to the discussion of Ripley (1977). Ripley commented that it was possible to extend the moment decomposition results to higher moments of homogeneous and isotropic processes. This is also true of isotropic processes but the associated analysis would be exceedingly complicated. Is some simpler, perhaps approximate analysis possible? How can one determine when the first and second moments are not sufficiently informative and, in that case, where should one stop - the third, fourth or even higher moments? These are important questions but as yet no answers seem to be available.

4.6 Extensions to multitype point processes

Ripley (1976a) indicated how second-order methods can be used to investigate the interactions between two point processes which are defined on the same space X and which are jointly stationary under some group G of transformations. Suppose that there are several point processes $Z_1, Z_2, \ldots, Z_k$ which are defined on $\mathbb{R}^2$ and which are jointly stationary under rotations about the origin. If $A \in C$, the class of bounded measurable sets in $\mathbb{R}^2$, let $Z_i(A)$ be the number of points of type i in A. Cross moments are defined by

$$\mu^{ij}(A_1 \times A_2) = E\{Z_i(A_1)Z_j(A_2)\}$$

for $A_1, A_2 \in C$ and $i,j = 1,\ldots,k$. Clearly μ^{ii} is the second moment measure μ_i^2 of the isotropic process Z_i defined on $\mathbb{R}^2$.

Just as μ^2 can be summarised by the function $K(r,s,\theta)$, μ^{ij} can be summarised by

$K^{ij}(r,s,\theta)$ = expected number of ordered pairs of distinct points $(\underset{\sim}{x},\underset{\sim}{y})$ such that $\underset{\sim}{x}$ is from the Z_i process and $|\underset{\sim}{x}| \leq r$, $\underset{\sim}{y}$ is from the Z_j process and $|\underset{\sim}{y}| \leq s$ and $\cos^{-1}\{\underset{\sim}{x}.\underset{\sim}{y}/(|\underset{\sim}{x}||\underset{\sim}{y}|)\} \leq \theta$.

Denote the radial intensity function of the Z_i process by $\lambda_i(\cdot)$, $i = 1,\ldots,k$. Provided that $\lambda_i(\underset{\sim}{x}) \simeq \lambda_i(\underset{\sim}{y})$ and that $\lambda_j(\underset{\sim}{x}) \simeq \lambda_j(\underset{\sim}{y})$ for $|\underset{\sim}{x}-\underset{\sim}{y}| \leq t$, the function

$K_1^{ij}(r,t)$ = expected number of ordered pairs $(\underset{\sim}{x},\underset{\sim}{y})$ of distinct points such that $\underset{\sim}{x}$ is from the Z_i process and $|\underset{\sim}{x}| \leq r$ and $\underset{\sim}{y}$ is from the Z_j process and $|\underset{\sim}{x}-\underset{\sim}{y}| \leq t$.

should contain most of the information about the cross moment structure of two processes between which there are no substantial long range interactions. It is preferred to K^{ij} for the same reasons as K_1 is preferred to K^* in the case of a single process. It can be estimated by $\hat{K}_1^{ij}(r,t)$, the obvious analogue for the two process situation of $\hat{K}_1(r,t)$. If the processes Z_i and Z_j, $i \neq j$, are defined on some sector S and are jointly θ-stationary on S, then the above results can clearly be generalised.

To test for the absence of interaction between the processes Z_i and Z_j, $i \neq j$, proceed as follows. First identify the edges of the sector S and consider the observed patterns on the surface of the cone so formed. Calculate $\hat{K}_1^{ij}$ at some set of evaluation points $\{(r,t)\}$, using distances measured on the surface of the cone rather than Euclidean distances. Generate an envelope of values for this function under the assumption of no interaction between the Z_i and Z_j processes by retaining the largest and smallest values of this function at each evaluation point for a series of simulated patterns. Each simulated pattern is obtained by randomly spinning the observed pattern of points from, say, the Z_j process about the axis of the cone. If $\hat{K}_1^{ij}$ lies within the simulation envelope at all evaluation points, the null hypothesis of no interaction is accepted. If $\hat{K}_1^{ij}(r,t)$ lies above the envelope this is taken as evidence of 'positive' association, that is of a tendency for points from the Z_i process to occur 'close to' points from the Z_j process. If $\hat{K}_1^{ij}(r,t)$ falls below the envelope, 'negative' association is postulated. Both the functions $\hat{K}_1^{ij}$ and $\hat{K}_1^{ji}$ should be examined in this way when looking for possible interactions between the two processes. The significance level can again be estimated by the rejected proportion of a further

sample of simulated patterns.

This test for the absence of interaction requires no knowledge of the marginal distributions of the processes save that $\lambda_i(\underset{\sim}{x}) \approx \lambda_i(\underset{\sim}{y})$ for $|\underset{\sim}{x}-\underset{\sim}{y}| \leq t$, the interpoint range of interest. Intuitively one would expect the sampling fluctuations of $\hat{K}_1^{ij}$ to increase as the Z_i and Z_j processes become more clustered. Because of this, evidence of association between two processes, one or both of which is thought to be highly clustered, should be treated with considerable scepticism.

CHAPTER 5: THE ESTIMATION OF THE MARGINAL RADIAL AND ANGULAR PROBABILITY DENSITIES AND THE DETECTION OF ANGULAR NON-UNIFORMITY

5.1 Introduction

Two requirements have to be met before $\hat{K}_1$ can be used to analyse a spatial pattern. The first is that it is reasonable to assume that the underlying point process is θ-stationary on some sector. The second is that it is possible to estimate fairly accurately the radial intensity or, equivalently, the marginal radial probability density function (pdf) of the process restricted to this sector. This estimate is needed when simulating the patterns used to find the envelope values for $\hat{K}_1$. In general there is no a priori reason for assuming a particular parametric form for the marginal radial pdf. It seems sensible to use some nonparametric density estimate.

Wertz (1978) surveys existing methods of statistical density estimation. Whether one uses histograms, kernel density estimates or sums of orthogonal functions to estimate the pdf, some subjectivity is always present in the final choice of the estimate. In the case of histograms the subjectivity is in the choice of bin width and in the positioning of the end points of the bins. For kernel density estimates it is in the choice of the kernel and of the smoothing parameter. For sums of orthogonal functions the difficulty lies in deciding when a sufficient number of terms have been included.

In most applications it is reasonable to suppose that the marginal radial pdf is a continuous function. This is so for the sporophore patterns illustrated in Figures 4.1(a)-(c). It was seen in the last Chapter that spurious effects of clustering or regularity can be

detected by a $\hat{K}_1$ analysis when the marginal radial pdf is not estimated sufficiently accurately. Therefore it was decided to use a suitable continuous estimate of this function in preference to a histogram.

This Chapter is concerned with kernel density estimators, in effect, smoothed histograms. Continuous estimators of both the marginal radial and angular pdf's are suggested. The estimate of the angular pdf is used to detect departures from the null hypothesis of angular uniformity. Angular clustering, regularity and trend can be detected in this way. Should angular trend be found, the estimate of the angular pdf can be used to partition the region of interest into sectors within each of which the assumption of angular uniformity can be checked in more detail.

The ideas described apply to any data set with some preferred reference point provided the position of this point is known and taken to be the origin. Ths sporophore patterns are analysed using these techniques.

5.2 Kernel density estimators: some existing results

The kernel density estimator was introduced by Rosenblatt (1956). Suppose for the moment that $x_1,\ldots,x_N$ is a sample of independent and identically distributed observations from a population with pdf $f(\cdot)$. The kernel density estimator is defined by

$$f_N(x) = (Nh)^{-1} \sum_{i=1}^{N} k\{(x - x_i)/h\}.$$

The function $k(\cdot)$ is called the kernel and the constant h is known as the smoothing parameter. Both k and h need to be specified. It is assumed that $h \to 0$ as $N \to \infty$.

Epachenikov (1969) showed that a kernel which consists of part of a parabola is optimal in the sense that it minimises the 'relative global error' $[\int E\{(f_N - f)^2\}] / \int f^2$. For practical purposes any reasonable kernel gives near optimal results in this sense and the choice of kernel function is not critical. However, the choice of smoothing parameter is crucial. Oversmoothing, which corresponds to taking a large value for h, introduces bias. Undersmoothing gives rise to an estimate with unnecessarily large random variation.

Silverman (1978) investigated the limiting behaviour of h as $N \to \infty$ required for the best rate of uniform convergence in probability of f_N to f. His results are proved under fairly mild conditions and concern the second derivative f_N'' of the kernel density estimate. The function f_N'' can be thought of as the sum of a systematic component $E(f_N'')$ whose variation is closely connected to that of f'' and of a random component $f_N'' - E(f_N'')$.

Silverman suggested that a series of test graphs can be used to find a suitable value of h: choose a value of h which gives noticeable random fluctuations in f_N'' but which are not so large as to obscure the systematic variation of this function. (This method is subjective.) It formalises the intuitive notion that the character of f_N'' should change more rapidly with changing h than does f_N itself and so it should be easier to use f_N'' rather than f_N to select an appropriate amount of smoothing. In all the applications to be discussed, the shape of the test graph changed rapidly as h was varied and it was not difficult to find a suitable value of this parameter. The test graph method will obviously fail if $f'' = 0$ and consequently there is no systematic variation in f_N''.

The results quoted so far in this Section generalise to the situation where $\underset{\sim}{x}_1,\ldots,\underset{\sim}{x}_N$ are a sample of <u>independent</u> and identically distributed vectors of observations from a multivariate distribution with pdf $f(\cdot)$. If $\underset{\sim}{x} = (x_1,\ldots,x_\ell)$ and f_N is the kernel density estimate, then the test graph is

$$\nabla^2 f_N(\underset{\sim}{x}) = \partial^2 f_N/\partial x_1^2 + \ldots + \partial^2 f_N/\partial x_\ell^2.$$

When $\ell = 2$, contour or perspective plots can be used to compare test graphs. It is not clear what should be done if $\ell > 2$.

There are very few results on the asymptotic behaviour of kernel density estimates formed from a sample of <u>dependent</u> observations. Rosenblatt (1970) proved consistency and asymptotic normality of the estimates when the observations form a Markov sequence. There are no theoretical results to justify the use of the test graph method in any situation involving dependent observations.

The yearly patterns of each sporophore type are illustrated in Figures 5.1(a)-(i). It may be that in each of these patterns the observations are dependent; indeed this must be so for the visually clustered patterns of <u>Laccaria laccata</u>. Thus there is no theoretical justification for using the test graph method or, indeed, for using kernel estimates of the densities associated with these patterns. Nevertheless this is precisely what is done in the next Section. It is hoped that the 'local character' of f_N and of f_N'' ensures that they are robust to the types of departures from independence which occur in the sporophore patterns. In a small simulation study of patterns from simple cluster processes and from hard core processes it was reassuring to note the close agreement between the kernel estimates

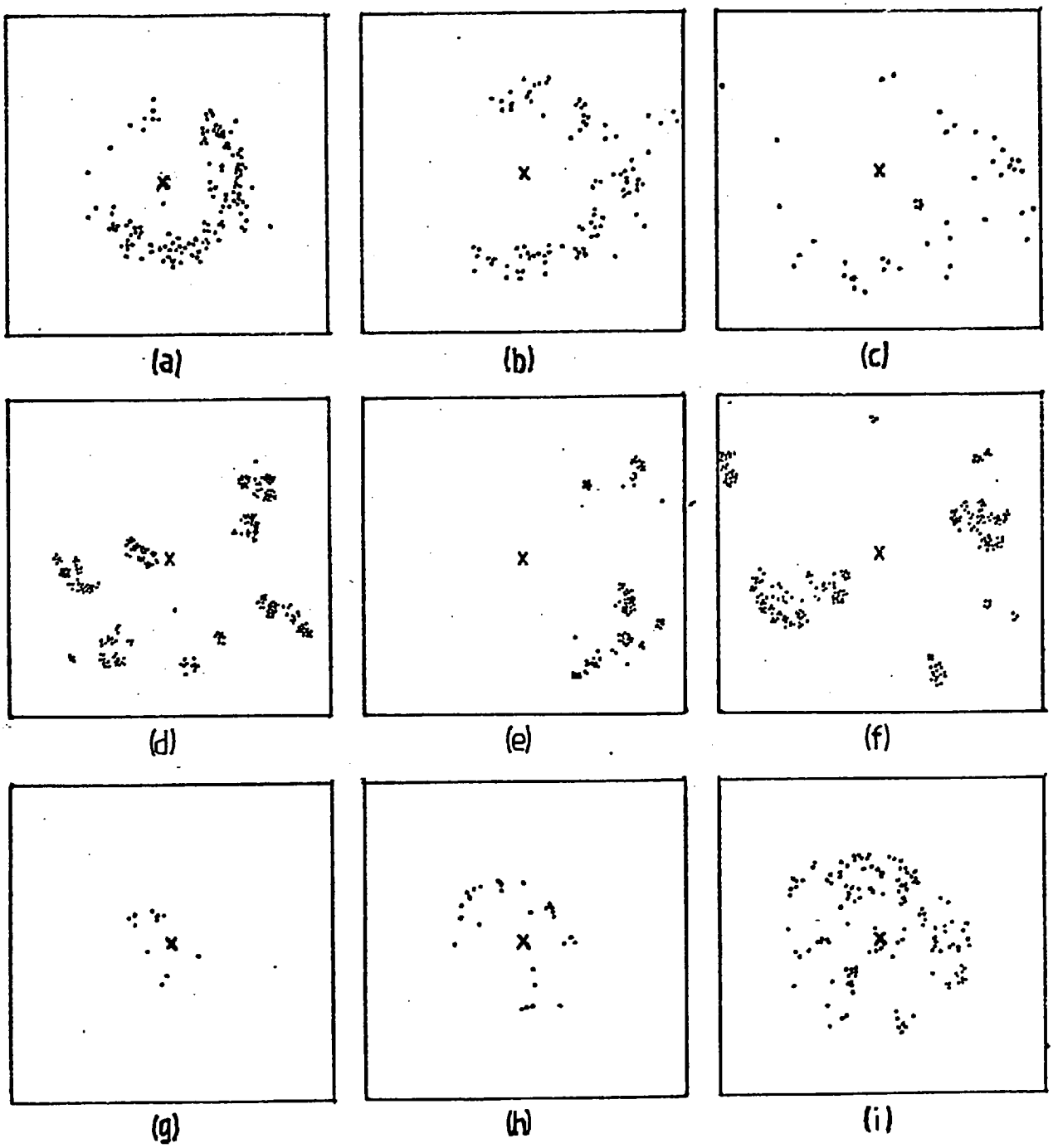

Figure 5.1. Sporophore patterns in a square of side 3 metres around a birch tree x.
(a), (b), (c) Hebeloma spp. in 1975, 1976, 1977.
(d), (e), (f) Laccaria laccata in 1975, 1976, 1977.
(g), (h), (i) Lactarius pubescens in 1975, 1976, 1977.

of the radial pdf's and their known true values.

In the preceding discussion h has been held constant for all values of $\underset{\sim}{x}$. Breiman, Meisel and Purcell (1977) suggest that it is intuitively more reasonable to allow h to depend on the nearest neighbour distances from $\underset{\sim}{x}$ to the data points. Wagner (1975) established the consistency of a type of variable kernel estimator in the one-dimensional case. Variable kernel estimators would appear to be well-suited to clustered data sets but they will not be used in the following Sections.

5.3 The one-dimensional kernel estimates of the marginal radial pdf's

If $\{\underset{\sim}{u}_i\}$, $\underset{\sim}{u}_i = (r_i, \theta_i)$ in polar coordinates, denote the positions of the sporophores in a particular pattern of N points, then the marginal radial kernel density estimate is defined to be

$$\hat{g}_r(s) = (Nh)^{-1} \sum_{i=1}^{N} k_q\{(s-r_i)/h\}$$

and the associated test graph is

$$\hat{g}_r''(s) = N^{-1}h^{-3} \sum_{i=1}^{N} k_q''\{(s-r_i)/h\} .$$

The kernel k_q used here is the quartic kernel

$$k_q(x) = \begin{cases} |x|^4/4 - |x|^3/2 + 1/2 , & |x| \leq 1, \\ |x|(2 - |x|)^3/4 , & 1 \leq |x| \leq 2, \\ 0 , & |x| \geq 2, \end{cases}$$

which satisfies conditions (a)-(h) of Silverman (1978), p.8.

(Epachenikov's optimal quadratic kernel does not satisfy these conditions and for this reason the near optimal quartic kernel seemed preferable.)

The device suggested by Boneva, Kendall and Stefanov (1971) was used to ensure that $\hat{g}_r(0) = 0$. This involved augmenting the set $\{r_i\}$ by a reflected copy of itself $\{-r_i\}$ and subtracting the contribution to $\hat{g}_r$ from each of the points in the latter set. This constraint was imposed because $\hat{g}_r(s)$ estimates the marginal radial pdf which is proportional to $s \int_0^{2\pi} \lambda(s,\phi)d\phi$. Here $\lambda(s,\phi)$ is the intensity of the underlying stochastic process at the point (s,ϕ) and it is assumed that $\int_0^{2\pi} \lambda(s,\phi)d\phi$ is bounded, a reasonable assumption for the sporophore patterns.

Figures 5.2(a)-(c) illustrate the test graphs of the kernel estimates of the 1975 Hebeloma spp. radial pdf for h = 75, 100 and 125 millimetres. These suggest taking h = 100 millimetres. Appropriate values of h for each of the other sporophore patterns were, with one exception, chosen in the same way. The exception is the 1975 pattern of Lactarius pubescens. This contained only eleven sporophores, too few for the meaningful formation of a kernel density estimate and so is not considered in the remainder of this Chapter.

Figures 5.3(a)-(c) illustrate the kernel estimates of the radial pdf in each year for (a) Hebeloma spp. (b) Laccaria laccata and (c) Lactarius pubescens. The number of sporophores in each associated pattern is shown in parentheses. To facilitate comparison between the preferred radial distance for each sporophore type, the same estimates are illustrated year by year in Figure 5.4. A detailed discussion of the radial behaviour of the sporophores is given in Chapter 6; many features are immediately obvious from Figures 5.3 and 5.4.

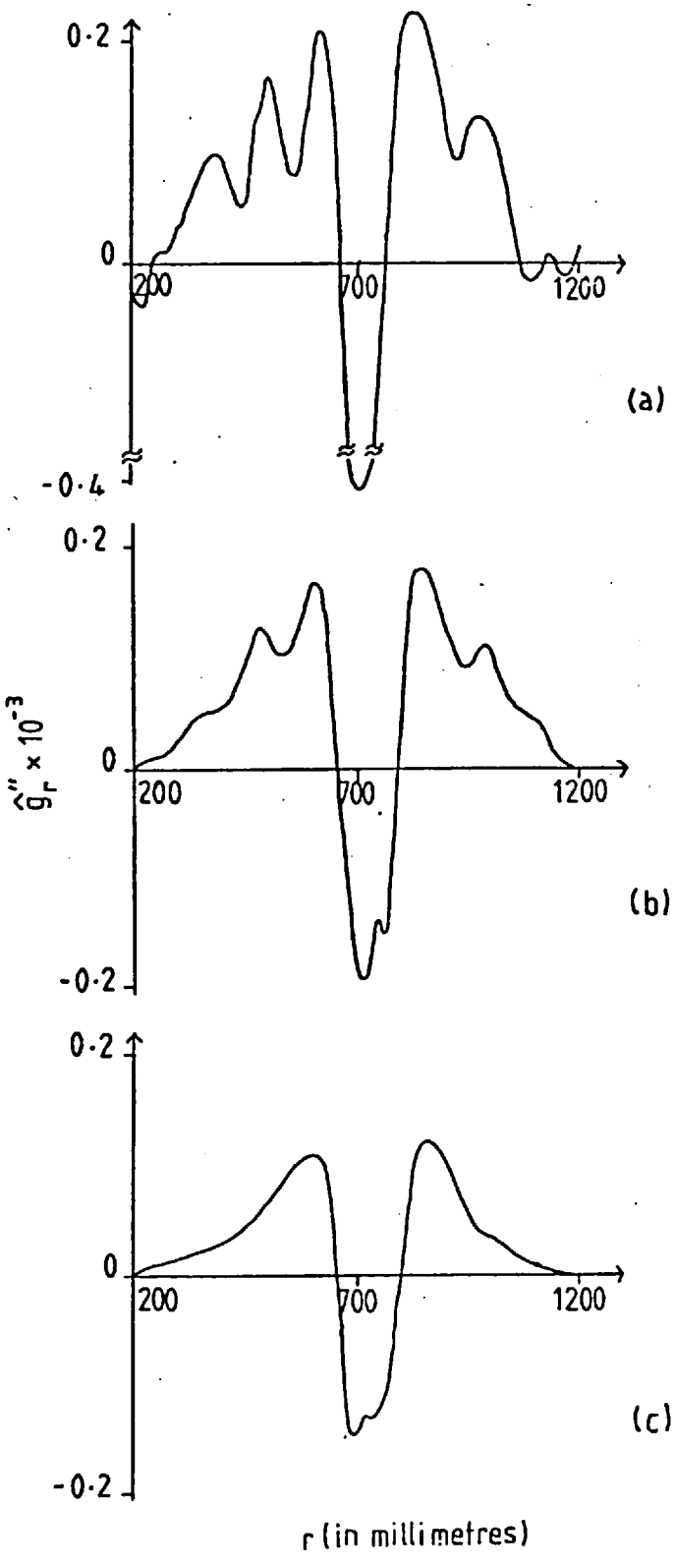

Figure 5.2. Test graphs for the 1975 Hebeloma spp. pattern of 133 sporophores with the smoothing parameter equal to (a) 75 (b) 100 (c) 125 millimetres.

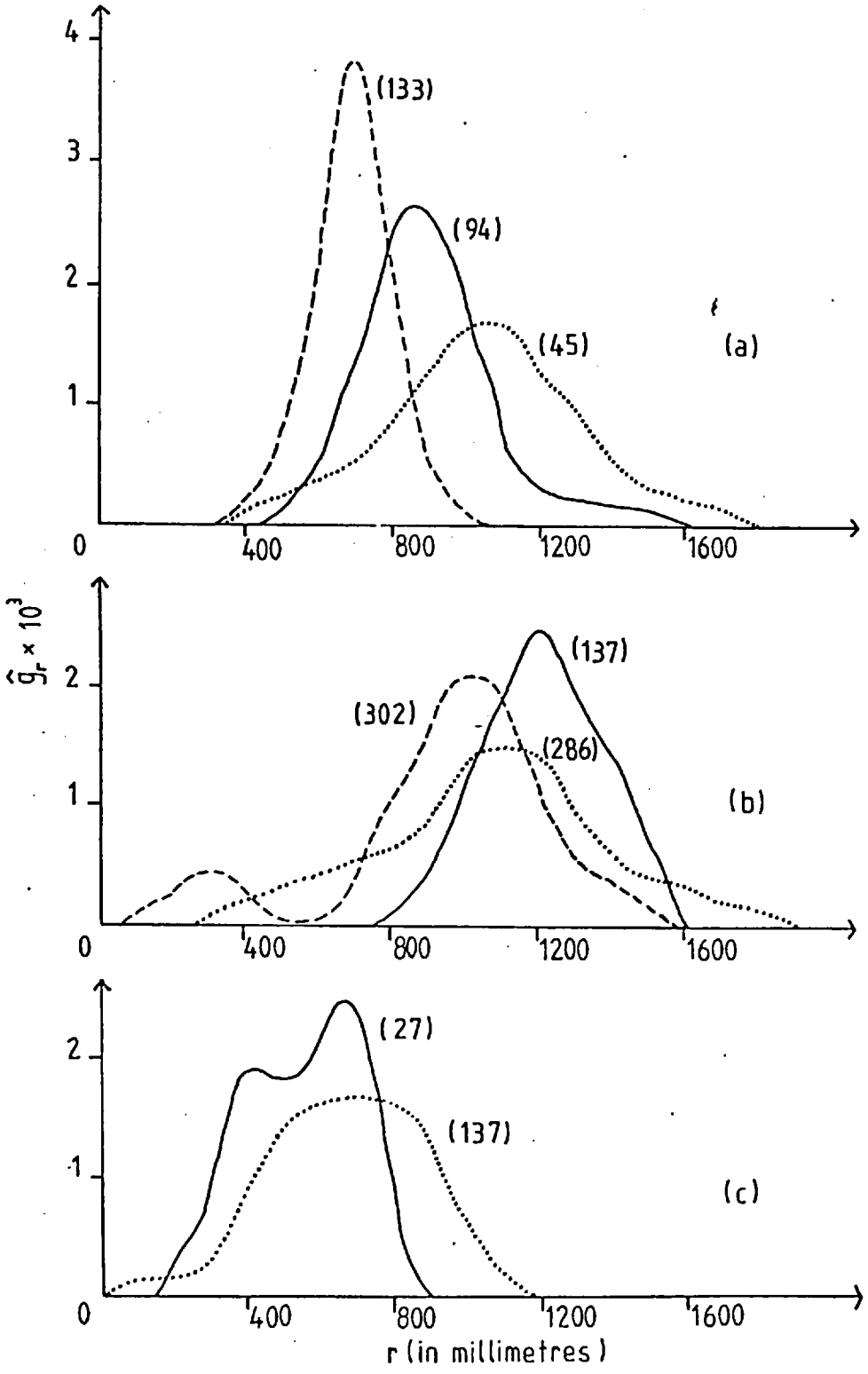

Figure 5.3. The kernel density estimates $\hat{g}_r$ of the radial pdf versus the radial distance r for (a) Hebeloma spp. (b) Laccaria laccata (c) Lactarius pubescens in 1975 ---, 1976 ——, 1977···· . The number of sporophores in each pattern is shown in parentheses.

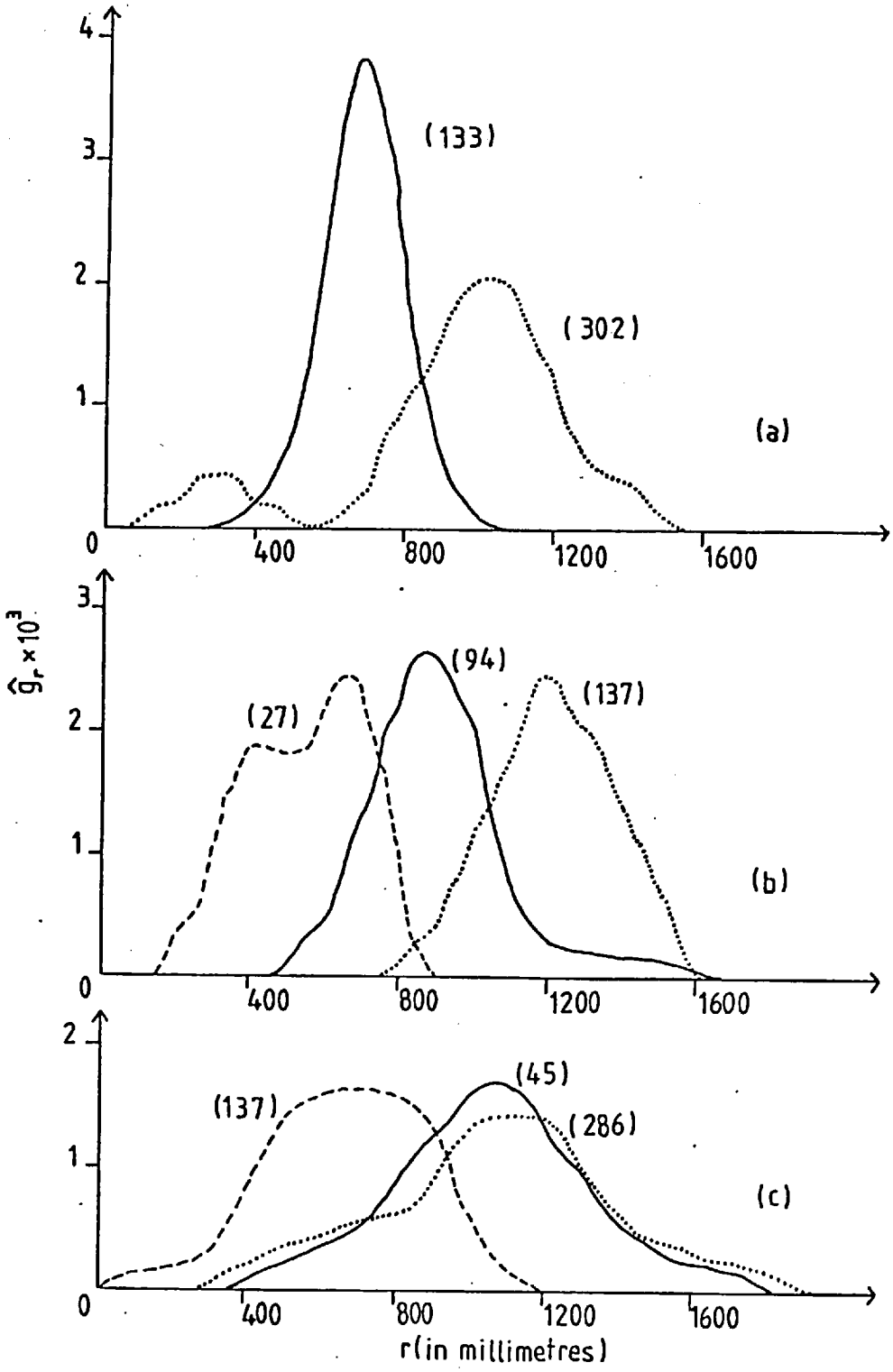

Figure 5.4. The kernel density estimate $\hat{g}_r$ of the radial pdf versus the radial distance r for (a) 1975 (b) 1976 (c) 1977. —— Hebeloma spp., ···· Laccaria laccata, ---- Lactarius pubescens. The number of sporophores in each pattern is shown in parentheses.

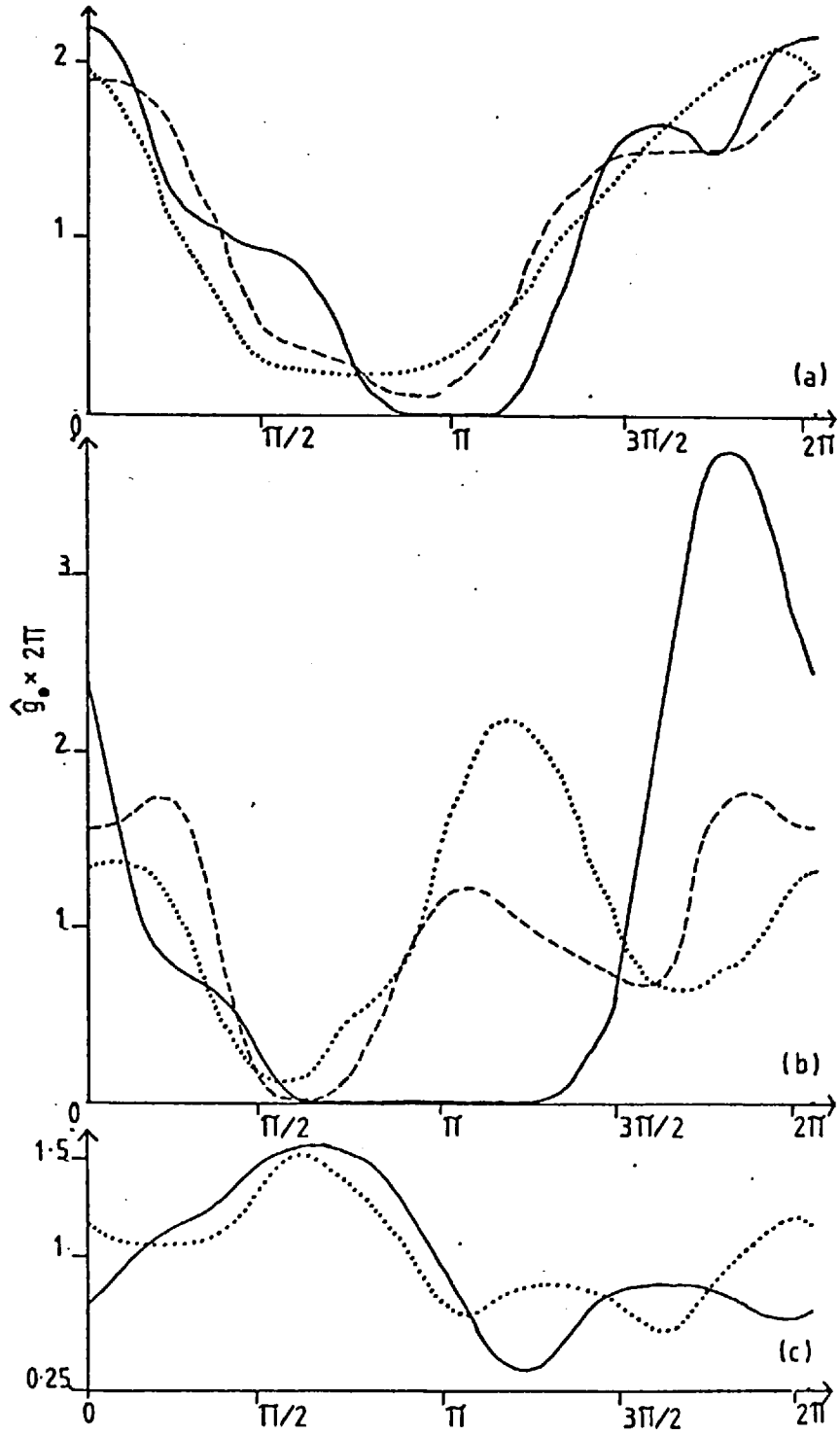

Figure 5.5. The kernel density estimate $\hat{g}_\theta$ of the angular pdf versus the angular coordinate for (a) Hebeloma spp. (b) Laccaria laccata (c) Lactarius pubescens in 1975 ----, 1976 ____, 1977 ···· .

5.4 The one-dimensional kernel estimates of the angular pdf's

The test graph method cannot be used to find a suitable value of the smoothing parameter to use in the analogous kernel estimate $\hat{g}_\theta$ of the marginal angular pdf if the process generating the observed sporophore pattern is isotropic. (In this case $E(\hat{g}_\theta) = (2\pi)^{-1}$ and there is no systematic component in $\hat{g}_\theta$"). Some alternative technique is required.

The method adopted was to suitably scale the smoothing parameter h_r selected for the radial density estimate and then to use this scaled value $h_\theta = \alpha h_r$, say, in computing

$$\hat{g}_\theta(\phi) = (Nh_\theta)^{-1} \sum_{i=1}^{N} k_q\{(\phi-\theta_i)/h_\theta\} .$$

The continuity condition $\hat{g}_\theta(0) = \hat{g}_\theta(2\pi)$ was satisfied by augmenting the set $\{\theta_i\}$ by two translated copies of itself, $\{\theta_i - 2\pi\}$ and $\{\theta_i + 2\pi\}$, and then calculating $\hat{g}_\theta$ for this enlarged data set (see Boneva et al., 1971).

The scaling factor α was defined to be

$$\alpha = 2\pi/\hat{L}$$

where

$$\hat{L} = \inf\{s-t : \hat{g}_r(x) = 0 \quad \forall\, x \in [s,t]^c\},$$

the length of the smallest interval outside which the radial density estimate was identically zero. This value for α was chosen since, in the sense to be described, it gave the same relative amount of smoothing for $\hat{g}_\theta$ as for the radial density estimate $\hat{g}_r$. The N radial observations lay inside an interval of length $\hat{L}$. There is some biological evidence to suggest that this length was determined by the width of the annulus

about the tree within which the tree root system favoured the growth of that type of mycorrhiza and the subsequent production of sporophores (see Ford et al, 1980). It therefore seemed reasonable to set the smoothing parameter h_θ used in finding the angular density estimate from the N angular observations lying inside the interval of length 2π equal to $(h_r/\hat{L})2\pi$.

Figures 5.5(a)-(c) illustrate the resulting estimates for the marginal angular pdf's for each sporophore type in successive years. These estimates are examined in detail in Chapter 6.

5.5 Alternative estimates of the marginal radial and angular pdf's

An obvious alternative approach is to find a two-dimensional estimate of the pdf of the underlying process. The marginal radial and angular pdf's found from this estimated pdf will be denoted $\hat{f}_r$ and $\hat{f}_\theta$ respectively. The two-dimensional kernel estimate based on the set of N observations $\{\underset{\sim}{u}_i\}$ is given by

$$f_N(\underset{\sim}{u}) = N^{-1}h^{-2} \sum_{i=1}^{N} k\{(\underset{\sim}{u}-\underset{\sim}{u}_i)/h\} \qquad (5.1)$$

with the obvious notation. It would certainly be an advantage if k is chosen to facilitate the integration needed to find $\hat{f}_r$ and $\hat{f}_\theta$ from f_N. By using the two-dimensional Gaussian kernel

$$k_g(\underset{\sim}{x}) = (2\pi)^{-1} \exp(-|\underset{\sim}{x}|^2/2) \quad , \quad \underset{\sim}{x} \in \mathbb{R}^2 \qquad (5.2)$$

one can obtain explicit expressions for $\hat{f}_r$ and $\hat{f}_\theta$ as follows. Change to polar coordinates in (5.2) and substitute in (5.1) to obtain for $\underset{\sim}{u} = (s,\phi)$

$$f_N(s,\phi) = \frac{s}{2\pi N h^2} \sum_{i=1}^{N} \exp\left[-\frac{\{s^2 + r_i^2 - 2sr_i \cos(\phi-\theta_i)\}}{2h^2}\right] .$$

Integrate over ϕ and s respectively to find

$$\hat{f}_r(s) = \frac{s}{2Nh^2} \exp\left(-\frac{s^2}{2h^2}\right) \sum_{i=1}^{N} \exp\left(-\frac{r_i^2}{2h^2}\right)\{I_0(s_i) + I_0(-s_i)\}$$

where $s_i = sr_i/h^2$ and $I_0(z)$ is the Bessel function,

$$I_0(z) = \pi^{-1} \int_0^{\pi} \exp(z \cos \phi)d\phi,$$

and

$$\hat{f}_\theta(\phi) = \frac{1}{2\pi Nh} \sum_{i=1}^{N} \{h \exp\left(-\frac{r_i^2}{2h^2}\right) + \sqrt{(2\pi)}t_i \, \Phi\left(\frac{t_i}{h}\right)\exp\left(\frac{t_i^2 - r_i^2}{2h^2}\right)\}$$

where $t_i = r_i \cos(\phi-\theta_i)$ and $\Phi(\cdot)$ is the standard normal cumulative distribution function. A suitable value for h is selected by considering either contour or perspective plots of

$$\nabla^2 f_N(s,\phi) = (2\pi Nh^6)^{-1} \sum_{i=1}^{N} (t_i^2-2h^2)\exp\{-t_i/(2h^2)\}$$

where now $t_i = s^2 + r_i^2 - 2sr_i \cos(\phi-\theta_i)$.

Since it is important that a 'good' estimate of the radial pdf is used in a $\hat{K}_1$ analysis, it will certainly be reassuring if $\hat{f}_r$ is very similar to $\hat{g}_r$. Figures 5.6(a)-(c) are perspective plots of $\nabla^2 f_N$ for the 1975 Hebeloma spp. pattern (Figure 5.1(a)) with h = 60, 80 and 100 millimetres. A value of 80 millimetres was selected for h and the resulting estimates $\hat{f}_r$ and $\hat{f}_\theta$ are illustrated in Figure 5.7. The close agreement between $\hat{f}_r$ and $\hat{g}_r$ for this pattern can be seen in

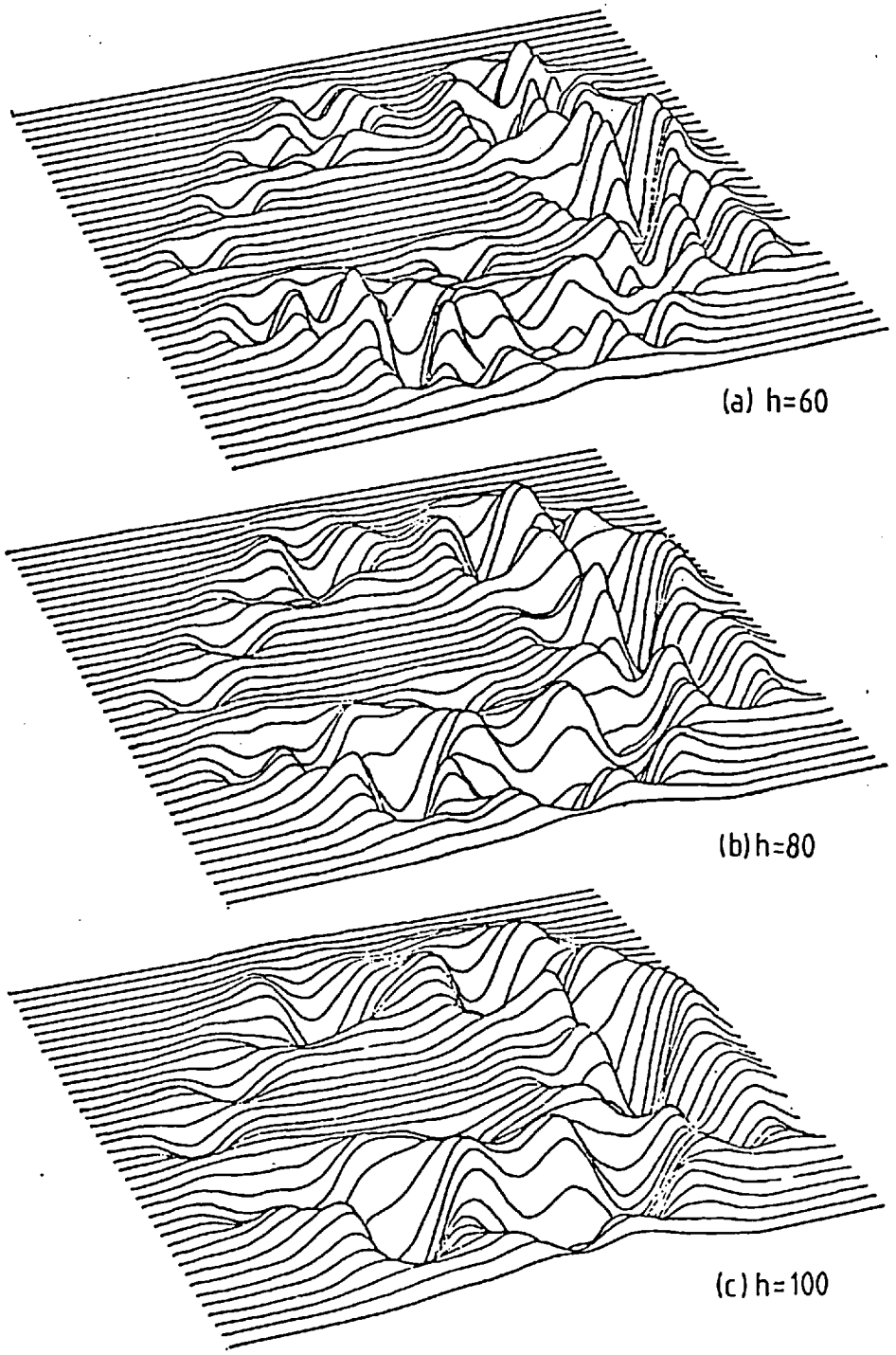

Figure 5.6. Perspective plots of the test graphs for the 1975 Hebeloma spp. pattern using a smoothing parameter of h millimetres.

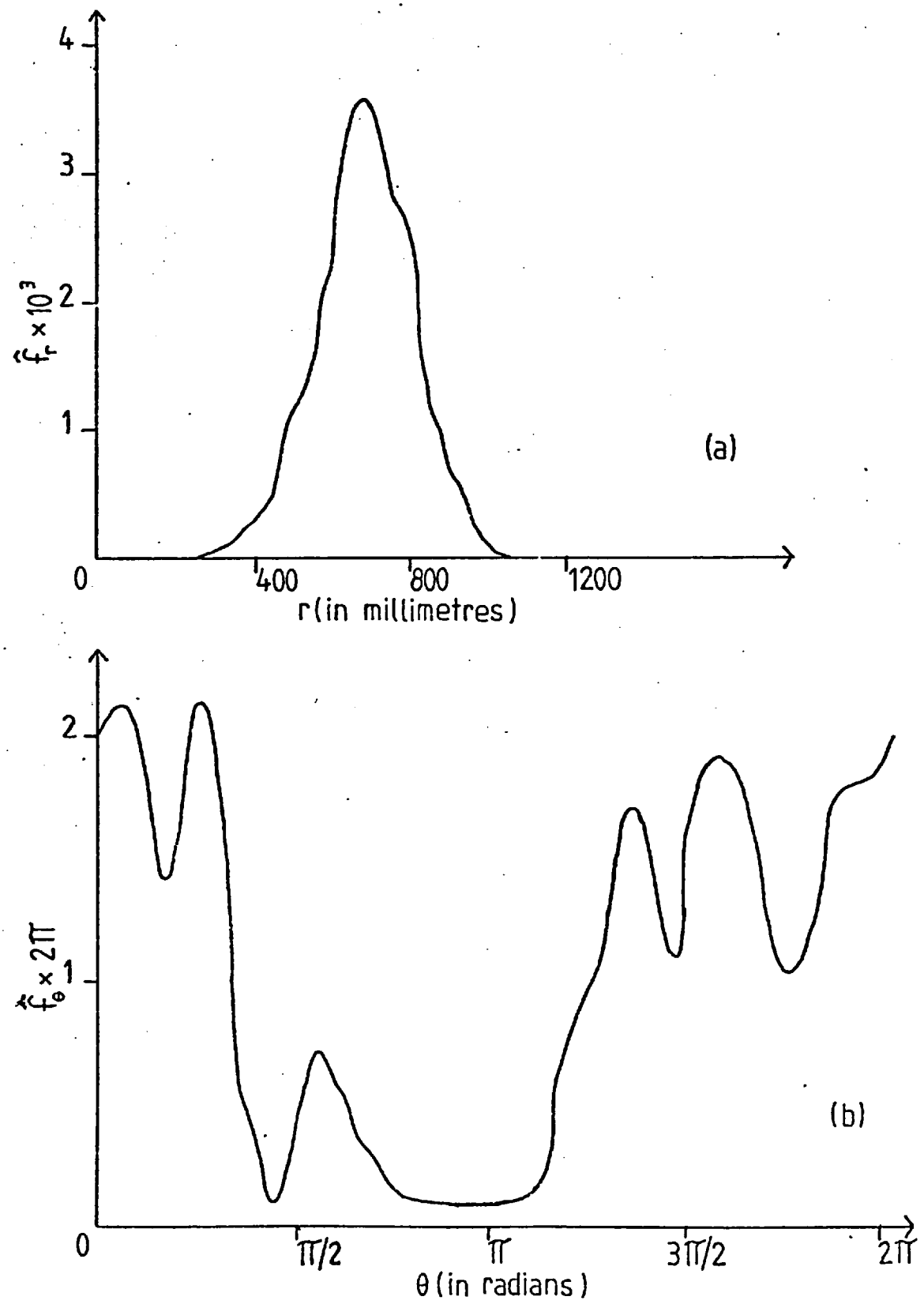

Figure 5.7. The estimates (a) $\hat{f}_r$ and (b) $\hat{f}_\theta$ of the marginal radial and angular pdf's for the 1975 Hebeloma spp. pattern of 133 sporophores.

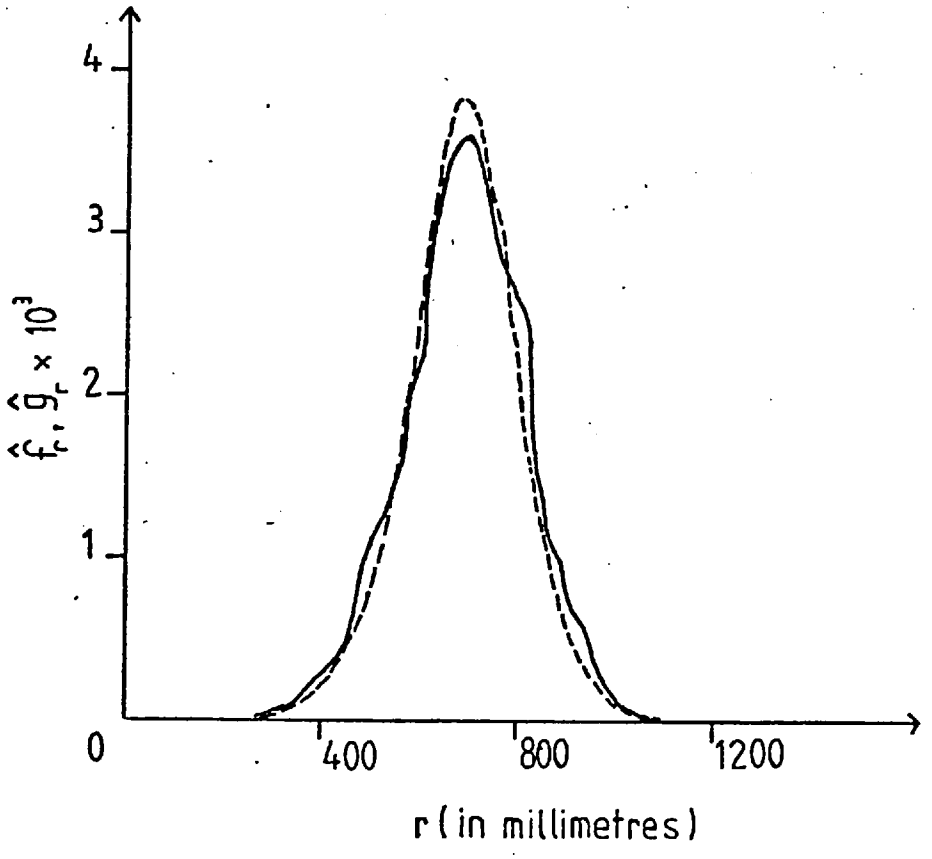

Figure 5.8. The estimates ——— $\hat{f}_r$ and ---- $\hat{g}_r$ of the radial pdf for the 1975 Hebeloma spp. pattern of 133 sporophores.

Figure 5.8. Similar agreement was found between the two estimates of the radial pdf for each of the remaining sporophore patterns.

A comparison of the appropriate curve in Figure 5.5(a) with that in Figure 5.7(b) shows that, for the 1975 Hebeloma spp. pattern, $\hat{g}_\theta$ and $\hat{f}_\theta$ are not nearly as visually similar as are $\hat{g}_r$ and $\hat{f}_r$. In particular $\hat{g}_\theta$ is much smoother than $\hat{f}_\theta$ although both indicate the same underlying trend. This is true of these angular density estimates for each of the sporophore patterns.

One explanation for this difference is that a constant smoothing parameter independent of the radial distance r is used in calculating $\hat{g}_\theta$. For $\hat{f}_\theta$ the angular distance over which the contribution to this estimate from each observation is spread is inversely proportional to r. Thus an observation far from the origin has a much greater influence on the shape of $\hat{f}_\theta$ than on that of $\hat{g}_\theta$. An idea not pursued here is that in some sense a combination of these two estimates might be preferable to either one.

An alternative explanation for the difference between $\hat{g}_\theta$ and $\hat{f}_\theta$ is that h_θ (found by rescaling h_r) is not a suitable choice for the smooth parameter in $\hat{g}_\theta$. It has not been necessary to consider this problem in more detail or to choose between $\hat{g}_\theta$ and $\hat{f}_\theta$ because both have very similar abilities to detect angular non-uniformity as shown in the next Section. Hence there is nothing to choose between these estimates for the purpose to which they are put in analysing the sporophore patterns.

The density estimates $\hat{f}_r$ and $\hat{f}_\theta$ take longer to compute than do $\hat{g}_r$ and $\hat{g}_\theta$. For example, computing and plotting four perspective plots of $\nabla^2 f_N$ and then calculating and plotting $\hat{f}_r$ and $\hat{f}_\theta$ for a pattern of 100 points takes about 120 seconds on the Cyber 174 at Imperial College.

The corresponding time taken to find $\hat{g}_r$ and $\hat{g}_\theta$ is about 10 seconds. For all the patterns examined it was usually easier to select a suitable smoothing parameter from the test graphs of $\hat{g}_r$" than from perspective plots of $\nabla^2 f_N$.

In general it should be sufficient to calculate only $\hat{g}_r$ and $\hat{g}_\theta$ as a preliminary step in a $\hat{K}_1$ analysis. If one wishes to 'check' these estimates, $\hat{f}_r$ and $\hat{f}_\theta$ can also be found: $\hat{f}_r$ should be in close agreement with $\hat{g}_r$ and $\hat{f}_\theta$ should lead to the same conclusions as $\hat{g}_\theta$ concerning the angular distribution. The radial and angular density estimates are, of course, useful summary statistics even when no subsequent $\hat{K}_1$ analysis is envisaged.

One final remark concerning the two-dimensional kernel density estimate f_N can be made if the radial and angular coordinates of any point in the pattern are independent. In such situations it seems reasonable to expect that $f_N(s,\phi) \approx \hat{f}_r(s).\hat{f}_\theta(\phi)$. Thus, although it is unnecessary to calculate f_N for the purposes of finding $\hat{f}_r$ and $\hat{f}_\theta$, some insight into the dependence structure of the underlying process might be obtained by comparing $f_N(s,\phi)$ with $\hat{f}_r(s).\hat{f}_\theta(\phi)$.

Remarkably close visual agreement between the perspective plots of $f_N(s,\phi)$ and $\hat{f}_r(s).\hat{f}_\theta(\phi)$ for the 1975 Hebeloma spp. pattern of 133 points can be seen in Figures 5.9(a) and (b). Similar agreement was found for all the remaining patterns of Hebeloma spp. and those of Lactarius pubescens. This suggests that any dependence between the positions of points in patterns of these sporophore types is not 'strong'. The positions of points in the visually highly clustered patterns of Laccaria laccata must clearly be highly dependent. As expected, the corresponding perspective plots were very different for each of these patterns.

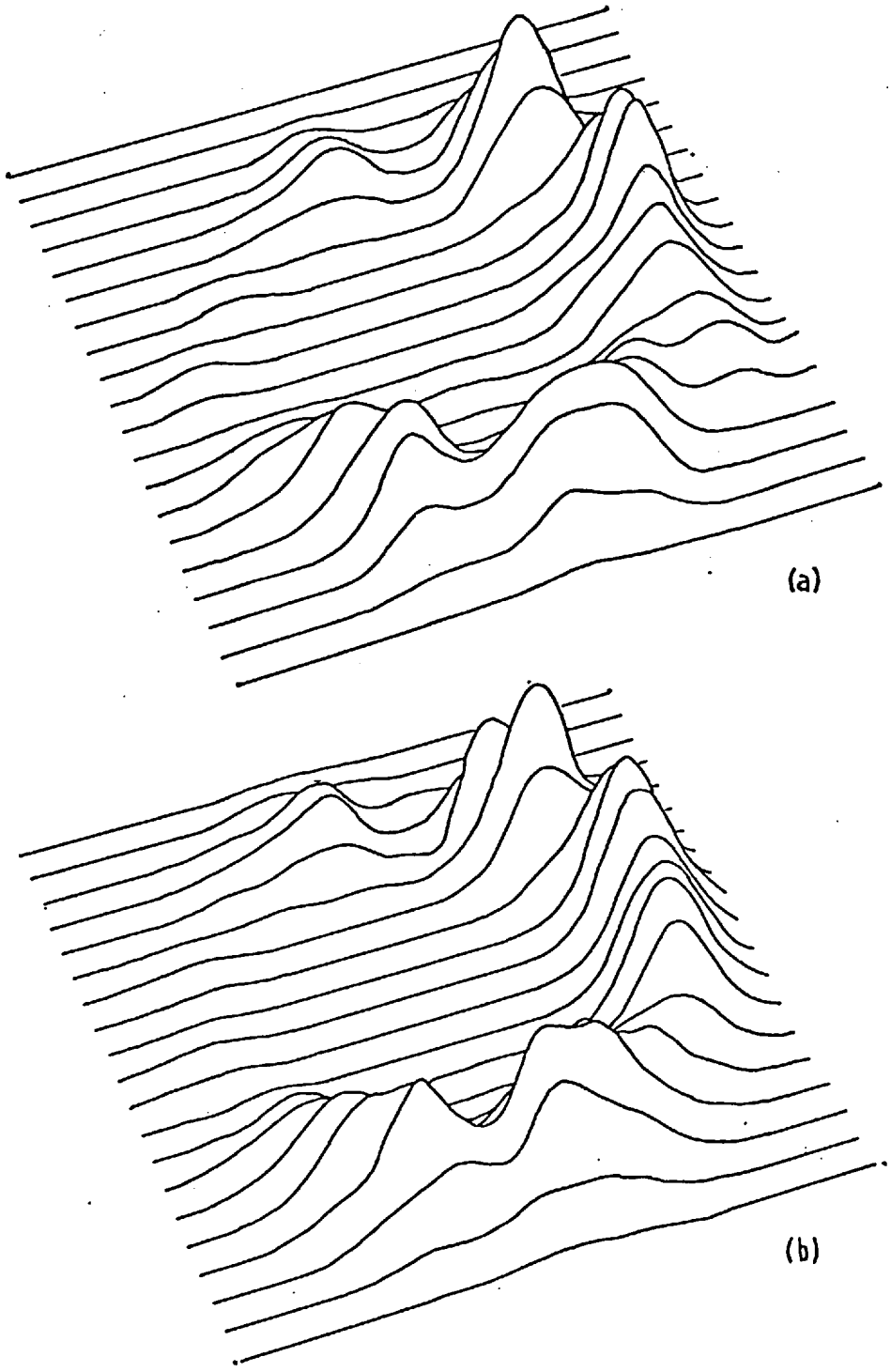

Figure 5.9. Perspective plots of (a) $\hat{f}_N(s,\phi)$ and (b) $\hat{f}_r(s).\hat{f}_\theta(\phi)$ for the 1975 Hebeloma spp. pattern of 133 sporophores.

5.6 Tests for angular uniformity

If the stochastic process underlying an observed pattern of N points is isotropic, then $E(\hat{g}_\theta) \equiv E(\hat{f}_\theta) \equiv (2\pi)^{-1}$. As N increases plots of $\hat{g}_\theta(\phi)$ and $\hat{f}_\theta(\phi)$ versus ϕ would be expected to resemble more and more closely straight lines parallel to the ϕ axis and passing through $(0,(2\pi)^{-1})$. If the stochastic process is anisotropic, the same plots would be expected to give an increasingly more accurate description of the angular trend.

It is intuitively reasonable to expect that the angular density estimates from an isotropic clustered pattern should fluctuate more about $(2\pi)^{-1}$ than those from a Poisson pattern with the same radial pdf and the same number of points. This behaviour suggests possible tests of the null hypothesis of an isotropic Poisson process against clustered alternatives, all processes having the same radial pdf. For example, one could consider

$$\text{(i)} \quad \int_0^{2\pi} |\hat{g}_\theta(\phi) - (2\pi)^{-1}| d\phi \quad \text{or} \quad \text{(ii)} \quad \sup_{\phi \in [0,2\pi]} |\hat{g}_\theta(\phi) - (2\pi)^{-1}|$$

or

$$\text{(iii)} \quad \int_0^{2\pi} |\hat{f}_\theta(\phi) - (2\pi)^{-1}| d\phi \quad \text{or} \quad \text{(iv)} \quad \sup_{\phi \in [0,2\pi]} |\hat{f}_\theta(\phi) - (2\pi)^{-1}| \ .$$

Large values of these statistics indicate possible angular clustering and small values, possible angular regularity.

Monte Carlo tests of the null hypothesis of angular uniformity are employed because there are no relevant small sample results concerning the distributions of these statistics. To test for angular uniformity in some pattern of N points using (i) or (ii) proceed as follows. Find a suitable estimate $\hat{g}_r$ and hence calculate $\hat{g}_\theta$ and the observed

value $M_{(\cdot)}$ of the statistic $(\cdot)$. Generate 100 samples each of N uniformly and independently distributed variates on $[0,2\pi)$. Each sample can be thought of as the angular coordinates of points in a pattern from an isotropic Poisson process. Suppose that h_θ was the smoothing parameter used to calculate $\hat{g}_\theta$ for the pattern of interest. Use the same smoothing parameter to calculate 100 values of the statistic $(\cdot)$ corresponding to each of the 100 samples. Let m be the percentage of these 100 values which exceed $M_{(\cdot)}$. A small value of m, say $m \leq 5$, indicates possible angular clustering and hence possible clustering in the pattern of interest. A large value of m, say $m \geq 95$, indicates possible angular regularity. The obvious significance levels can be attached to the appropriate one or two-sided tests.

An analogous procedure is followed when statistics (iii) and (iv) are used to test for angular uniformity. It is slightly more complicated since it is necessary to simulate 100 patterns each of N points from an isotropic Poisson process with the same radial pdf as that estimated for the pattern of interest. This complication is a consequence of the radial dependence of the amount of smoothing used in forming $\hat{f}_\theta$.

Table 5.1 contains the results of a simulation study of the performance of these statistics against certain clustered and regular alternatives. The patterns examined were simulations of either simple cluster processes or fixed range inhibition processes. In all cases, with the notation of Section 4.3,

$$\lambda_0(x) \propto \quad x \exp(-x^2/2).$$

Figures 5.10(a) and (c) illustrate a clustered pattern and a regular pattern respectively. The associated angular density estimates are illustrated in Figures 5.10(b) and (d).

Clustered Patterns:			m			
N	μ	D	(i)	(ii)	(iii)	(iv)
100	2	0.8	18	24	6	8
		0.4	22	24	16	10
	4	0.8	9	1	0	0
		0.4	8	1	0	0
	10	0.8	1	1	0	0
		0.4	1	0	0	0
Regular Patterns:			m			
N	c	D	(i)	(ii)	(iii)	(iv)
100	0	0.2	50	81	54	30
		0.3	94	95	92	82
100	0.1	0.3	86	79	80	74
125			86	87	96	98
150			80	95	90	98

Table 5.1

The value $M_{(\cdot)}$ of statistic $(\cdot)$ was calculated for a simulated pattern of N points from the simple cluster or fixed range interaction process of interest. A further 100 values of statistic $(\cdot)$ were calculated from 100 simulations of an isotropic Poisson process. The percentage m of these values which exceeded $M_{(\cdot)}$ is shown. Here μ = average number of points per cluster, c = coefficient of inhibition and D = cluster diameter or range of interaction.

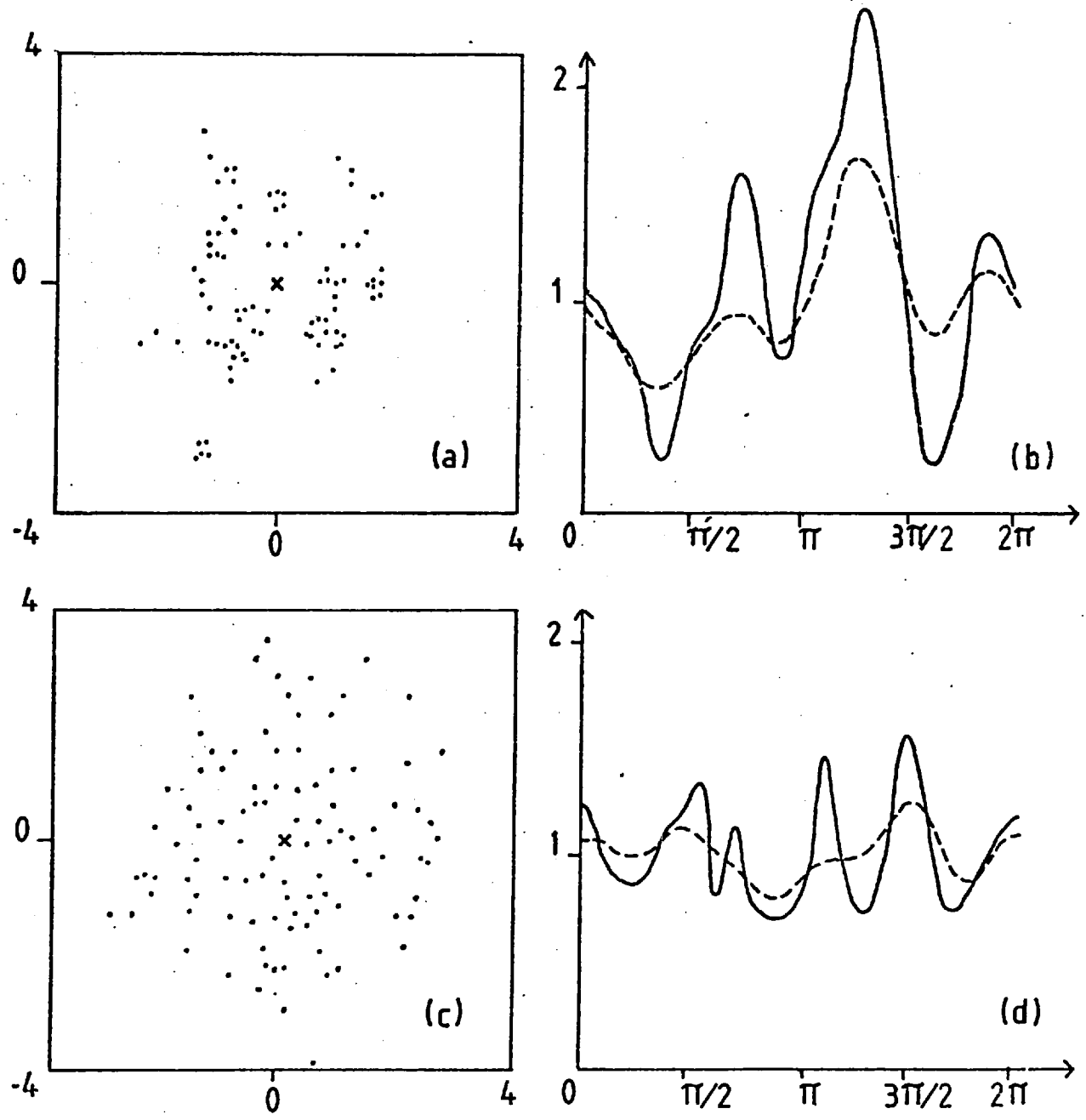

Figure 5.10. Simulations of (a) simple cluster process, N = 100, $\mu = 4$, D = 0.8, (c) fixed range interaction process, N = 100, $c = 0.1$, D = 0.3. The estimates ——— $\hat{f}_\theta$ and ---- $\hat{g}_\theta$ of the angular pdf's are shown enlarged by a factor 10^3 in (b) and (d).

All the statistics appear to detect clustering in a pattern. Although the m values are fairly large for the more regular patterns, none of the statistics is a reliable indicator of this feature of a pattern. This is not surprising. With obvious exceptions, there is no reason to expect that the spacing apart of points in a regular pattern should be reflected in a similar sort of one-dimensional 'regularity' of the angular coordinates of these points. None of the statistics is clearly superior to any other and (i) and (ii) are recommended because of their computational ease.

It should be stressed that large values of the statistics and corresponding small values of m can also be obtained if anisotropy is present. Care must therefore be taken in interpreting the results of the above method applied to actual data. For example, consider the 1975 Hebeloma spp. pattern for which $m = 0$ ($p < 0.01$) in all four cases. This extreme value is caused by the obvious angular trend in the data (see Figures 5.5(a) and 5.7(b)) rather than by any visible clustering in the pattern.

This example suggests a means of dividing the region of interest into sectors within each of which the hypothesis of angular uniformity can be checked in more detail. For example, the 1975 Hebeloma spp. pattern splits into two sectors H, a sector of high sporophore intensity, and its complement H^c of low sporophore intensity where

$$H = \{(s,\phi) : s \geq 0, \quad \phi \in [0,2\pi), \quad \hat{g}_\theta(\phi) \geq (2\pi)^{-1}\}.$$

If one is then interested in testing for angular uniformity within the sector H, simply identify the edges of this sector and use the obvious analogues of statistics (i) and (ii) for the resulting pattern on the

surface of the cone. The corresponding m values of 64 and 61 respectively lead one to accept the hypothesis that within the sector H the pattern has a uniform angular distribution. In particular it is therefore meaningful to proceed with a $\hat{K}_1$ analysis of the pattern in this sector. Similar results for the other sporophore patterns are summarised in the next Chapter.

CHAPTER 6: AN ANALYSIS OF THE SPATIAL PATTERNS FORMED BY SPOROPHORES GROWING ABOUT A YOUNG BIRCH TREE

6.1 Introduction

The techniques developed in Chapters 4 and 5 are used in this Chapter to analyse the sporophore patterns illustrated in Figures 4.1(a)-(c). Ford et al (1980) summarise the known facts concerning the biological background of these data sets. Only a brief description is given here.

Figures 4.1(a),(b),(c) are maps of the positions of the sporophores which grew around a single birch tree (Betula pendula) during the years 1975, 1976 and 1977, respectively 4, 5 and 6 years after planting. All the sporophores appeared during the months July-October. The tree was one of a plot of sixty planted in 1971 in a square lattice pattern with a three metre spacing at Bush Estate, Midlothian, Scotland. Several types of sporophores were identified. Hebeloma spp., Laccaria laccata and Lactarius pubescens were found in all three years and a further species, Inocybe lanuginella appeared for the first time in 1977. Because only four sporophores belonging to the last species were observed, this species has been omitted from the study.

Each of the observed fungal species is able to form sheathing mycorrhizas which grow in a symbiotic relationship with birch tree roots (Trappe, 1962). When soil cores from beneath selected groups of sporophores were examined mycorrhizas of the same type were always present. This seems to indicate a close connection between mycorrhizas and sporophores, the fruiting bodies of the fungus.

Biologists believe that a better description of the sporophore distributions may help in understanding the processes which affect

the colonisation of the tree root system by mycorrhizal fungi. The direct observation of this colonisation is very difficult. Moreover, observation usually results in damage to or destruction of either mycorrhizas or roots or both, thereby making it impossible to observe the same undisturbed system from one year to the next. This is why any indirect information provided by the sporophore distributions is of such interest. Eventually biologists hope to be able to encourage the development of young trees by implanting their root systems with the preferred distribution of mycorrhizas. Such an ambitious project will not be discussed further here.

Ford et al used 'classical' statistical techniques to provide some insight into the important characteristics of sporophore distribution around a single tree. As they observe, "a different form of analysis is necessary if some of the interesting questions regarding patterns of development in sporophore production are to be investigated".

The first of their two suggestions is "to develop an alternative technique of analysis which provides information on different scales of association and is not affected by non-stationarity". The $\hat{K}_1$ analysis does precisely this under certain assumptions which can be at least partially checked in practice using the methods of Chapter 5. This analysis goes some way towards answering such questions as "Do sporophores of different species occur together or are they separated?" and "Do sporophores in one year occur in the same place as sporophores of the same or different species in the preceding year?" (Ford et al, 1980).

Some simple stochastic processes which could have generated the observed pattern of each sporophore type in each year are proposed. These models are fitted using the $\hat{K}_1$ technique. They are a first

attempt to pursue the second of the suggestions made by Ford et al, namely "to use a modelling approach" to describe the patterns of sporophore development. The results of this Chapter provide preliminary information for any future work aimed at understanding the process of mycorrhizal colonisation of a tree root system.

6.2 The marginal radial and angular distributions

In this Section the marginal radial and angular distributions of the sporophore patterns are examined in detail. The methods of the previous Chapter can be used to find kernel density estimates $\hat{g}_r$ and $\hat{g}_\theta$ of the respective pdf's. These estimates are illustrated in Figures 5.3, 5.4 and 5.5. Except where specifically mentioned, the 1975 Lactarius pubescens pattern of only eleven sporophores is not considered in this Chapter.

It is clear from Figure 5.3 that the shape of the radial density curve for each sporophore type changed from year to year and that, in general, there was a definite outward movement from the tree. Ford et al (1980) used rank sum tests (Hollander and Wolfe, 1973, pp.124-125) to investigate this movement. With one exception they found that between 1975 and 1976 and again between 1976 and 1977 the mean distance from the tree for each type of sporophore increased significantly ($p < 0.05$). The exception was Laccaria laccata whose mean distance decreased a non-significant amount in the latter period.

A quick glance at Figure 5.4 reveals that within each year the mean distances from the tree for Lactarius pubescens, Hebeloma spp. and Laccaria laccata are arranged in ascending order. A comparison was made using ranked sum tests. It was found that in each year the difference between the mean distance of Lactarius pubescens and that

of Hebeloma spp. was significant ($p < 0.05$). Except in 1977, the difference between the mean distance of Hebeloma spp. and that of Laccaria laccata was also significant at this level.

The observed differences in mean distances, both between sporophore types in a single year and between years for a single type, must be interpreted with care. It could be that the types do not 'interact' in any way and that each simply has its own preferred radial distance. Alternatively the presence of one type could 'promote' or 'inhibit' the growth of another. There is no way of discriminating between these two cases on the basis of the radial density estimates. The results of the multitype $\hat{K}_1$ analysis of Section 6.4 enable such interpretations to be made.

The angular density estimates are illustrated in Figure 5.5. For each sporophore type in each year the null hypothesis of angular uniformity was rejected using the tests of Section 5.6. In the case of Laccaria laccata in 1975 and 1977 it was felt that this departure from angular uniformity was due to the obvious clustering in the patterns rather than to any underlying trend. In 1976, a year of severe drought, both clustering and angular trend were visually obvious for this sporophore type.

Table 6.1 summarises the results obtained when the method at the end of Chapter 5 was used to partition the region about the tree into high and low intensity sectors in each year for Hebeloma spp. and for Lactarius pubescens. This method was also used to determine the high intensity sector for Laccaria laccata in 1976. Table 6.1 contains the results of tests for angular uniformity on the surface of the cone formed by identifying the edges of the high intensity sector for the pattern of interest. These tests led to acceptance of the null

hypothesis of angular uniformity on the appropriate high intensity sector in each year for both Hebeloma spp. and Lactarius pubescens. The rejection of this test for Laccaria laccata in 1976 was interpreted as evidence of angular clustering rather than of angular trend in the high intensity sector.

Figures 6.1(a)-(c) illustrate the preferred sectors for the three sporophore types. About 80% of the Hebeloma spp. and 70% of the Lactarius pubescens sporophores in each year lay in the relevant high intensity sector. Biologists have found evidence of the effects of sunlight and shade and of damp and dry soil on the development of different types of sporophores. It is possible that the obvious preferences of certain sporophore types for particular sectors about the tree are due to environmental variability. Further biological investigations are required before such behaviour can be confirmed in the present situation. Because so few sporophores lay in the low intensity sectors it was decided to omit these parts of the patterns from any further analysis. With large data sets the patterns in these sectors could, of course, be analysed in the same way as the patterns in the high intensity sectors.

6.3 Modelling the sporophore patterns

The absence of angular trend in a sector is a necessary condition for θ-stationarity of the underlying process in this sector. Unfortunately it is not a sufficient condition. There are no known tests for θ-stationarity in a sector. In order to proceed with a meaningful $\hat{K}_1$ analysis of a particular sporophore pattern, it was necessary to assume that the underlying process was θ-stationary on the high intensity sector in which no angular trend had been detected.

Type	Year	H	N	N_H	h	m	
						(i)	(ii)
Hebeloma spp.	1975	$[4.02, 2\pi) \cup [0, 1.13]$	133	114	3.39	64	61
	1976	$[4.34, 2\pi) \cup [0, 1.26]$	94	75	3.20	14	22
	1977	$[4.15, 2\pi) \cup [0, 0.82]$	45	37	2.95	53	43
Laccaria laccata	1975	$[0,2\pi)$	302	302	2π	0	0
	1976	$[4.71, 2\pi) \cup [0, 0.50]$	137	118	2.07	0	0
	1977	$[0,2\pi)$	286	286	2π	0	0
Lactarius pubescens	1975	———	-	-	-	-	-
	1976	$[0.44, 3.08]$	27	17	2.64	76	78
	1977	$[5.72, 2\pi) \cup [0, 2.83]$	137	96	3.39	11	21

Table 6.1

Values for each annual pattern of each sporophore type: N, total number of sporophores; N_H, number of sporophores in the high intensity sector whose angular coordinates are given by H; h, angular 'length' of this sector. Simulations of the relevant θ-stationary Poisson process on H were used to obtain 100 values of statistic $(\cdot)$, (i) $= \int_H |\hat{g}_\theta(\phi) - 1/h| d\phi$ and (ii) $= \sup_{\phi \in H} |\hat{g}_\theta(\phi) - 1/h|$ where $\hat{g}_\theta$ is the estimated angular density on H obtained by identifying the edges of this sector. The percentage m of these values which exceeded the corresponding value for the pattern of interest is shown.

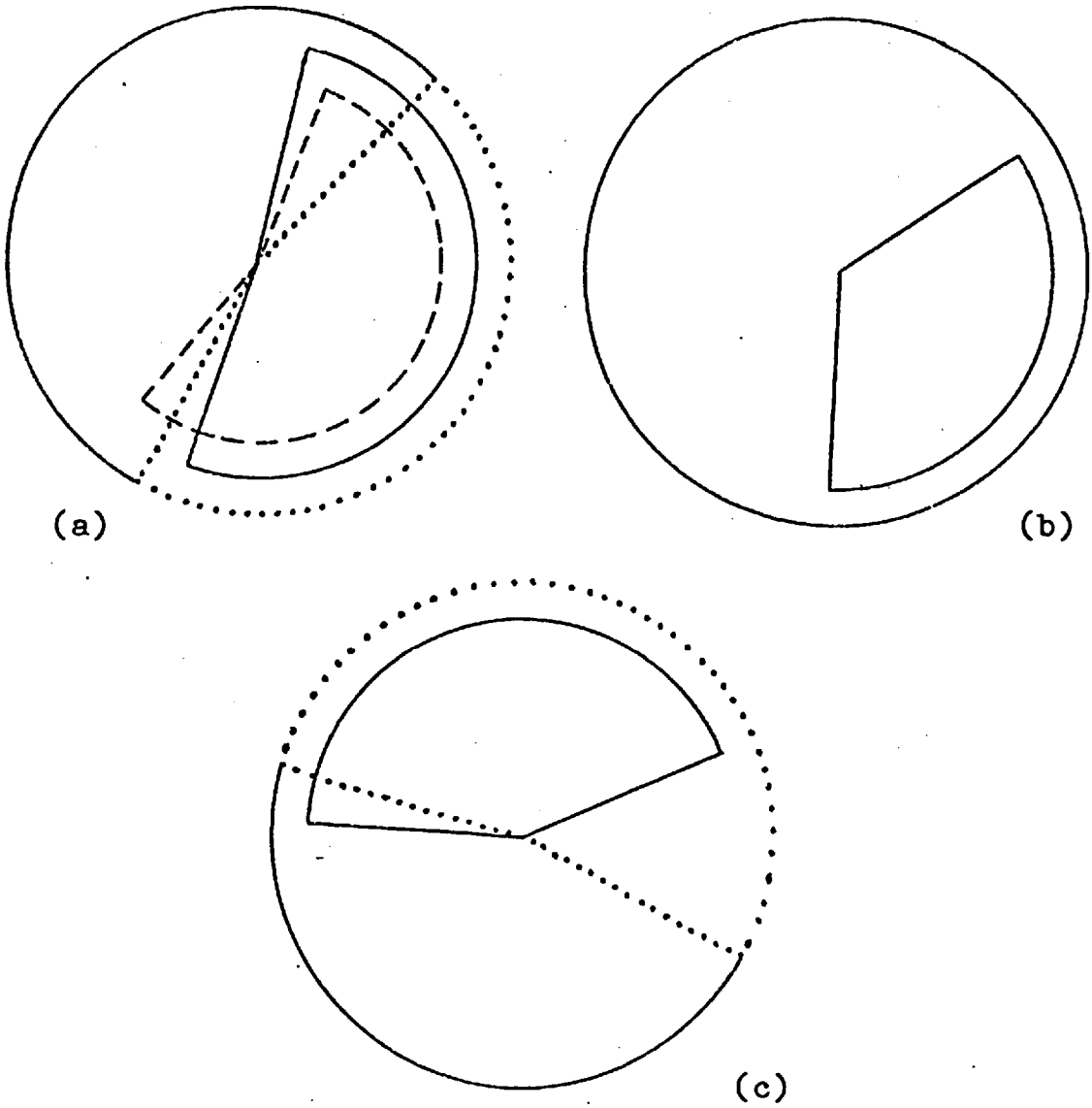

Figure 6.1. The high intensity sectors in 1975 ----, 1976—— and 1977 ···· for (a) Hebeloma spp. (b) Laccaria laccata (in 1975 and 1977 the whole area about the tree) and (c) Lactarius pubescens.

A series of K_1 analyses were used first to test whether any of the yearly patterns for Hebeloma spp. or for Lactarius pubescens in the appropriate high intensity sector could be accounted for by a θ-stationary Poisson process with variable radial intensity. The visually obvious clustering of Laccaria laccata made a similar test for this sporophore type unnecessary. The methods of Section 4.4 were used to simulate outcomes of a θ-stationary Poisson process on the appropriate high intensity sector. The radial intensity in this sector was taken to be that estimated from the sporophore pattern of interest in this region. In each case this intensity hardly differed from that calculated previously for the whole pattern and so has not been illustrated here. The simulated patterns were used to calculate envelope values for $\hat{K}_1(r,t)$ at a selection of points (r,t). Figures 6.2(a)-(e) show the results of these $\hat{K}_1$ analyses for the yearly patterns of Hebeloma spp. and Lactarius pubescens. The results are based in each case on 100 simulated patterns. It is clear that in each year both types of sporophores showed evidence of clustering within the appropriate preferred sector.

A series of $\hat{K}_1$ analyses were next used to assess the fit of the simple cluster model introduced in Section 4.3 to these same yearly patterns in the relevant high intensity sectors. The radial intensity of the cluster centres was taken to be proportional to the estimated radial intensity of the sporophore pattern of interest in this region. The methods of Section 4.4 were used to simulate patterns of N_H points. Each pattern contained a Poisson number, mean ν, of cluster centres. Thus there were about $\mu = N_H/\nu$ points per cluster, each cluster being of fixed diameter D.

The results for the 1975 Hebeloma spp. pattern of 133 points illustrated in Figure 4.1(a) are now discussed in detail. This pattern is shown enlarged in Figure 6.3 and from Table 6.1 it is seen that in this case $N_H = 114$. A visual examination of the pattern in the high intensity sector was made in the light of the earlier decision to reject a θ-stationary Poisson null hypothesis. This examination led to the conclusion that there might be clusters of two to three points on average within discs of about 100 millimetres diameter. Figure 6.4(a) illustrates the results of a $\hat{K}_1$ analysis testing the fit of a simple cluster process with $\mu = 114/45$ and D = 100 millimetres. This process was too clustered at the larger radial distances r for small interpoint distances t.

When a process is tested and found to be too clustered, three options are available: either μ can be decreased (that is, ν increased) or D can be increased or both these changes can be made simultaneously. It is clear that increasing only D must increase the interpoint distances at the larger values of r where the clusters can be assumed to be placed further apart on average since the estimated radial intensity is a decreasing function of r for large r. Figure 6.4(b) shows that holding $\mu = 114/45$ and setting D = 150 millimetres improved the fit of the simple cluster model in the sense that $\hat{K}_1$ lay within the simulation envelope for more of the selected values of (r,t). However, the simulated process was still too clustered for small values of t and large values of r. Decreasing μ and keeping D fixed must increase the average distance between points in each cluster. When $\mu = 114/50 \approx 2.3$ and D = 150 millimetres it was found that $\hat{K}_1$ lay within the simulation envelope for all selected values of (r,t). Decreasing μ still further to $\mu = 114/60$ and holding D constant produced a process which was insufficiently clustered for small values

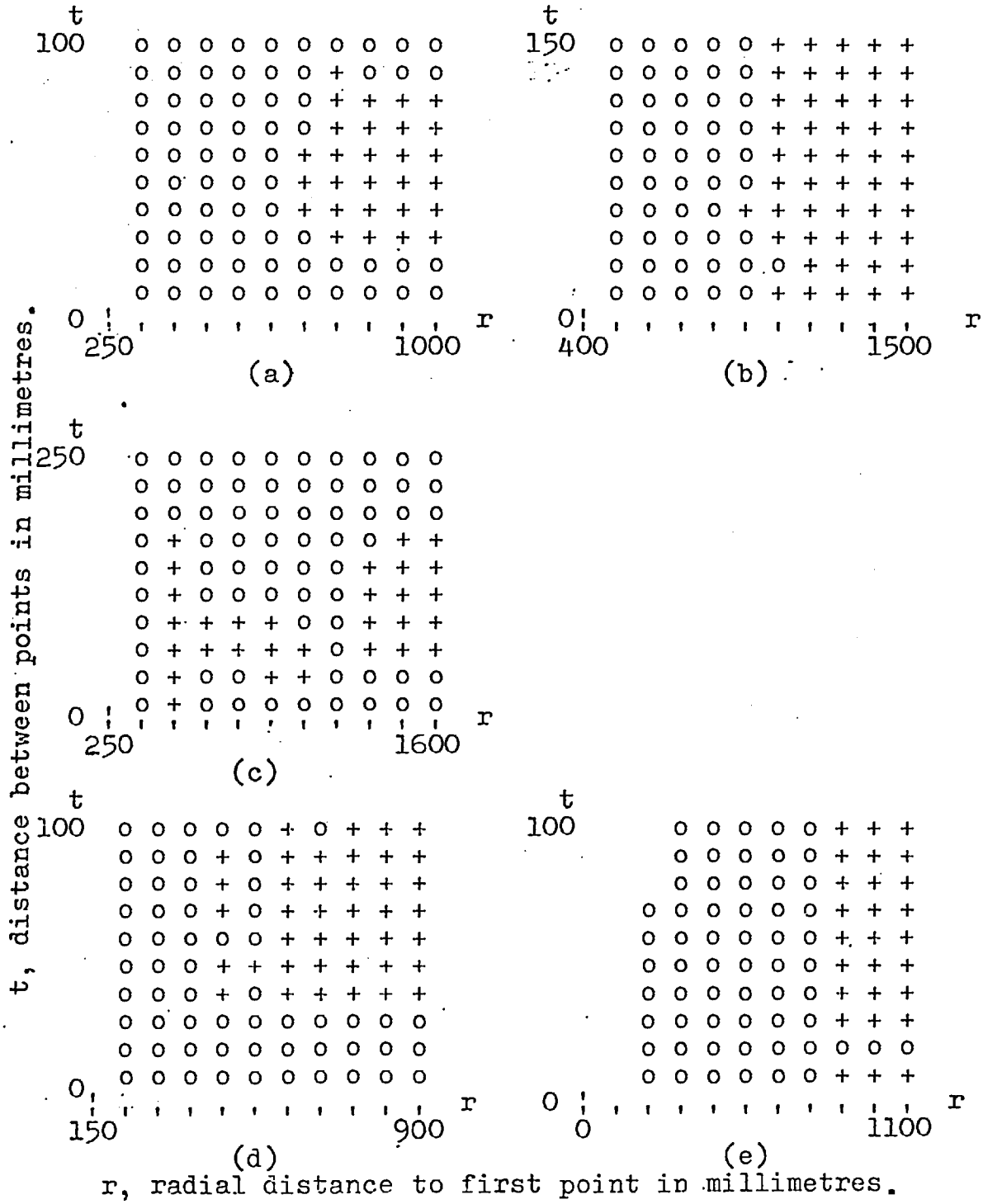

Figure 6.2. Results of $\hat{K}_1$ analyses for Hebeloma spp. in (a) 1975 (b) 1976 (c) 1977 and for Lactarius pubescens in (d) 1976 (e) 1977. The selected points (r,t) for which $\hat{K}_1$ lay within or above the envelope values obtained from 100 simulations of a Poisson process with the relevant radial intensity are marked 0 and + respectively.

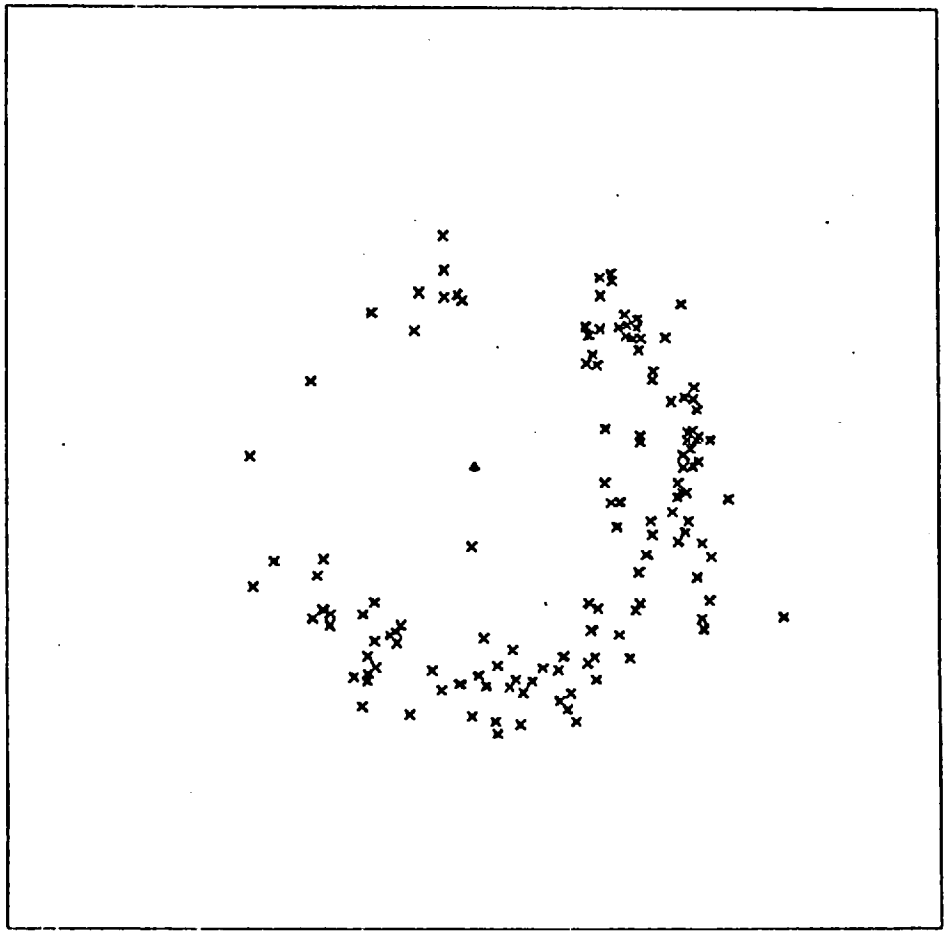

Figure 6.3. The 1975 Hebeloma spp. pattern. Sporophores marked x, the tree ▲ . The square is of side 3 metres.

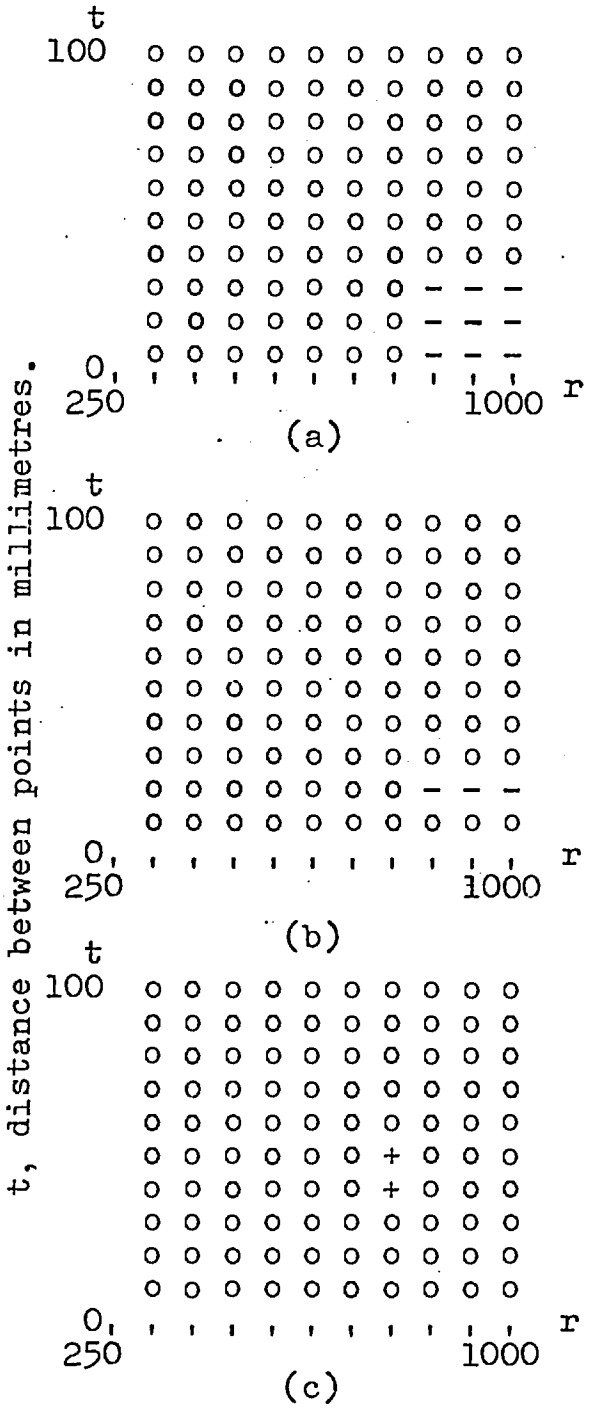

Figure 6.4. Results of $\hat{K}_1$ for the 1975 Hebeloma spp. pattern. The envelope values at a selection of points (r,t) were obtained from 100 simulations of a simple cluster process with about μ points per cluster of diameter D millimetres. (a) μ = 114/45, D = 100; (b) μ = 114/45, D = 150; (c) μ = 114/60, D = 150. Values of (4,5) at which $\hat{K}_1$ lay within, above or below the envelope are shown 0, + and - respectively.

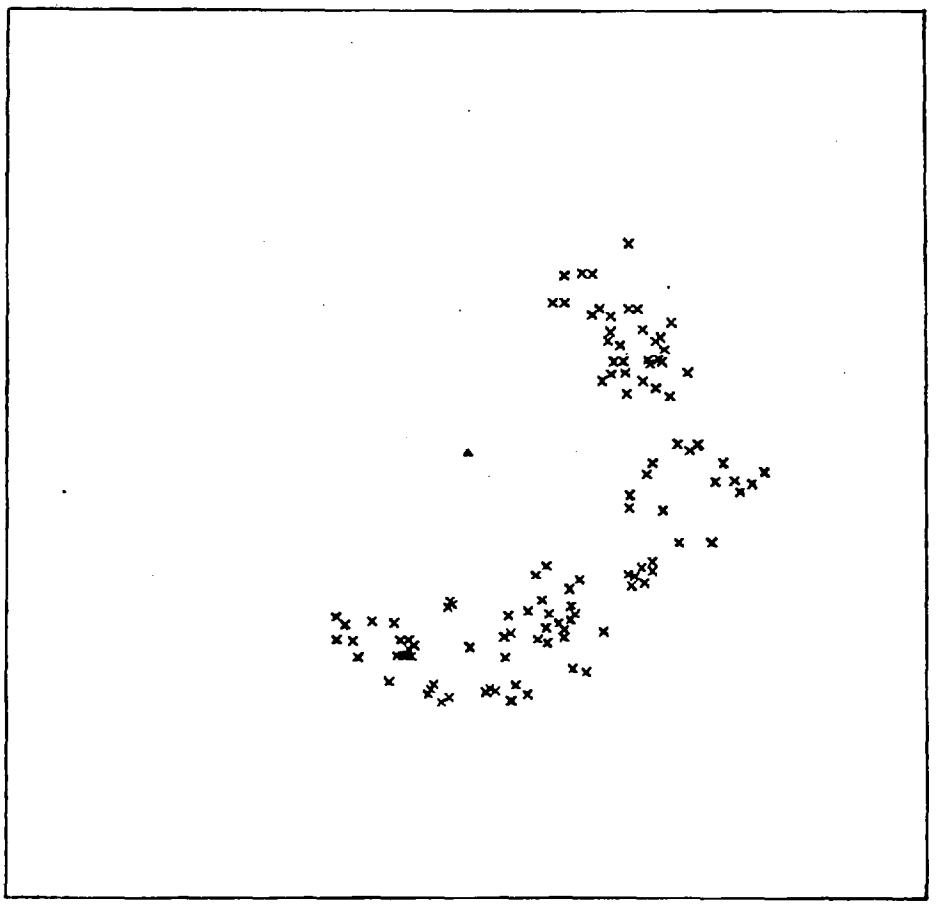

Figure 6.5. A realisation of a simple cluster process containing 114 points in the high intensity sector of the 1975 Hebeloma spp. pattern. There are about $\mu = 2.3$ points per cluster of 150 millimetres diameter. The radial intensity of the cluster centres is proportional to that estimated from the 1975 Hebeloma spp. pattern.

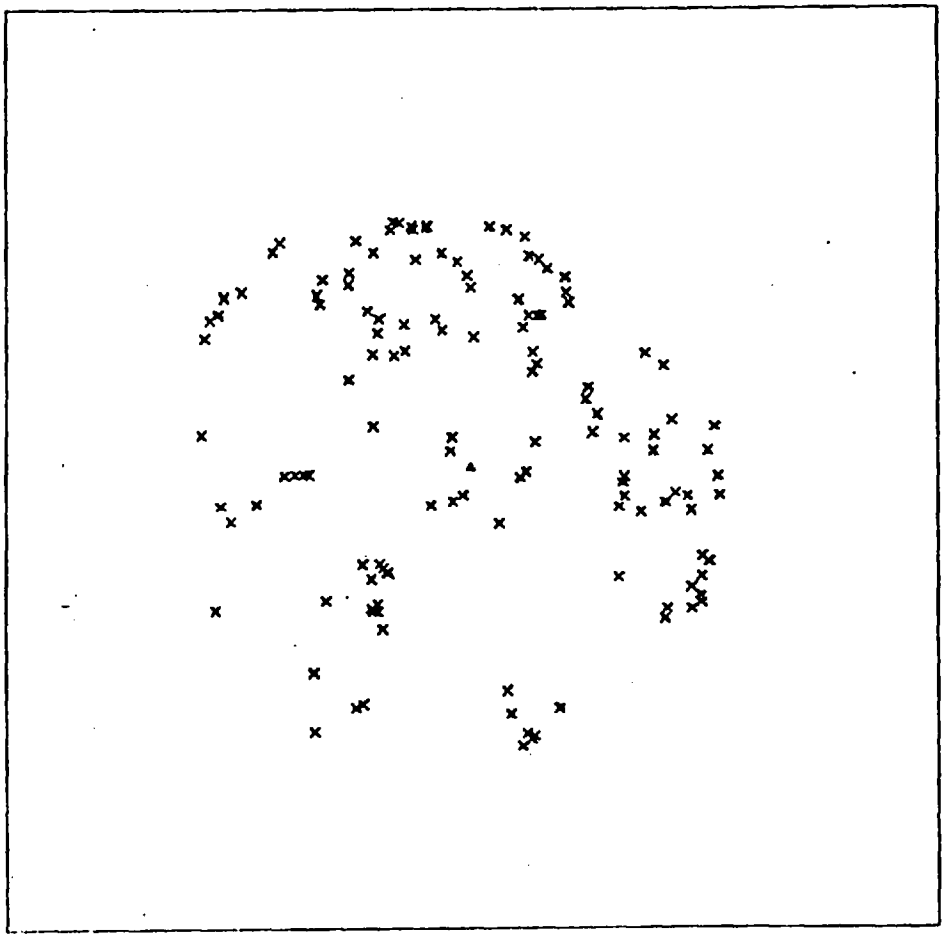

Figure 6.6. The 1977 Lactarius pubescens pattern. Sporophores marked x, the tree ▲. The square is of side 3 metres.

of t, see Figure 6.4(c).

These investigations show that the fit of the model to the 1975 Hebeloma spp. pattern in the preferred sector was fairly sensitive to changes in the values of the parameters μ and D. Figure 6.5 illustrates a realisation of 114 points in the appropriate sector from a simple cluster process with $\mu \approx 2.3$, D = 150 millimetres and a cluster centre radial intensity equal to that estimated from the 1975 Hebeloma spp. pattern in this sector. This Figure should be compared with the relevant part of Figure 6.3.

The patterns for Hebeloma spp. in the preferred sectors for 1976 and 1977 were examined in the same way. It was very pleasing to find that precisely the same simple cluster model with $\mu \approx 2.3$, D = 150 millimetres and with the appropriate radial intensities for the cluster centres could account for the observed patterns. In both cases the fit was again reasonably sensitive to changes in the values of μ and D.

The 1977 Lactarius pubescens pattern illustrated in Figure 5.1(i) is shown enlarged in Figure 6.6. It was found that a simple cluster model with $\mu \approx 2.8$, D = 150 millimetres and having the appropriate radial intensity could account for that part of the pattern in the high intensity sector. The same parameter values and model could also account for that part of the 1976 pattern of this sporophore type which lay in the relevant preferred sector. Fairly small changes in the parameter values again produced processes whose fit was not as satisfactory.

The 1975 Laccaria laccata pattern of 302 sporophores illustrated in Figure 5.1(d) is shown enlarged in Figure 6.7. A close visual examination of the clumps of sporophores evident in this pattern revealed a finer clustered structure within each clump. It was found

that because of this feature a simple cluster model failed to fit sufficiently well for small values of t. For example, Figure 6.8(a) illustrates the best fit obtained when a series of simple cluster processes with different parameter values were considered. A more elaborate model reflecting the structure within each clump is clearly required.

The double cluster model introduced in Section 4.3 seemed an obvious contender. Figure 6.8(b) illustrates the results of comparing $\hat{K}_1$ with simulation envelope values found from 20 simulations of a double cluster process with a Poisson number (mean $\mu_L = 12$) of large clumps of diameter $D_L = 300$ millimetres, each large clump containing a Poisson number (mean $\mu_S = 8$) of small clusters of diameter $D_S = 60$ millimetres. Since there were $N_H = 302$ points in each simulated pattern, there were about $\mu = N_H/(\mu_S\mu_L) \approx 3.1$ points per small cluster. This process was not sufficiently clustered for small values of t. By decreasing μ_S to 6 and so having about $\mu \approx 4.2$ points per cluster and keeping the other parameter values fixed, it was found that $\hat{K}_1$ lay within the simulation envelope at all the evaluation points (r,t). The radial intensity of the centres of the large clumps was taken to be proportional to the estimated radial intensity of the points in the pattern of interest. Figure 6.9 illustrates a realisation of the fitted process. This Figure should be compared with Figure 6.7.

The complete 1977 pattern and the high intensity sector of the 1976 pattern of Laccaria laccata were analysed in the same way. It was found that the same double cluster process with on average 6 small clusters of 60 millimetres diameter per large clump of 300 millimetres diameter and with about 4.2 points per small cluster, produced a satisfactory fit in each case when the appropriate radial intensity

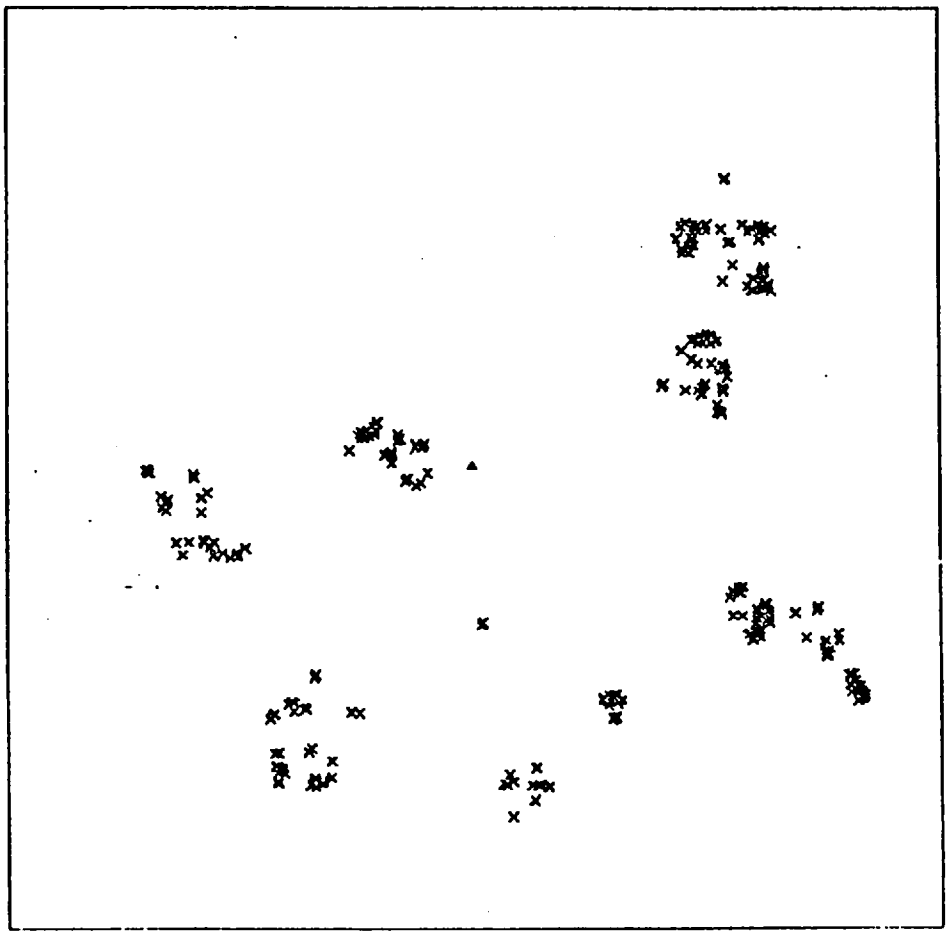

Figure 6.7. The 1975 Laccaria laccata pattern. Sporophores marked x, the tree ▲. The square is of side 3 metres.

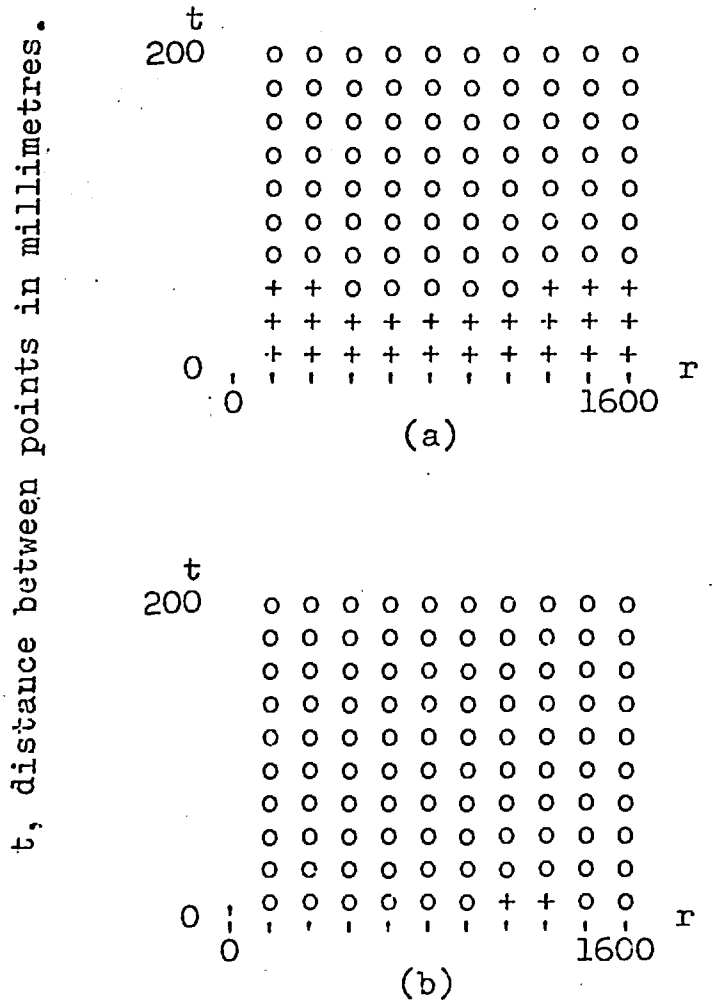

Figure 6.8. Results of $\hat{K}_1$ analyses for the 1975 Laccaria laccata pattern. The envelope values at a selection of points (r,t) were obtained from 20 simulations of (a) a simple cluster process with about $\mu = 302/12$ points per cluster of 300 millimetres diameter and (b) a double cluster process with about $\mu = 3.1$ points per small cluster of 60 millimetres diameter and on average $\mu_S = 8$ small clusters per large clump of 300 millimetres diameter. Values of (r,t) at which $\hat{K}_1$ lay within or above the envelope are shown 0 and + respectively.

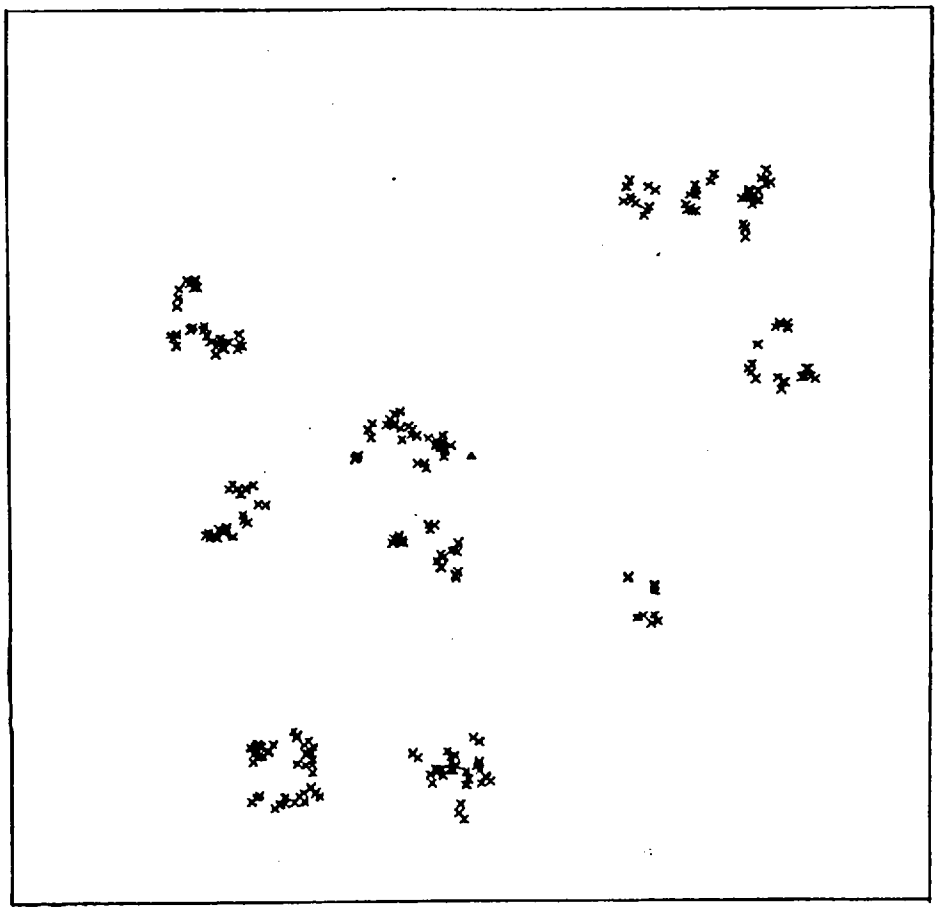

Figure 6.9. A realisation of a double cluster process containing 302 points. There are on average $\mu_S = 6$ small clusters of 60 millimetres diameter per large clump of 300 millimetres diameter. There are about $\mu = 4.2$ points per small cluster and the radial intensity of the large clumps is proportional to that estimated from the 1975 Laccaria laccata pattern. The squares are of side 3 metres.

was used for the centres of the large clumps. The fit for each of the yearly patterns of Laccaria laccata was fairly sensitive to changes in the values of these parameters. A total of 20 rather than 100 simulations was used to find the envelope values for each $\hat{K}_1$ analysis because of the large number of sporophores involved. If there are N_H sporophores in the high intensity sector of a pattern, then the time taken for a $\hat{K}_1$ analysis increases proportionally to N_H^2.

The most important aspect of the results of the $\hat{K}_1$ analyses is that for each sporophore type the essential features of the fitted cluster model in the appropriate high intensity sector were unaltered from one year to the next. Only the changing radial distribution of the cluster centres and the fluctuations in overall numbers of each sporophore type were required to account for the differences in the observed patterns. The change in radial distribution is possibly connected with the outward growth of the tree root system. Any physical explanation for the fitted models will only be possible after further biological research. However, it is hoped that the postulated models might provide a useful starting point for such studies.

In the above no attempt has been made to consider 'interactions' either between types in the same year or within types over several years. This problem is taken up in the next Section.

6.4 Interactions

If the annual patterns of the sporophores are superimposed on one another, then the pattern of a certain kind of sporophore in a particular year can be thought of as the outcome of one of nine types in the resultant multitype process. In Section 4.6 it was shown how a multitype $\hat{K}_1$ analysis could be used to search for 'interaction' between any two

types in a sector within which the joint distribution of both types is θ-stationary. It will be assumed that the intersection of the two appropriate high intensity sectors is such a θ-stationary sector when any two of the nine types are considered together. No statistical tests of such an assumption are yet available. However, it is not possible to make statements concerning 'interaction' unless some such stationarity is assumed and so provides the necessary replication for subsequent inference.

As before the 1975 Lactarius pubescens pattern was omitted from this analysis. Two effects must be borne in mind in this application of the multitype $\hat{K}_1$ method. The first is the size of the assumed θ-stationary sector for the joint distribution of any two types and how many points in the realisation of each type lay in this sector. This is determined by the extent of coincidence of the relevant high intensity sectors for the two types of interest. The second effect is the amount of overlap of the radial distributions of the two types of interest.

It can be seen from Figure 6.1 that the area of intersection of the appropriate high intensity sectors for any two of the yearly patterns of the same kind of sporophore is substantial. Thus there are certainly a sufficient number of points from each of the annual patterns of the same kind of sporophore lying in such a common sector for the application of a multitype $\hat{K}_1$ analysis. Any evidence of 'interaction' can only be obtained from a region in which the marginal radial densities of the two patterns also overlap. It can be seen from Figure 5.3 that for any two yearly patterns of the same kind of sporophore such a region contains a substantial number of points from each pattern. Therefore the multitype $\hat{K}_1$ analysis should give an indication of the presence or absence of any 'interaction within sporophore types'.

Similar considerations, this time using Figures 5.4 and 6.1, reveal that multitype $\hat{K}_1$ analyses should yield useful information about the 'interaction between sporophore types' in a given year in the following cases:

(a) between Hebeloma spp. and Laccaria laccata in each year

(b) between Hebeloma spp. and Lactarius pubescens in 1977

(c) between Laccaria laccata and Lactarius pubescens in 1977.

In 1976 too few points lay within the region of radial overlap in the common high intensity sectors of the two types in (b) and of those in (c) for meaningful multitype $\hat{K}_1$ analyses.

The results of the $\hat{K}_1^{ij}$ analyses are shown in Table 6.2. In each case the envelope values are based on 25 simulated patterns obtained as indicated in Section 4.6 by randomly spinning one pattern relative to the other on the surface of the cone formed by identifying the sides of the common high intensity sector. The number of points from each yearly pattern which fell in this sector is also shown. It is clear that there are no detectable 'interactions' either 'between' or 'within' sporophore types except in the case of Laccaria laccata. This kind of sporophore showed evidence of 'attraction' between any two of the three annual patterns, especially between those in 1976 and 1977 and between those in 1975 and 1977. The results of the relevant $\hat{K}_1^{ij}$ analyses are illustrated in Figure 6.10(a)-(c). As explained in Section 4.6, $\hat{K}_1^{ij}$ can be expected to have a larger variance the more clustered the two patterns under consideration. In view of this and the very marked clustering evident in all three patterns of Laccaria laccata, the results indicating 'attraction' between these patterns should be interpreted with some caution.

Type	*Hebeloma* spp.	*Laccaria laccata*	*Lactarius pubescens*
Hebeloma spp.	75-76 N (101,75)	75 N (114,234)	75 ———
	76-77 N (72,37)	76 N (55,118)	76 ———
	75-77 N (105,37)	77 N (37,124)	77 N (18,35)
Laccaria laccata		75-76 A (131,118)	75 ———
		76-77 A (118,115)	76 ———
		75-77 A (302,286)	77 N (123,96)
Lactarius pubescens			75-76 ———
			76-77 N (17,65)
			75-77 ———

Table 6.2

Results of $\hat{K}_1^{ij}$ analyses investigating possible 'interaction' within or between sporophore types given in the diagonal or the off-diagonal cells respectively. The years or year of interest are given, then N or A indicating evidence of no 'interaction' or of 'attraction' respectively followed by the number of sporophores of each pattern in the common high intensity sector. The total number of sporophores in 1975, 1976, 1977 are (a) *Hebeloma* spp. 133, 94, 45 (b) *Laccaria laccata* 302, 137, 286 (c) *Lactarius pubescens* 11, 27, 137.

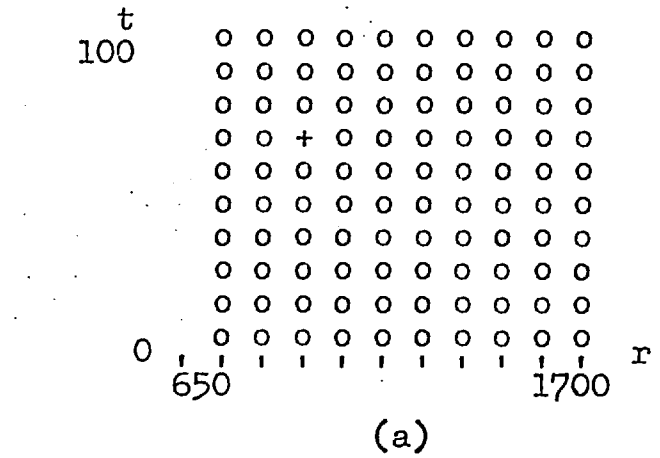

(a)

t in millimetres.

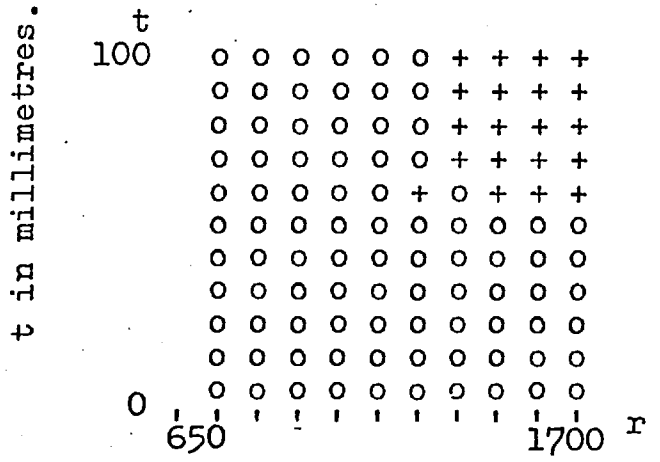

(b)

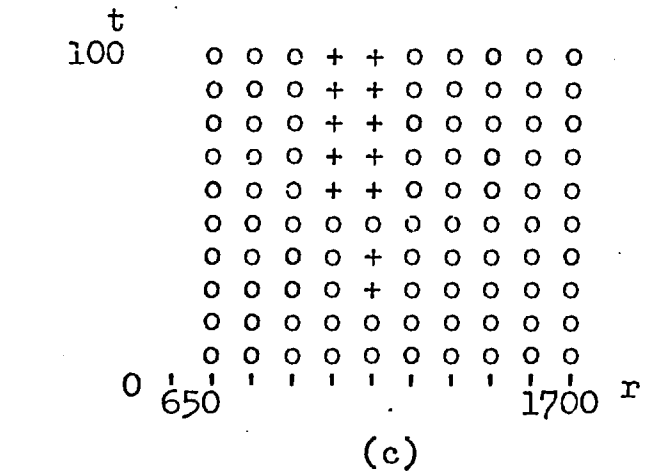

(c)

r in millimetres.

Figure 6.10. The results of multitype $\hat{K}_1$ analyses of the following pairs of Laccaria laccata patterns (a) 1975 and 1976 (b) 1976 and 1977 (c) 1975 and 1977. The envelope values at a selection of points (r,t) were obtained from 25 simulations in each case. Values of (r,t) at which $\hat{K}_1^{ij}$ lay within or above the envelope are shown 0 and + respectively.

6.5 Conclusions

The results of this Chapter suggest that Hebeloma spp. and Lactarius pubescens prefer to grow in certain sectors about the tree. In 1976, a year of drought, Laccaria laccata showed similar behaviour but such behaviour was not evident for this sporophore type in 1975 or 1977. The average distance from the tree for each type of sporophore increased over the three year period of observation. In any year the sporophores of Lactarius pubescens were on average closer to the tree than those of Hebeloma spp. The sporophores of Laccaria laccata were on average furthest from the tree. The annual number of sporophores of Hebeloma spp. decreased over the three year period whilst that of Lactarius pubescens increased. Although the numbers of sporophores of Laccaria laccata in 1975 and 1977 were comparable, there were substantially fewer sporophores of this type in 1976.

The yearly patterns of each sporophore type in the relevant high intensity sectors showed evidence of clustering. A simple cluster model was fitted to the patterns of Hebeloma spp. and to those of Lactarius pubescens. The fitted processes were essentially the same for each sporophore type in all three years, the only difference being a change in the radial intensity of the cluster centres from one year to the next. For the Hebeloma spp. patterns the fitted processes consisted of clusters each containing about 2.3 points. The processes fitted to the Lactarius pubescens patterns contained about 2.8 points per cluster. The clusters were of 150 millimetres diameter for both sporophore types. Double cluster processes each consisting of large clumps of 300 millimetres diameter which contained on average 6 small clusters each of 60 millimetres diameter were fitted to the Laccaria laccata patterns. The small clusters contained about 4.2 points each

and only the changing radial intensity of the clump centres was required to account for the differences between the annual patterns. There was evidence of possible 'attraction' between the yearly patterns of Laccaria laccata but no other 'interactions' either 'between' sporophore types in the one year or 'within' a particular type over the three years were detected.

REFERENCES

BARTLETT, M.S. (1963). The spectral analysis of point processes. J. Roy. Statist. Soc. B25 264-296.

BATCHELER, C.L. and HODDER, R.A.C. (1975). Tests of a distance technique for inventory of pine populations. N.Z. J. Forestry Science 5 3-17.

BESAG, J.E. and GLEAVES, J.T. (1974). On the detection of spatial pattern in plant communities. Bull. Int. Statist. Inst. 45(1) 153-158.

BONEVA, L.I., KENDALL, D.G. and STEFANOV,I. (1971). Spline transformations: three new diagnostic aids for the statistical data analyst. J. Roy. Statist. Soc. B33 1-70.

BREIMAN, L., MEISEL, W. and PURCELL, E. (1977). Variable kernel estimates of multivariate densities. Technometrics 19 135-144.

BROWN, D. and ROTHERY, P. (1978). Randomness and local regularity of points in a plane. Biometrika 65 115-122.

CLARK, P.J. and EVANS, F.C. (1954). Distance to nearest neighbour as a measure of spatial relationships in populations. Ecology 35 445-453.

COX, T.F. and LEWIS, T. (1976). A conditioned density ratio for analysing spatial patterns. Biometrika 63 483-491.

DIGGLE, P.J. (1975). Robust density estimation using distance methods. Biometrika 62 39-48.

DIGGLE, P.J. (1977). A note on robust density estimation for spatial point patterns. Biometrika 64 91-95.

DIGGLE, P.J. (1979). On parameter estimation and goodness-of-fit testing for spatial point patterns. Biometrics 35 87-101.

DIGGLE, P.J., BESAG, J. and GLEAVES, J.T. (1976). Statistical analysis of spatial point patterns by means of distance methods. Biometrics 32 659-667.

EPACHENIKOV, V.A. (1969). Nonparametric estimation of a multivariate probability density. Theory Prob. Appl. 14 153-158.

FINNEY, D.J. (1947). Volume estimation of standing timber by sampling. Forestry 21 179-203.

FINNEY, D.J. (1948). Random and systematic sampling in timber surveys. Forestry 22 64-99.

FINNEY, D.J. (1950). An example of periodic variation in forest sampling. Forestry 23 96-111.

FINNEY, D.J. (1953). The estimation of error in the systematic sampling of forests. J. Indian Society Agricultural Statistics 5 6-16.

FORD, E.D., PELHAM, P.A. and MASON, J. (1980). Spatial patterns of sporophore distribution around a young birch tree in three successive years. Trans. British Mycological Society (to appear)

HINES, W.G.S. and HINES, R.J. O'Hara (1979). The Eberhardt statistic, and the detection of nonrandomness of spatial point distributions. Biometrika 66 73-79.

HOLGATE, P. (1965a) Some new tests of randomness. J. Ecology 53 261-266.

HOLGATE, P. (1965b) Tests of randomness based on distance methods. Biometrika 52 345-353.

HOLGATE, P. (1972). The use of distance methods for the analysis of spatial distribution of points. Lewis (1972) 122-135.

HOLLANDER, M. and WOLFE, D.A. (1973). Nonparametric Statistical Methods. Wiley, New York.

HOPKINS, B. (1954). A new method of determining the type of distribution of plant individuals. Annals of Botany 18 213-227.

KELLY, F.P. and RIPLEY, B.D. (1976). A note on Strauss's model for clustering. Biometrika 63 357-360.

LEHMANN, E.L. (1975). Nonparametrics. Statistical Methods Based on Ranks. Holden-Day, San Francisco.

LEWIS, P.A.W. (Editor) (1972). Stochastic Point Processes. Wiley, New York.

MATÉRN, B. (1960). Spatial Variation. Meddelanden från Statens Skogsforskningsinstitut 49,5. 1-144.

MATÉRN, B. (1971). Doubly stochastic Poisson processes in the plane. Patil et al (1971) I 195-213.

MILNE, A. (1959). The centric systematic area-sample treated as a random sample. Biometrics 15 270-297.

MORISITA, M. (1957). A new method for the estimation of density by the spacing method applicable to non-randomly distributed populations. Physiol. Ecol. Kyoto 7 134-144.

MOUNTFORD, M.D. (1961). On E.C. Pielou's index of non-randomness, J. Ecology 49 271-275.

PATIL, G.P., PIELOU, E.C. and WATERS, W.E. (Editors) (1971). Statistical Ecology. Proceedings of the International Symposium on Statistical Ecology, New Haven, 1969. Penn. State Univ. Press, College Town, Pennsylvania.

PERSSON, O. (1964). Distance methods. Studia Forestalia Suecica 15, 1-66.

PERSSON, O. (1971). The robustness of estimating density by distance measurements. Patil et al (1971) II 175-190.

PIELOU, E.C. (1959). The use of point-to-plant distances in the study of the pattern of plant populations. J. Ecology 47 607-613.

QUENOUILLE, M.H. (1949). Problems in plane sampling. Annals Math. Statist. 20 355-375.

RIPLEY, B.D. (1976a) The second-order analysis of stationary point processes. J. Appl. Prob. 13 255-266.

RIPLEY, B.D. (1976b). On stationarity and superposition of point processes. Annals of Probability 4 999-1005.

RIPLEY, B.D. (1976c). The disintegration of invariant measures. Math. Proc. Camb. Phil. Soc. 79 337-341.

RIPLEY, B.D. (1977). Modelling spatial patterns. J. Roy. Statist. Soc. B39 172-212.

RIPLEY, B.D. (1979a). Tests of 'randomness' for spatial point patterns. J. Roy. Statist. Soc. B41 368-374.

RIPLEY, B.D. (1979b). Simulating spatial patterns: dependent samples from a multivariate density. Applied Statistics 28 109-112.

ROSENBLATT, M. (1956). Remarks on some non-parametric estimates of a density function. Annals Math. Statist. 27 832-837.

ROSENBLATT, M. (1970). Density estimates and Markov sequences. In Nonparametric Techniques in Statistical Inference, M.L. Puri (Editor) 199-210. Cambridge University Press, London.

SILVERMAN, B.W. (1978). Choosing the window width when estimating a density. Biometrika 65 1-11.

STRAND, L. (1972). A model for stand growth. IUFRO Third Conference Advisory Group of Forest Statisticians. INRA, Paris. 207-216.

STRAUSS, D.J. (1975). A model for clustering. Biometrika 63 467-475.

TRAPPE, J.M. (1962). Fungus associates of ectotrophic mycorrhizae. Botanical Review 28 538-606.

WAGNER, T.J. (1975). Nonparametric estimates of probability densities. IEEE Transactions in Information Theory 21 438-440.

WERTZ, W. (1978). Statistical Density Estimation. A Survey. Vandenhoeck and Ruprecht, Gottingen.